American Mineralogist, Volume 99, pages 914–942, 2014

What Lurks in the Martian Rocks and Soil? Investigations of Sulfates, Phosphates, and Perchlorates

Mössbauer parameters of iron in phosphate minerals: Implications for interpretation of martian data‡

M. Darby Dyar[1,*], Erica R. Jawin[1,†], Elly Breves[1], Gerard Marchand[1], Melissa Nelms[1], Melissa D. Lane[2], Stanley A. Mertzman[3], David L. Bish[4] and Janice L. Bishop[5]

[1]Department of Astronomy, Mount Holyoke College, South Hadley, Massachusetts 01075, U.S.A.
[2]Planetary Science Institute, Tucson, Arizona 85719, U.S.A.
[3]Department of Earth and Environment, Franklin and Marshall College, Lancaster, Pennsylvania 17603, U.S.A.
[4]Department of Geological Sciences, Indiana University, 1001 East 10th Street, Bloomington, Indiana 47405, U.S.A.
[5]SETI Institute/NASA-Ames Research Center, Mountain View, California 94043, U.S.A.

Abstract

Phosphate minerals, while relatively rare, show a broad range of crystal structure types with linkages among PO_4 tetrahedra mimicking the hierarchy of polymerization of SiO_4 tetrahedra seen in silicate minerals. To augment previous Mössbauer studies of individual phosphate species and groups of species, this paper presents new Mössbauer data on 63 different phosphate samples, and integrates them with data on more than 37 phosphate species in 62 other studies from the literature. Variations in Mössbauer parameters of different sites in each mineral are then related to both the local polyhedral environment around the Fe cations and the overall structural characteristics of each species. The entire aggregated Mössbauer data set on phosphate minerals is juxtaposed against parameters obtained for spectra from the MIMOS spectrometers on Mars. This comparison demonstrates that signatures from many different phosphate or sulfate mineral species could also be contributing to Mars Mössbauer spectra. Results underscore the conclusion that unique mineral identifications are generally not possible from Mössbauer data alone, particularly for paramagnetic phases, although combining Mössbauer results with other data sets enables a greater level of confidence in constraining mineralogy. This study provides a wealth of new data on Fe-bearing phosphate minerals to bolster future analyses of Mössbauer spectra acquired on Mars.

Keywords: Mossbauer, Mars, phosphates, alluaudite, arrojadite, vivianite, triphylite

Introduction

Phosphate minerals have tremendous economic importance owing to their roles as components of fertilizer and animal feed supplements, lending significance to the many minerals in this class. Phosphorus (P) is also used in food products as a preservative, stabilizer, and thickener, and phosphoric acid is used in many carbonated drinks. Li phosphates are rapidly emerging as excellent candidates for producing batteries for green energy storage and transportation uses (e.g., Takahashi et al. 2002; Yang et al. 2003; Deniard et al. 2004; Kang and Ceder 2009), so this group of minerals has been increasingly studied in recent years.

From a more theoretical perspective, phosphate minerals are significant for their broad array of crystal structures, which are grouped by composition and designated on the basis of the cation that occupies the tetrahedral sites. Thus by definition (Huminicki and Hawthorne 2002), normal phosphates contain P in 4-coordination with O (PO_4), hydrated normal phosphates have PO_4 as well as H_2O, anhydrous phosphates contain PO_4 and OH, while hydrated phosphates contain PO_4, OH, and H_2O. Finally, phosphate minerals are key indicators of rock paragenesis because their variable oxidation and hydration states make them valuable markers of oxidation/reduction and pH in geological environments. The latter characteristic is particularly useful to planetary explorations.

Phosphates commonly occur together with sulfates because both mineral classes are based on tetrahedral anion groups of similar size and high charge. There is ample evidence for the presence of phosphate minerals on Mars, based on their presence in martian meteorites, their identification in remotely sensed data, and on the high levels of P seen in chemical analyses of martian soils, float rocks, and bedrock. Knowledge of the specific minerals present will provide critical information about the diverse environments in which they formed (e.g., acidic/alkaline, hydrated/dehydrated, degree of oxidation, etc.). Sulfates are widespread on Mars, hence, it is likely that phosphate minerals will continue to be identified at many locations on Mars as well.

The authors of this paper are united in a broad research effort aimed at analyzing and characterizing a broad range of the 549 known phosphate mineral species, using a wide variety of techniques including electron microprobe, X-ray diffraction, extended-visible/near infrared/midinfrared reflectance spectroscopy, thermal emission spectroscopy, and Mössbauer spectroscopy. Such a complete study of phosphates will provide well-characterized sample spectra that will be critical for

* E-mail: mdyar@mtholyoke.edu
† Present address: Department of Geological Sciences, Brown University, Providence, Rhode Island 02912, U.S.A.
‡ Special collection papers can be found on GSW at http://ammin.geoscienceworld.org/site/misc/specialissuelist.xhtml.

0003-004X/14/0506–914$05.00/DOI: http://dx.doi.org/10.2138/am.2014.4701

interpreting past and future data from Mars. The results of this effort lay the necessary groundwork for future mission data and meteorite data interpretation that will allow for the determination of which phosphates exist on Mars and for constraints to be placed on their environments of formation.

This paper seeks to relate the Mössbauer parameters of Fe-bearing phosphate minerals to both the local polyhedral environment around the Fe cations and the overall structural characteristics of each species. The foundation for these comparisons has been laid by the thorough discussion and classification of phosphate minerals presented by Huminicki and Hawthorne (2002). It seems logical to assume that minerals of the same structure classes will have similar spectral features. Similarly, mineral species that belong to the same hydration sequence might also be assumed to have similar spectra. However, little work has been done to explore or test this hypothesis. This project was designed to examine general trends in Mössbauer spectroscopy of phosphate minerals at 295 K; Mars temperature measurements have been acquired for some phosphates, but will be considered in a future paper. Accordingly, this paper presents new data on 63 different phosphate samples, integrates them with data on more than 37 phosphate species in 62 other studies from the literature, and then places the entire data set in a crystal chemical context.

Background

The primary motivation for this study was a desire to better interpret Mössbauer results from the Mars Exploration Rovers Spirit and Opportunity (Klingelhöfer et al. 2003). In support of this objective, it is useful to review the existing lines of evidence for the presence of phosphate minerals on Mars.

Phosphate minerals on Mars and from Mars

The presence of phosphate minerals on Mars is supported by multiple lines of evidence: their presence in martian meteorites, experimental work to simulate the hydrothermal alteration of P-rich precursors in basaltic environments, and data on the high levels of P reported in martian soils, float rocks, and bedrock by α particle X-ray spectrometers (APXS) on the Mars Pathfinder (Rieder et al. 1997, 2003) and Mars Exploration Rovers (Brückner et al. 2008; Campbell et al. 2009). Although meteorite studies identify the specific species present in each sample through direct study, the experimental and rover data constrain but do not uniquely identify the likely phosphate mineralogy. The latter problem results not only from assumptions made about bulk compositions in the experiments, but also on the lack of available spectroscopic data on rare sulfate and phosphate minerals. A companion paper to this one considers the variations in Mössbauer parameters of a wide array of sulfate minerals to help address this issue. The current paper focuses on ^{57}Fe Mössbauer parameters of Fe-bearing phosphate minerals. Knowledge of the specific minerals present will provide critical information about the diverse environments in which they formed (e.g., acidic/alkaline, hydrated/dehydrated, degree of oxidation, etc.). To place this work in proper context, it is helpful to briefly review the literature on proposed martian phosphate mineralogy.

Phosphates on Mars indicated by meteorites. Both primary igneous and secondary phosphates have been identified through direct observation of the Shergottite-Nakhlite-Chassignite (SNC) meteorite suite that is thought to be derived from Mars (Gooding et al. 1988; Gooding and Wentworth 1991; Gooding 1992; McSween 1994; Mittlefehldt 1994; Dreibus et al. 1996; Treiman 1996; Mojzsis and Arrhenius 1998; McCoy et al. 1999; Bridges and Grady 1999; Bridges and Warren 2003; Greenwood et al. 2003; Bouvier et al. 2005; Greenwood and Blake 2006; Hui et al. 2011; Stopar et al. 2013). Shergottites in particular contain a wide variety of phosphate minerals. EETA79001 has been extensively studied (Gooding 1992; Jull et al. 1995), and contains an assemblage of secondary minerals that includes carbonate, sulfates, and the phosphate minerals holtedahlite [$Mg_{12}(PO_3OH,CO_3)(PO_4)_5(OH,O)_6$], collinsite [$Ca_2(Mg,Fe)(PO_4)_2{\cdot}2H_2O$], and anapaiite [$Ca_2Fe(PO_4)_2{\cdot}4H_2O$] (Gooding et al. 1988). Dofar 378 contains 1.4% Ca phosphate (Ikeda et al. 2006).

McSween et al. (1996) found 3.5 modal percentage of whitlockite [$Ca_9(Mg,Fe)(PO_4)_6(PO_3OH)$] in QUE94201. Boctor et al. (1998) and Greenwood et al. (2003) reported the merrilite and chlorapatite [$Ca_5(PO_4)_3Cl$] in Allan Hills 84001 and Los Angeles, while McCoy et al. (1999) found whitlockite and apatite in Zagami. Overall, Nakhlites and Chassignites to date contain primarily apatite, while the Shergotittes exhibit much more mineralogical diversity.

The assemblages of Ca- and Mg-phosphates identified in martian meteorites commonly include Ca-carbonate and Ca-sulfate minerals, which strongly imply alkaline formation environments (e.g., Gooding 1992), akin to similar terrestrial assemblages. As an example, the secondary mineral assemblage in EET79001 suggests a low-temperature, saline fluid with a pH above ~7 (Mojzsis and Arrhenius 1998). Although the mineral assemblages in the meteorites imply the former presence of more basic waters on Mars, the current remote-sensing observations by the Mars Exploration Rovers (MERs) (see next section) have implied that sulfates and phosphates observed directly on Mars likely formed in acidic systems (e.g., Clark et al. 2005; Morris et al. 2005; Tosca et al. 2005; Greenwood and Blake 2006).

The high-P content of the SNC meteorites (Banin et al. 1992) relative to terrestrial rocks likely is due to a high-P abundance in the martian mantle. Dreibus et al. (1996) and Wänke and Dreibus (1998) estimate that the mantle P abundance is ~10× higher than that of the Earth, supporting the possibility for phosphates on Mars being more common than for the Earth. The phosphates in the martian meteorites are generally thought to be primary, late crystallization, igneous minerals, with few exceptions (Gooding and Wentworth 1991; Mojzsis and Arrhenius 1998). Dreibus et al. (1996) also found that the phosphates in the Shergotty, Zagami, and ALHA77005 SNCs are leached readily by diluted acids, suggesting that if moderate to very acidic waters were present on Mars, highly mobile primary phosphates would dissolve, and low-temperature, secondary phosphate precipitation could be a globally significant process.

Experiments that constrain phosphate mineralogy. Experiments by Guidry and Mackenzie (2003) show increased dissolution of terrestrial igneous and sedimentary apatites at decreased pH. Tosca et al. (2004) evaluated simulated chemical weathering of Mars-like basaltic rocks exposed to an acid-fog environment and found that some Fe-phosphate minerals precipitated from the fluids. Hurowitz et al. (2006) contrasted experimental data with results from the Mars Exploration Rovers,

and concluded that phases with high ratios of P_2O_5 to CaO such as monetite ($CaHPO_4$), brushite ($CaHPO_4 \cdot 2H_2O$), or merrilite [$Ca_{18}Na_2Mg_2(PO_4)_{14}$] are among the species likely present on surfaces in the Watchtower and Champagne localities.

Many workers have focused their attention on the Paso Robles locality investigated by the Spirit rover. This locality has been especially well-studied because it contains both phosphate-rich soils and rocks interpreted to be the result of extensive alteration of primary materials that were high in P (e.g., Gellert et al. 2006; Ming et al. 2006; Yen et al. 2007). The rocks in this locality were suggested by Ming et al. (2006) to contain either fluorapatite [$Ca_5(PO_4)_3F$] or brushite [$Ca(HPO_4) \cdot 2H_2O$]. Lane et al. (2008) later used visible near-infrared reflectance, thermal emission, and Mössbauer data to suggest that ferristrunzite [$Fe^{3+}Fe^{3+}_2(PO_4)_2(OH)_3 \cdot 5H_2O$] or strengite ($FePO_4 \cdot 2H_2O$) are present there. These results were tested experimentally by Hausrath et al. (2013), who suggested that ferrian giniite or hydrated monocalcium phosphate [MCP; $Ca(H_2PO_4) \cdot 2H_2O$] should be observed at Paso Robles if their precursor was a Ca-phosphate such as apatite. They support the idea that the alteration conditions at Paso Robles were oxidizing, acidic, and hydrothermal, but acknowledge that the Mössbauer parameters of different Fe^{3+} phosphates and sulfates might be indistinguishable.

Phosphates on Mars indicated by in situ observations. Rocks and soils on Mars have indicated the presence of P that is thought to reside in phosphates. In situ bulk element analyses at the Viking, the Pathfinder (PF), and both MER landing sites indicate that P is present in the typical martian soil at 0.36 wt% P (e.g., Toulmin et al. 1977; Clark et al. 1982; Rieder et al. 1997, 2004; Dreibus and Haubold 2004; Foley et al. 2003; Gellert et al. 2004, 2006; Schmidt et al. 2009; McGlynn et al. 2012). Water-lain reworked sulfate-rich bedrock at the MER Meridiani site is thought to contain a phosphate component as well (e.g., Rieder et al. 2004; Clark et al. 2005). Some float rocks in Gusev crater, such as Wishstone, Champagne, and Watchtower, and Ben's Clod, have high-P contents, too, indicating the presence of phosphates (e.g., Gellert et al. 2006; Hurowitz et al. 2006; Ming et al. 2006; Usui et al. 2008). The highest values of P detected to date have been measured in some soils on Mars including undisturbed Crumble (at 0.6 wt% P), and a disturbed soil called Paso Robles (PR, discussed further below) that exhibited a strong phosphorus contribution (2.4 wt% P) [see Fig. 18 in Gellert et al. (2006); Ming et al. (2006)].

Enriched and varying values of P (and S, Br, and Cl) indicate alteration of basalts in an aqueous, acidic environment (e.g., Rieder et al. 2004; Gellert et al. 2006; Tosca et al. 2005). Greenwood and Blake (2006) note that the globally homogenized martian soil has a positive correlation of P, S, and Cl, which are all soluble components of the soil. The S and Cl in the martian rocks and soils likely originated through volcanic exhalations; however, the P may be a product of acidic weathering of igneous Ca-phosphate minerals in the plentiful martian basalts. Acidic water is indicated because circum-neutral waters would contain less P in the resulting soils due to decreased Ca-phosphate solubility. Greenwood and Blake (2006) argue that because of the different sources, S and Cl vs. P, the P/S and P/Cl ratios should be variable in the soils across Mars, but generally are not, indicating mixing in a global acidic ocean (although they state that the global soil could have originated in smaller, separate acidic waters or by localized acid-thin-film or acid-fog alteration, but whose sediments subsequently were transported by wind and globally mixed). Furthermore, aeolian mixing would not explain the uniformly high-P content of the ancient Meridiani Planum bedrock, which is better explained by percolating acidic waters.

The key to understanding the phosphate history on Mars is to first identify and determine phosphate mineralogy and chemistry, and then to relate the identified stabilities and compositions to the environment of formation and water chemistry. To date only a few specific basic (alkaline) phosphate phases have been identified by study of the martian meteorites (e.g., chlorapatite, whitlockite, merrillite, holtedahlite, collinsite, anapaite, and possibly Mg-phosphate pentahydrate), but the chemistry of the in situ secondary phosphates in the martian soils (typical global soil, Paso Robles) and bedrock (e.g., Meridiani) on Mars is still conjecture.

Phosphate crystal structures

Phosphate structures are commonly composed of PO_4^{3-} tetrahedra bonded with (the vast majority of) cations in octahedral or larger coordination polyhedra; tetrahedral Fe^{3+} occupancy (i.e., in P-deficient structures) is rare. Interpretation of the Mössbauer spectra of these structures is greatly simplified because it is generally a matter of distinguishing among octahedral sites occupied by Fe^{3+} and Fe^{2+}. These distinctions are described using the positions of the peaks in doublets of a Mössbauer spectrum using the terms isomer shift (IS, δ, or sometimes center shift) and quadrupole splitting (QS, ΔE_Q, or Δ), expressed in velocity units by convention in this field.

Isomer shift is caused by overlap between the nucleus and the *s*-electron charge distributions that causes a shift in the nuclear energy levels in the Fe atom. Isomer shift is most sensitive to oxidation state and less sensitive to distortions in the surrounding site geometry. Isomer shift is measured as the offset of the doublet's centroid from zero velocity, and its value in silicates is generally low (0.25–0.5 mm/s) for octahedral Fe^{3+} and much higher (>1.10 mm/s) for octahedral Fe^{2+}. Its error is usually given as ±0.02 mm/s (Dyar 1984; Dyar et al. 2008).

Quadrupole splitting results from interactions between the nuclear quadrupole moment and the gradient of the surrounding electric field, which cause the I = 3/2 level to split into two sublevels. QS is the separation between the two component peaks, and is sensitive to both oxidation state and site geometry. As an example, consider Fe^{2+} in perfectly octahedral (sixfold) coordination. The electronic configuration of Fe^{2+}, $3d^6$, is in general high spin for minerals, i.e., $t_{2g}^4 e_g^2$. The sixth electron populates the three degenerate (all the same energy) t_{2g} levels equally, so spherical symmetry is maintained and, ignoring lattice terms, there is no quadrupole splitting. However, a distortion of the octahedral environment lifts the degeneracy of the t_{2g} levels, leading to unequal occupancy of the *d* orbitals and a large contribution to Δ from the electronic field. In high-spin Fe^{3+}, which has electronic configuration $t_{2g}^3 e_g^2$, the *d* orbitals remain equally populated even when the octahedral environment is distorted, and the electronic field remains spherical. Of course, in both cases, asymmetry in the lattice field causes $^{[6]}Fe^{2+}$ and $^{[6]}Fe^{3+}$ to split the I = 3/2 level, but in general, Δ for Fe^{2+} (>1.5 mm/s) >> Δ for Fe^{3+} (<1.3 mm/s). In general, the larger the Δ value, the more distorted the

coordination polyhedron surrounding the Fe atom (Burns and Solberg 1990; Dyar et al. 2006). The error of Δ on fitted spectra is usually given as ±0.02 mm/s (Dyar 1984; Dyar et al. 2008).

Given that the parameters have wide ranges, it should be possible to assign certain ranges of parameters to particular types of bonding environments or coordination polyhedra, which is one of the goals of this paper. Thus this paper presents Mössbauer spectra of well-characterized phosphate minerals and seeks to determine characteristic parameters for minerals with different structure types. In some cases, these are the first Mössbauer measurements of Fe^{3+}/Fe^{2+} ratios for these mineral species. Overall, the results shed light not only on variations of parameters with structure types, but on stoichiometry and charge-balancing substitutions in these phases and the breadth of parageneses and redox environments in which these minerals form. The second goal of this paper is to determine if the Mössbauer parameters of phosphate minerals are distinctive enough to have been detected by the Mars Exploration Rover Mössbauer spectrometers.

Experimental and analytical procedures

Samples for this project (listed in Table 1 in order by Dana number) were selected from the collections of the coauthors, purchased from collectors, or came from E. Cloutis (U. Winnepeg), the National Museum of Natural History (Smithsonian), and the Harvard Mineralogical Museum. Diversity of samples from multiple localities was sought so that compositional variability within each group could be assessed. All samples were kept in dry air in a desiccator when not being analyzed. Samples were first hand-picked to purify them, a step that was critical because many of these phases occur as intergrowths with other minerals. This job was made more difficult by the fact that many phosphates coexist with other phases of the same or similar color, making it necessary to distinguish coexisting phases on the bases of morphology and subtle hue and shade variations. However, it is important to note that in some cases, individual species were mingled with other species at such a small scale that it is unrealistic to expect that pure separates could be created. In such cases, minor contributions in spectra from the impurities would be expected and are noted in Table 1. One of the advantages of the current study is that more than one example of most species was analyzed, and so the diagnostic spectral characteristics that various samples have in common can be identified despite the presence of potential impurities.

A majority of the separates was then analyzed by XRD to confirm their purity and make unequivocal phase identifications. XRD analyses were conducted at Franklin and Marshall College and Indiana University. Samples were then prepared for Mössbauer spectroscopy by mixing the phosphates with sucrose, then gently mixing them into a homogeneous powder to fill the sample holder. 295 K Mössbauer spectra were then acquired using a source of 100–40 mCi ^{57}Co in Rh, which was used on a WEB Research Co. (now See Co.) model W100 spectrometer. Run times ranged from 12–96 h, and results were calibrated against α-Fe foil. Spectra were not corrected for thickness effects because the goal of this study was to compare peak positions rather than peak areas.

Table 1. Samples studied

Dana number	Mineral species	Sample number	XRD results	Locality
38.1.1.1	triphylite	DD193-B	triphylite, quartz, hureaulite, whiteite, and minor tavorite and lipscombite	Sandamab, Namibia
38.1.1.1	triphylite	DD271-A	50% triphylite and 50% parascholzite	Hagendorf, Bavaria, Germany
38.1.1.1	triphylite	DD301B	75–80% triphylite and 15–25% jahnsite	Tip Top pegmatite, Black Hills, South Dakota
38.1.1.1	triphylite	DD305-A	50% triphylite, 50% parascholzite	Serra Branca pegmatite, 12 km south of Pedra Lavrada, Paraíba, Brazil
38.1.1.1	triphylite	DD308-A	45% triphylite, 45% dolomite and 10% hydroxylapatite	Boqueirãozinho pegmatite, Parelhas, Rio Grande du Norte, Brazil
38.1.1.1	triphylite	DD308-T	65% muscovite and 35% triphylite	Boqueirãozinho pegmatite, Parelhas, Rio Grande du Norte, Brazil
38.1.1.1	triphylite	MDD7	55% triphylite and 45% muscovite	Baviere, Germany
38.1.1.1	triphylite	ML-P38	65% triphylite and 35% quartz	Tip Top Mine, Custer Co., South Dakota
38.1.1.2	lithiophilite	DD135	ferroan lithiophyllite	Serra Branca pegmatite, 12 km south of Pedra Lavrada, Paraíba, Brazil
38.1.2.1	maricite	MDD14	80% maricite and 20% vivianite	Big Fish River, Yukon, Canada
38.1.4.11	ferrisicklerite	DD162-A	65–70% ferrisicklerite, with 30–35% Li-rich alluaudite	Les Moulins Mine, Saint-Luc, Anniviers Valley, Wallis, Switzerland
38.2.3.2	hagendorfite	DD184	50–60% hagendorfite, 25–30% triphylite, and 10–20% wolfeite	Hagendorf, Bavaria, Germany
38.2.3.2	hagendorfite	DD237	70–75% hagendorfite, and 25–30% triphylite	Dyke Lode, Custer, Custer Co., South Dakota
38.2.3.3	varulite	DD321	70% poor crystallinity varulite, and 15% each hureaulite and chlorapatite	Varuträsk, Sweden
38.2.3.5	ferroalluaudite	ML-P14	allauadite	Pleasant Valley Pegmatite, Custer Co., South Dakota
38.2.3.6	alluaudite	ML-P40 (2)	allauadite	Helen Beryl Mine, Custer Co., South Dakota
38.3.3.1	graftonite	ML-P24	75% graftonite and 25% triphylite	Bull Moose Mine, near Custer, Custer Co., South Dakota
38.4.1.2	purpurite	DD227	40–50% purpurite, 30–40% ferrisicklerite, and 10–20% quartz	Sandamab, Namibia
38.4.1.2	purpurite	DD270	80% albite and 20% purpurite	Sidi Bou Othmane, Jbilet, Marrakech, Morocco
39.2.1.1	hureaulite	ML-P31-A	60% hureaulite and 40% pentamanganese	Lavra da Cigana, Galileia, Minas Gerais, Brazil
40.2.2.1	fairfieldite	DD171	No XRD data for this sample, but it is from a known locality for this mineral.	Hagendorf, Bavaria, Germany
40.2.2.2	messelite	DD228	No XRD data for this sample, but it is from the type locality.	Messel, Darmstadt, Hesse, Germany
40.3.2.4	landesite	ML-P26	No XRD data for this sample, but it from a known locality for this mineral.	Cigana Mine, Galileia, Brazil
40.3.5.1	ludlamite	DD219	60–70% ludlamite, and 30–40% siderite	Mina Colavi, Saavedra Prov., Potosí Dist., Bolivia
40.3.6.1	vivianite	DD171	85–90% vivianite, and 10–15% triphylite	Hagendorf, Bavaria, Germany
40.3.6.1	vivianite	DD311	85–90% vivianite, and 10–15% sodium iron phosphate	Mina Huanuni, Cerro Morococala, Oruro Dept., Bolivia
40.3.6.1	vivianite	DD312A	70–80% vivianite, and 20–30% barite.	Ovidor, Catalao, Goiás, Brazil
40.3.6.1	vivianite	DD315A	Vivianite	Kertsch, Kazahkstan
40.3.6.1	vivianite	DD323	50% siderite, 20% goethite, 20% vivianite, 10% dilithium silicate.	Ovidor, Catalao, Goiás, Brazil
40.3.7.1	bobierrite	MDD11	pure bobierrite	Cross Cut Creek, Rapid Creek, Yukon, Canada
40.3.9.1	metavivianite	DD319	60–70% natrolite, and 30–40% metavivianite	Hamilton, Victoria, Australia
40.4.1.2	strengite	DD293-A	90% strengite, 10% goethite, and trace quartz	Kirunavaara, Kiruna, Lapland, Sweden
40.4.1.2	strengite	ML-P16	60% plagioclase and 40% strengite	Boa Vista Mine, Minas Gerais, Brazil

(Continued on next page)

Spectra were fit with Lorentzian doublets using the MEX_FielDD program acquired from the University of Ghent courtesy of E. De Grave. Isomer shifts (IS or δ), and quadrupole splittings (QS or Δ) of the doublets were allowed to vary, and widths (full-width at half maximum) of all peaks were coupled to vary in pairs. All major Fe species were represented by well-resolved quadrupole pairs so the fits were straightforward, though it was sometimes necessary to fit small doublets representing impurities (Table 2[1]).

Results: Mössbauer parameters

Mössbauer parameters for all samples studied at room temperature are given in full in Table 2[1]. To simplify the discussion, minerals are discussed in alphabetical order. In cases where several species constitute a group of similar structures, the discussion is grouped under a single group heading.

Crystal structures and related Mössbauer parameters

Alluaudite group. Minerals in the alluaudite group include the species itself [$NaCaFe^{2+}(Mn,Fe^{2+},Fe^{3+},Mg)_2(PO_4)_3$], ferroalluaudite [$NaCaFe^{2+}(Fe^{2+},Mn,Fe^{3+},Mg)_2(PO_4)_3$], varulite [$NaCaMn(Mn,Fe^{2+},Fe^{3+})_2(PO_4)_3$], and hagendorfite [$(Na,Ca)MnFe_2(PO_4)_3$]. The basic structure has four large coordination polyhedra, one of which is 8-coordinated in face-sharing chains parallel to [001] (Moore 1971a; Moore and Ito 1979). The other three are 6-coordinated polyhedra designated M1, M2, and M3. The M1 and pairs of M2 polyhedra share edges and form staggered chains parallel to the {101} plane, with the M1 site being larger than M2 and highly distorted. The chains are connected by PO_4 tetrahedra to form sheets, and channels between the sheets parallel to the *c* axis contain 8-coordinated X1 sites and 4-coordinated X2 sites. Hatert et al. (2000) proposed three additional "A" sites, also in the channels. This mineral group has been very well-studied because synthetic materials with the alluaudite structure have potential for the manufacture of batteries because Li can fit into the channels.

Mössbauer parameters of the various species in this group have already been characterized in a large number of synthetic samples. In alluaudite, Korzenski et al. (1998) studied $NaFe_{3.67}(PO_4)_3$ and reported three doublets assigned to the Fe1, Fe2, and Fe3 sites. Subsequently Hermann et al. (2002) measured samples spanning a range of x = 0, 0.25, 0.5, and 0.75 for $Na_{1-x}Li_xMnFe_2(PO_4)_3$ and observed that δ decreases

[1] Deposit item AM-13-517, Table 2. Deposit items are available two ways: For a paper copy contact the Business Office of the Mineralogical Society of America (see inside front cover of recent issue for price information). For an electronic copy visit the MSA web site at http://www.minsocam.org, go to The American Mineralogist Contents, find the table of contents for the specific volume/issue wanted, and then click on the deposit link there.

Table 1.—*Continued*

Dana number	Mineral species	Sample number	XRD results	Locality
40.4.3.2	phosphosiderite	ML-P22	phosphosiderite	Stewart mine, near pala, San Diego County, California
41.6.1.2	triplite	DD129	65–70% dolomite, 25% quartz, and 5–10% triplite	Boqueirãozinho pegmatite, Parelhas, Rio Grande du Norte, Brazil
41.6.1.2	triplite	DD302	triplite	Córdoba, Argentina
41.6.2.1	wagnerite	DD330	wagnerite	Hålsjöberg (Horrsjöberg), Sweden
41.6.4.1	satterlyite	MDD18	satterlyite and vivianite	Kulan Camp, Rapid Creek, Yukon, Canada
41.6.7.1	tarbuttite	DD306	90% tarbuttite, 10% parascholzite	Reaphook Hill. 40 miles south of Blinman, Flinders Range, South Australia
41.7.2.1	arrojadite	ML-P25	65% arrojadite and ~35% natrite	Locality unknown (collection of Pierre Hanin (?))
41.7.4.1	lulzacite	DD197	55% siderite, 35% lulzacite, and 10% bonshtedtite	Bois-de-la-Roche Quarry, Saint-Aubin-des-Châteaux, Loire-Atlantique, France
41.9.1.1	kulanite	MDD16	kulanite	Stonemane Camp, Rapid Creek, Yukon, Canada
41.9.1.1	kulanite	ML-P32	kulanite	Rapid Creek, Yukon, Canada
41.9.2.2	frondelite	DD130	~55% frondelite, 35% phosphosiderite, and 10% quartz	Boca Rica Pegmatite, Galiléia, Minas Gerais, Brazil
41.10.1.1	lazulite	DD125	80% lazulite, with 10% each augelite and quartz	Rapid Creek, Yukon, Canada
41.10.1.1	lazulite	DD206	No XRD data for this sample	Area A, Rapid Creek, Richardson Mountain District, Yukon Territory, Canada
41.10.1.1	lazulite	DD208	No XRD data for this sample	Formacáo Claim, Diamantina, Minas Gerais, Brazil
41.10.1.4	barbosalite	DD134	50% barbosalite and 50% mitridatite	Bull Moose Mine, Custer Co., South Dakota
41.10.1.4	barbosalite	DD248-A	50% barbosalite, 40% pyrite, and 10% phosphosiderite	Bull Moose Mine, near Custer, Custer Co., South Dakota
41.10.2.1	lipscombite	MDD9	90% poorly crystalline lipscombite with minor hydroxylapatite	Anloua, Adamaoua Plateau, Cameroon
41.11.1.1	trolleite	DD157	trolleite with much amorphous material	Sandamab pegmatite, Namibia
42.7.1.1	childrenite	ML-P29	may be in solid solution with eosphorite	Linopolis, Minas Gerais, Brazil
42.7.4.1	arsenocrandallite	DD150	No XRD data for this sample, but the Mössbauer parameters are consistent with what is expected by comparison with jarosite and the sample is from the type locality.	Dolores Propspect, Pastrana, Mazarrón-Águilas, Muricia, Spain
42.7.7.1	roscherite	DD274	solid solution with eosphorite	Laranjeiras Claim, Galiléia, Minas Gerais, Brazil
42.7.7.3	zanazziite	DD337	No XRD data for this sample.	Santa Maria, Jenipapo, Itinga, Minas Gerais, Brazil
42.9.1.2	dufrénite	ML-P34-D	dufrénite, pharmacosiderite, and hureaulite	Lone Tree Mine, Humboldt County, Nevada
42.9.2.2	gormanite	MDD13	pure gormanite	Big Fish River, Yukon, Canada
42.9.3.4	chalcosiderite	ML-P39	minor (~5–10%) dickite impurity	Wheal Phoenix, Cornwall, Great Britain
42.11.3.1	whiteite	DD329	90–95% whiteite with 5–10% synthetic tuite	Area A, Rapid Creek, Richardson Mountain District, Yukon Territory, Canada
42.11.9.1	strunzite	HMM108175	strunzite	Fitzgibbon Quarry, Alstead, New Hampshire
42.11.9.3	ferristrunzite	ML-P15	ferristrunzite + quartz	Blaton Hainaut, Belgium
42.11.10.1	laueite	DD210	No XRD data for this sample.	Palermo Mine, North Groton, New Hampshire
42.11.10.7	ferrolaueite	MDD20	ferrolaueite	Monmouth County, New Jersey
43.5.11.1	lüneburgite	DD218	No XRD data for this sample, but it is from same locality studied by Sen Gupta et al. (1991).	Bela Stena Mine, Piskanya, Balevats, Serbia, Yugoslavia

with increasing Li substitution. They report parameters of δ = 0.41–0.47 mm/s and Δ = 0.50–0.90 mm/s for Fe^{3+} and δ = 1.1–1.3 and Δ = 2.0–2.8 mm/s for Fe^{2+}. That group continued with studies of $NaMn(Fe_{1-x}In_x)_2(PO_4)_3$ alluaudite (Hatert et al. 2003), $Na_2(Mn_{1-x}Fe^{2+}_x)_2Fe^{3+}(PO_4)_3$ (Hatert et al. 2005) and several Na-Mn-Fe-bearing alluaudites (Hatert et al. 2004). These latter three papers develop a model in which Fe^{3+} and Fe^{2+} occupy only the M2 site (as first suggested by Moore 1971a) but there are multiple Mössbauer doublets because there are several different next-nearest neighbors surrounding the M2 sites. This model was used by Redhammer et al. (2005) to interpret the single Fe^{2+} doublet with of δ = 0.43 mm/s and Δ = 0.52 in their alluaudite spectrum.

In the two (natural) samples studied here (Fig. 1), alluaudite ML-P40 is 100% Fe^{3+} in a single octahedral doublet (δ = 0.43 mm/s, Δ = 0.44 mm/s), and "ferroalluaudite" ML-P14 is 90% Fe^{3+} (δ = 0.44 mm/s, Δ = 0.45 mm/s) and 10% Fe^{2+} (δ = 1.27 mm/s, Δ = 2.75 mm/s), both in 6-coordination. Given the context established by the previous work, it is concluded that both valence states of Fe occupy the M2 site.

Redhammer et al. (2005) acquired Mössbauer spectra of a hagendorfite sample from the type locality at Hagendorf, Bavaria, Germany. In their sample, Fe^{2+} is modeled with four doublets representing the M2 site, with parameters of δ = 1.19–1.24 mm/s and Δ = 1.40–2.94 mm/s at 298 K. Roughly 36% of the total spectral area was a Fe^{3+} doublet with δ = 0.43 mm/s and Δ = 0.53 mm/s at 298 K; this was also assigned to the M2 site. In this study, samples DD237 from Custer, South Dakota, and DD184, also from Hagendorf, were measured (Fig. 1). They show the same pattern of three Fe^{2+} doublets and one for Fe^{3+} with similar parameters (Table 2[1]).

Finally, varulite DD321 (Fig. 1) also has four doublets, but two are Fe^{2+} (δ = 1.29–1.42 mm/s and Δ = 2.34 and 1.12 mm/s, respectively) and two are for Fe^{3+} (δ = 0.30 and 0.35 mm/s and Δ = 0.77 and 0.34 mm/s, respectively). However, these are again likely to be in the M2 sites, though there is a possibility that the δ = 1.42 mm/s might represent Fe^{2+} in one of the larger sites.

Anapaite. Anapaite $[Ca_2Fe^{2+}(PO_4)_2{\cdot}4(H_2O)]$ was first described by Catti et al. (1979) as a framework structure of Ca (8-coordinated), Fe (6-coordinated), and P (4-coordinated) corner- and edge-sharing polyhedra. Each Fe is bonded to four H_2O molecules and two O^{2-} anions that are the corners of adjacent PO_4 tetrahedra. Eeckhout et al. (1999) present a thorough multi-temperature study of anapaite from Bellaver de Cerdena, Spain. Their sample displays a single doublet with δ = 1.19 mm/s and Δ = 2.49 mm/s at 300 K consistent with the single Fe site in the structure.

Arrojadite. Arrojadite $[KNa_4CaMn^{2+}_4Fe^{2+}_{10}Al(PO_4)_{12}(OH,F)_2]$ has an exceedingly complicated crystal structure (Moore et al. 1981) that has recently been revisited by Cámara et al. (2006), Chopin et al. (2006), and Yakubovich et al. (1986). It has 11 cation and anion sites with partial occupancies, with Fe in the M1 (a distorted tetrahedron), M2 (a distorted 5-coordinated square pyramid), M4, M5, M6 (all three are distorted octahedra), and M7 (octahedral) sites. Its Mössbauer spectrum is similarly complicated, as first presented by Shinno and Li (1998). They reported spectra with broad peaks to which they fit five quadrupole splitting distributions corresponding to M3, M4, M5, M6, and M7 sites (Table 2[1]).

In this study, arrojadite ML-P25 also has six Fe^{2+} doublets, again with a wide range of Δ from 0.97 to 2.98 mm/s (Table 2[1]). In general, the larger the Δ value, the more distorted the coordination polyhedron surrounding the Fe atom (Burns and Solberg 1990; Dyar et al. 2006). Although both Moore et al. (1981) and Cámara et al. (2006) suggested that Fe^{2+} is present in the four-coordinated M1 site, the Mössbauer parameters do not support this assignment. However, the other six doublets likely correspond to the remaining six sites, M2-7. The M2 site is 5-coordinated, and extremely distorted; this should result in the lowest value of δ but there is no clearly lower value for any of the six doublets. The other sites may be distinguished on the basis of the quadratic elongation parameter (λ), which provides a quantitative measurement of polyhedral distortion

$$\lambda = \sum_{i=1}^{n} \left(\frac{l_i}{l_o} \right)^2 / n \quad (1)$$

where l_i is the measured bond distance (where n = 6 for 6-coordination) and l_0 is the bond distance in a perfect (undistorted, equal volume) octahedron. Reported unitless octahedral λ values for the Rapid Creek sample studied by Cámara et al. (2006) are 1.0139 and 1.0126 for M3a and M3b, 1.0319 for M4, 1.0483 and 1.0456 for M5a and M5b, 1.0337 for M6, and 1.0228 and 1.0548 for M7a and M7b. If λ is truly and solely a function of site distortion measured in this way, then the site assignments would be as follows: Δ = 3.21 and 2.72 mm/s would be the M7 and M5 most distorted sites, Δ = 2.13 and 2.15 mm/s would represent M4 and M6, and Δ = 1.11 and 1.57 mm/s would represent M3. Shinno and Li (1998) assigned these observed features to Fe^{2+} in specific sites in the structure on the basis of distortion of their coordination polyhedra as represented by the parameters of quadrupole splitting distributions used to model them. Their assignments were not the same as those based on the bond distortion parameters: the distribution with Δ = 3.17 mm/s was assigned to M3, Δ = 2.77 mm/s to M6, Δ = 2.51 mm/s to M7, Δ = 2.07 mm/s to M4, and 1.52 mm/s to M5 (Shinno and Li 1998). These alternative methods for assigning spectral features could be resolved through comparison of site occupancies from single-crystal refinements, but this task is outside the scope of the present work.

Barbosalite. Barbosalite $[Fe^{2+}Fe^{3+}_2(PO_4)_2(OH)_2]$ is the Fe^{3+}-rich member of the lazulite group of hydroxyl-phosphates; its structure and spectra are discussed under the lazulite heading below.

Baricite. Baricite $[(Mg,Fe)_3(PO_4)_2{\cdot}8H_2O]$ is a member of the vivianite group and is discussed with that group below under the vivianite heading.

Bassetite. Although no sample of the uranyl phosphate bassetite $[Fe^{2+}(UO_2)_2(PO_4)_2{\cdot}8H_2O]$ was available for this study, it has been previously analyzed by De Grave and Vochten (1988) and Vochten et al. (1984). They find only a single doublet each for Fe^{2+} and Fe^{3+} in partially oxidized samples. However, they observe two distinct Fe^{2+} doublets in reduced samples when measured at 80 K, despite the fact that the crystal structure has only a single Fe site surrounded by PO_4 tetrahedra and UO_6 octahedra.

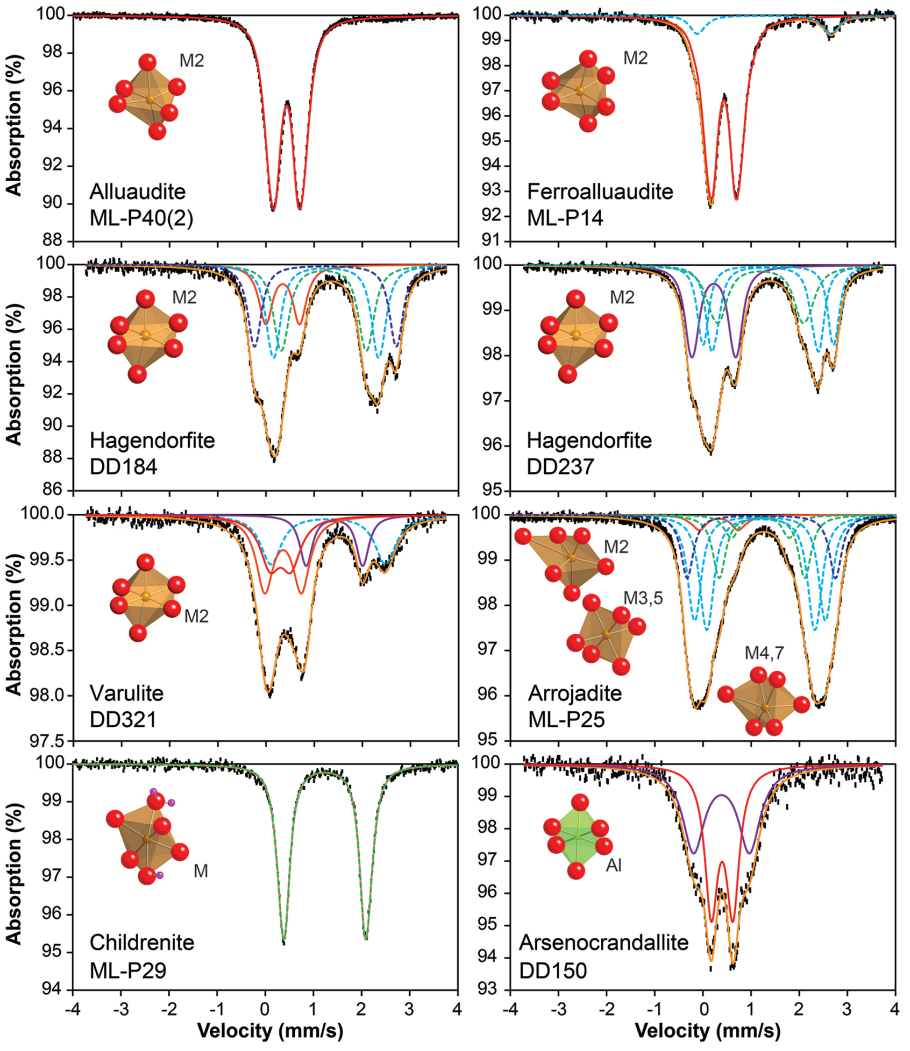

Figure 1. Mössbauer spectra and Fe coordination polyhedra created using CrystalMaker software and data from the American Mineralogist Crystal Structure Database, with citations to the crystal structure refinements from which the polyhedra were built following each mineral species name. Dashed lines representing Fe^{2+} in doublets with $\Delta = 1.43–1.99$ mm/s are shown in green, $\Delta = 2.00–2.85$ mm/s are light blue, $\Delta > 2.85$ mm/s are dark blue. Solid lines represent Fe^{3+} with $\Delta = 0.23–0.49$ mm/s in red, 0.5–0.79 mm/s in orange, and $\Delta > 0.80–1.55$ mm/s are purple. The fit envelope for each fit is shown as a thin solid line in gold. Alluaudite (Moore 1971a) ML-P40 and "ferroalluaudite" ML-P14 (Corbin et al. 1986) are predominantly Fe^{3+} in the M2 site. Two samples of hagendorfite, DD184 and DD237 (Redhammer et al. 2005), and varulite DD321 contain multiple doublets of Fe^{2+} and Fe^{3+}, but as with the other alluaudite group minerals, all Fe is assigned to the M2 site. There is no crystal structure refinement available for varulite, so the M2 polyhedron from Hagendorfite is illustrated there hypothetically. Arrojadite ML-P25 (Yakubovich et al. 1986) contains multiple Fe^{2+} doublets but their assignments to specific sites are unclear. Childrenite (Giuseppetti and Tadini 1984) ML-P29 has only one doublet corresponding to the Fe (M) site. In arsenocrandallite DD150 (Blount 1974), Fe^{3+} is substituting into the Al site, likely in polyhedra with two different combinations of next nearest neighbors. (Color online.)

Bobierrite. Bobierrite [$Mg_3(PO_4)_2 \cdot 8H_2O$] has a structure that is nearly identical to that of the vivianite group mineral species, and is discussed under that heading below.

Chalcosiderite. Chalcosiderite [$CuFe_6(PO_4)_4(OH)_8 \cdot 4H_2O$] is a member of the turquoise group; those structures are discussed under the turquoise heading below.

Childrenite group. The childrenite group of hydrous phosphates includes the species childrenite [$(FeMn)Al(PO_4)(OH)_2 \cdot H_2O$], eosphorite [$MnAl(PO_4)(OH)_2 \cdot H_2O$], ernstite [$(Mn_{1-x}Fe_x)Al(PO_4)(OH)_{2-x}O_x$], and sinkankasite [$H_2MnAl(PO_4)_2(OH)_2 \cdot 6H_2O$]. In childrenite, the Al octahedra [$AlO_2(OH)_3(H_2O)$] form a chain in the *c* direction, as do the more distorted, edge-sharing Fe octahedra [$(Fe,Mn)O_4(OH)H_2O$]. The chains are linked together by sharing H_2O and OH groups, respectively as well as PO_4 tetrahedra to form layers (Giuseppetti and Tadini 1984). The Mössbauer spectrum of childrenite was studied by Alves et al. (1980), who reported a single doublet with $\delta = 1.13$ mm/s (reported relative to sodium nitroprusside) and $\Delta = 1.73$ mm/s. In this study, sample ML-P29 (Fig. 1) also has only a single feature with $\delta = 1.24$ mm/s (relative to Fe) and $\Delta = 1.66$ mm/s.

Crandallite. The crystal structure of crandallite, $CaAl_3(OH)_6[PO_3(O_{½}(OH)_{½})]_3$, is analogous to that of alunite, with sheets made up of corner-sharing Al octahedra linked into trigonal and hexagonal rings (Blount 1974; Schwab et al. 1991; Goreaud and Raveau 1980), and quite similar to that of the phosphate mitridate (see below). Ca^{2+} cations (like K^{1+} in alunite) occupy the distorted cavities inside the 12-coordinated rings, close to four O^{2-} and four OH^- within the ring. If Fe^{3+} substitutes into this structure it likely occupies the Al octahedra.

In this study, sample DD150 (Fig. 1) is from the documented locality in Dolores Prospect, Pastrana, Mazarrón-Águilas, Murcia, Spain, but the sample was so small that XRD results could not be obtained. Its Mössbauer spectrum has two 6-coordinated Fe^{3+} doublets with parameters of $\delta = 0.39$ and 0.40 mm/s and $\Delta = 1.17$ and 0.46 mm/s, respectively. The larger doublet is indeed similar to what is observed in alunite, which is typically fit with a single doublet at ca. $\delta = 0.38$ mm/s and $\Delta = 1.20$ mm/s (Hrynkiewicz et al. 1965; Afanasev et al. 1974; Rothstein 2006; Kovács et al. 2008; and many others). So it is likely that this sample really is representative of the arsenocrandallite species, even without XRD corroboration.

Dufrénite. Five different minerals share the dufrénite structure and should have similar Mössbauer parameters: dufrénite $[Fe^{2+}Fe^{3+}_4(PO_4)_3(OH)_5 \cdot 2H_2O]$, natrodufrénite $[NaFe(Fe,Al)_5(PO_4)_4(OH)_6 \cdot 2H_2O]$, burangaite $[(Na,Ca)_2(Fe,Mg)_2Al_{10}(PO_4)_8(OH,O)_{12} \cdot 4H_2O]$, and matioliite $[NaMgAl_5(PO_4)_4(OH)_6 \cdot 2H_2O]$. The framework structure includes four octahedral sites; M1 and M3 share only corners, while M2 and M4 form face-sharing trimers of M4-M2-M4 octahedra. There are also two different types of PO_4 tetrahedra (Kampf et al. 2010). M1, M3, and M4 are smaller and thus favored by Al^{3+} and Fe^{3+}; the larger M2 site contains Fe^{2+}, Mn^{2+}, or Mg.

Sample ML-P34D in this study (Fig. 2) is the first published Mössbauer spectrum of dufrénite. It is solely Fe^{3+} in two different doublets with area ratios of 60:40: $\delta = 0.38$ and 0.38 mm/s and $\Delta = 0.54$ and 0.96 mm/s. This suggests that the doublet with the larger Δ represents Fe^{3+} in M1 and M3, with the smaller Δ doublet assigned to M4.

Fairfieldite. The crystal structure of fairfieldite $[Ca_2(Mn,Fe^{2+})(PO_4)_2 \cdot 2H_2O]$ was first described in successive papers by Zanazzi et al. (1969) and Fanfani et al. (1970). It is based upon chains of alternating $M^{2+}O_4(H_2O)_2$ octahedra and pairs of PO_4 tetrahedra (Huminicki and Hawthorne 2002), with the H_2O in a *trans* arrangement. The same geometry is found in the sulfate minerals yavapaiite $\{K[Fe^{3+}(SO_4)_2]\}$, kröhnkite $\{Na_2[Cu^{2+}(H_2O)_2(SO_4)_2]\}$, krausite $[KFe^{3+}(H_2O)_2(SO_4)_2]$, merwinite $[Ca_3Mg(SiO_4)_2]$, and brianite $[Na_2CaMg(PO_4)_2]$.

Sample DD171 (Fig. 2) in this study is the first known published Mössbauer spectrum of this phase. It has two Fe^{2+} doublets with $\delta = 1.06$ and 1.23 mm/s and $\Delta = 2.45$ and 2.94 mm/s, respectively. The remaining 25% of the total area is in a Fe^{3+} doublet with $\delta = 0.41$ mm/s and $\Delta = 0.94$ mm/s. Presumably, both Fe^{2+} and Fe^{3+} occupy the octahedral Fe site.

Farringtonite. Single-crystal studies of farringtonite, $[Mg_3(PO_4)_2]$ by Nord and Kierkegaard (1968) show that its structure is composed of MgO_5 square pyramidal 5-coordinated M1 sites, MgO_6 M2 octahedra, and PO_4 tetrahedra. The MgO_5 sites share edges to form Mg_2O_8 dimers (Huminicki and Hawthorne 2002) that link at the opposite ends to PO_4 and the M2 octahedra. There are two M1 sites for every one M2. The Mössbauer study by Nord and Ericsson (1985) presents spectra of synthetic farringtonite in solid solution with Zn. Using site occupancy arguments, they assign the doublet with $\delta = 1.10$–1.15 mm/s and $\Delta = 2.51$–2.94 mm/s to M1; the M2 site has $\delta = 1.25$–1.28 mm/s and $\Delta = 1.04$–1.97 mm/s.

Ferrisicklerite. The ferrisicklerite species, $Li(Fe,Mn)PO_4$, is one of three pairs of solid-solution series minerals with the same orthorhombic olivine-type structure (Huminicki and Hawthorne 2002): ferrisicklerite-sickerlite $[Li(Fe,Mn)PO_4$-$Li(Mn,Fe)PO_4]$, heterosite-purpurite ($FePO_4$-$MnPO_4$), and triphylite-lithiophilite ($LiFePO_4$-$LiMnPO_4$). Natrophilite ($NaMnPO_4$) and simferite $[Li(Mg,Fe,Mn)_2(PO_4)_2]$ also are similar. Ferrisicklerite can be considered an intermediate between triphylite and heterosite and sicklerite lies between lithiophyllite and purpurite (Huminicki and Hawthorne 2002). All the structures are composed of chains of edge-sharing LiO_6 or NaO_6 octahedra that run parallel to *a*. These are flanked by $(Fe^{2+}Mn^{2+}\square)O_6$ octahedra where $\square$ is a vacancy, many of which are vacant. Their Mössbauer spectra should be indistinguishable. Unfortunately, no sample of sickerlite was available for the current study, but other members of this group are well represented (see heterosite and triphylite). Literature data on ferrisicklerite support the presence of Fe only in the Mn2 site. Liu et al. (2005) report Mössbauer parameters of $\delta = 0.45$ and 1.23 mm/s and $\Delta = 0.90$ and 2.94 mm/s for Fe^{3+} and Fe^{2+}, respectively. Sample DD162-A (Fig. 2) in this study has two Fe^{3+} doublets ($\delta = 0.42$ and 0.44 mm/s, $\Delta = 0.47$ and 1.44 mm/s) and one Fe^{2+} doublet ($\delta = 1.22$ mm/s, $\Delta = 2.75$ mm/s).

Ferristrunzite. Ferristrunzite $[Fe^{3+}Fe^{3+}_2(PO_4)_2(OH)_3 \cdot 5(H_2O)]$ is described with the strunzite group, below.

Ferrolaueite. Ferrolaueite $[Fe^{2+}Fe^{3+}_2(PO_4)_2(OH)_2 \cdot 8(H_2O)]$ is discussed with laueite, below.

Frondelite. Frondelite $[MnFe_4(PO_4)_3(OH)_5]$ is described below as part of the discussion of the rockbridgeite group.

Giniite. The giniite $[Fe^{2+}Fe^{3+}_4(PO_4)_4(OH)_2 \cdot 2H_2O]$ structure refinement by Corbin et al. (1986) suggests an open framework structure with three different Fe octahedral sites. The basic structural unit is a set of edge-sharing octahedra with Fe3 (three corners shared with PO_4) in the center and Fe1 (FeO_6, with four corners shared with PO_4) and Fe2 (two corners shared with PO_4) at opposite edges. Of these sites, Fe3 is the most distorted, and the Fe1 and Fe2 sites are quite similar.

Rouzies et al. (1994) report results on a synthetic giniite sample with four Mössbauer doublets, two for each valence state. Fe^{3+} has parameters of $\delta = 0.42$ and 0.44 mm/s and $\Delta = 1.05$ and 0.41 mm/s. Fe^{2+} features with $\delta = 1.15$ and 1.24 mm/s and $\Delta = 2.61$ and 2.37 mm/s are described. The doublets for Fe^{2+} and Fe^{3+} with larger Δ have roughly twice the area of the smaller-Δ features. Rouzies et al. (1994) do not assign their doublets to specific sites. However, based on the Corbin et al. (1986) refinement and the doublet areas, the features with larger Δ for both Fe^{2+} and Fe^{3+} can now be assigned to a combination of Fe1 and Fe2, and the smaller doublets to Fe3.

Gladiusite. Gladiusite $[Fe^{3+}(Fe^{2+},Mg)_4(PO_4)(OH)_{11}H_2O]$ was first described by Liferovich et al. (2000) based upon a sample from the Kovdor complex in the Kola Peninsula, Russia. There are six octahedral M sites: M1, M3, and M5 contain only Fe^{3+}

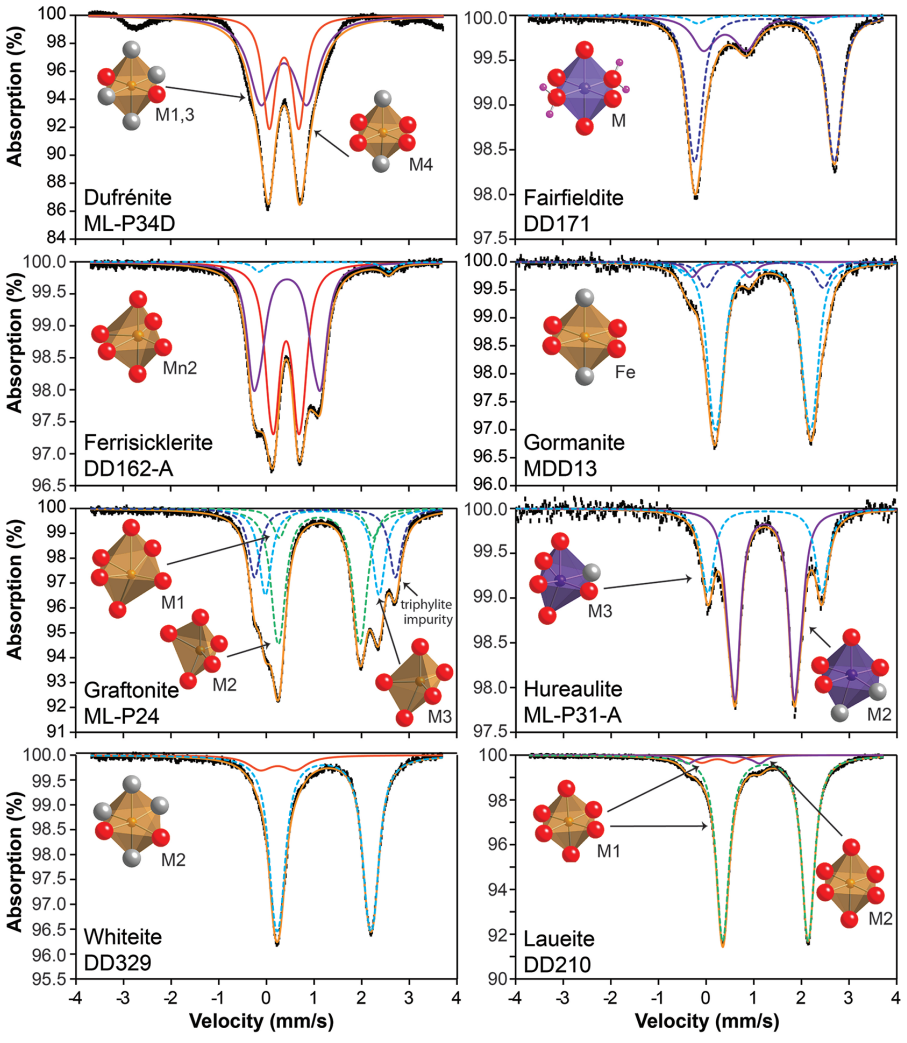

FIGURE 2. Mössbauer spectra and Fe coordination polyhedra, with citations to the crystal structure refinements from which the polyhedra were built. In dufrénite (Moore 1970), the Fe^{3+} doublet with the larger Δ represents Fe^{3+} in M1 and M3, with the smaller Δ doublet assigned to M4. In fairfieldite (Herwig and Hawthorne 2006) DD171, all three doublets represent occupancy in the single Fe site. Ferrisicklerite (Alberti 1976) DD162-A contains Fe^{3+} only in the Mn2 site. Gormanite (Le Bail et al. 2003) MDD13 is dominated by a Fe^{2+} doublet representing occupancy in the Fe site. Graftonite (Nord and Ericsson 1982) ML-P24 has Fe^{2+} in three different sites as indicated. Hureaulite (Moore and Araki 1973) ML-P31-A has Fe^{2+} only in the M2 and M3 sites. Whiteite (Gray et al. 2010) DD329 is the first published Mössbauer spectrum for this species, and both Fe^{3+} and Fe^{2+} are assigned to the M2 site. Laueite (Moore 1965) DD210 shows Fe^{2+} and Fe^{3+} occupancy of the M1 site, with a small Fe^{3+} doublet representing M2. (Color online.)

and Fe^{2+}, M2 and M4 are occupied by Fe^{3+}, Fe^{2+}, and Mg (as well as Mn in M2), and M6 has Fe^{2+} and Mg. M1 and M2 octahedra alternate and share *trans* edges to form a chain in the *c* direction. The chains also share edges with like M1/M2 chains to form "ribbons." M3/M4 and M5/M6 also form analogous ribbons that link through corner-sharing and phosphate groups.

Sokolova et al. (2001) detail the structure and Mössbauer spectra of that sample. They model one Fe^{3+} and two Fe^{2+} doublets (designated FeI and FeII) with parameters of $\delta = 0.33$, 1.11, and 1.19 mm/s and $\Delta = 0.45$, 2.45, and 1.39 mm/s, respectively. The narrow width of the FeI doublet suggests that it represents a single site or a group of highly uniform sites, while the larger width of FeII implies contributions from multiple sites with varying geometries. However, given the complex distribution of Fe among sites in this structure, it is not possible to assign the Mössbauer doublets to specific sites on the basis of this single sample.

Gormanite. Gormanite $[Fe_3^{2+}Al_4(PO_4)_4(OH)_6{\cdot}2H_2O]$ forms a solid-solution series with souzalite $[Mg_3Al_4(PO_4)_4(OH)_6{\cdot}2H_2O]$, and was first described by Sturman et al. (1981). Le Bail et al. (2003) refined the structure using synchrotron power diffraction data, and observed three distinct Al sites, one Mg site, and one Fe site. Sturman et al. (1981) reported wet chemical data that supported the presence of Fe^{2+} only in gormanite. However, optical spectroscopy (Chandrasekhar et al. 2003) reveals the presence of both Fe^{2+} and Fe^{3+} in a sample from the Yukon Territory.

In this study, the Mössbauer spectrum of sample MDD13

(also from the Yukon Territory) has four doublets (Fig. 2), three representing Fe^{2+} (δ = 1.19, 1.22, and 1.04 mm/s and Δ = 2.02, 2.54, and 2.98 mm/s, respectively) and one Fe^{3+} (δ = 0.31 mm/s and Δ = 1.22 mm/s). Of the total Fe, 77% is in the Fe^{2+} site with the lowest Δ, so that likely represents the Fe site in the structure. The other doublets, which are relatively small, cannot be assigned.

Graftonite. The crystal structure of graftonite [$Fe_3^{2+}(PO_4)_2$] was determined by Calvo (1968). The M1 is 6- or 7-coordinated and can accept considerable Ca^{2+} (Wise et al. 1990). Smaller divalent cations (Fe, Mn, Mg) occupy a 5-coordinated site (M2) and a 5- or 6-coordinated site (M3). The smaller polyhedra form edge-sharing chains parallel to the *c* axis while the larger sites occur in edge-sharing pairs that also share corners to make sheets in the *b*-*c* plane.

Nord and Ericsson (1982) used Mössbauer spectroscopy to study the cation distribution in nine synthetic graftonite samples covering the solid solution between graftonite and beusite [$Mn_3^{2+}(PO_4)_2$]. Their results show three doublets. At 295 K, Fe^{2+} in the M1 site has δ = 1.13–1.22 mm/s and Δ = 1.93–2.10 mm/s. Fe^{2+} in the M2 site has δ = 1.10–1.12 mm/s and Δ = 1.55–1.61 mm/s. Fe^{2+} in the M3 site has δ = 1.16–1.17 mm/s and Δ = 2.35–2.38 mm/s. In the current study, sample ML-P24 (Fig. 2) was fitted with four doublets, one of which (δ = 1.23 mm/s and Δ = 2.99 mm/s) is a triphylite impurity. Based on the previous work, the doublet with δ = 1.12 mm/s and Δ = 1.59 mm/s represents M2, the doublet at δ = 1.16 mm/s and Δ = 2.38 mm/s represents M3, and the feature at δ = 1.35 mm/s and Δ = 2.19 mm/s is the M1 site.

Hagendorfite. Hagendorfite [$(Na,Ca)MnFe_2(PO_4)_3$] is discussed with the other alluaudite group phases under the alluaudite heading above.

Heterosite. The structure of heterosite, ($FePO_4$), which occurs in solid solution with purpurite ($FePO_4$-$MnPO_4$) is discussed in detail under the listing above for ferrisicklerite. Unfortunately, no sample of heterosite was available for the current study, but other workers have characterized its Mössbauer characteristics. Aldon et al. (2010) finds ~300 K parameters for Fe^{3+} in heterosite of δ = 0.41 mm/s and Δ = 1.54 mm/s. Andersson et al. (2000) reports nearly identical values for δ = 0.42 mm/s and Δ = 1.52 mm/s for Fe^{3+} in heterosite. Fehr et al. (2010) finds two Fe^{3+} doublets in heterosite with slightly lower δ (0.36 and 0.33 mm/s) and Δ = 1.63 and 0.69 mm/s values that average to those reported by the previous workers. They could find no explanation for the presence of the two doublets.

Hureaulite. Hureaulite [$Mn_5^{2+}(H_2O)_4(PO_4H)_2(PO_4)_2$] is based upon five edge-sharing Mn^{2+}-bearing octahedra that share corners to create a sheet of octahedra parallel to (001) (Huminicki and Hawthorne 2002). There is only one M1 site and two each of M2 and M3. The groups of five linked octahedra also link through PO_4^{3-} tetrahedra to form slabs parallel to (001).

Mössbauer spectroscopy of hureaulite has been thoroughly studied by two different groups. Nomura and Ujihira (1982) studied seven samples in the Mn-Fe^{2+} solid-solution series. They assigned the most intense peak with the largest Δ to M2, with parameters of δ = 1.24–1.26 mm/s and Δ = 2.47–2.52 mm/s. The least intense doublet was assigned to M1, with δ = 1.23–1.25 mm/s and Δ = 1.48–1.70 mm/s, and the remaining doublet to M3, with δ = 1.23–1.24 mm/s and Δ = 1.20–1.32 mm/s.

Bustamante et al. (2005) report both a structure refinement and Mössbauer data for a synthetic sample. They calculated that the quadratic elongation λ is 1.0242, 1.0179, and 1.0617 for the M1, M2, and M3 sites. Bond angle variances (σ^2) of those sites are 81.7, 59.2, and 187.3. Angular variance (σ) was calculated using the expression:

$$\sigma = \sum_{i=1}^{n} \left(\theta_i - \theta_{avg}\right)^2 / \left(n-1\right) \quad (2)$$

where θ_i is the measured angle in the crystal structure (there are n = 12 angles in a six-coordinated site) and θ_{avg} is the bond angle for a perfect octahedron (all angles are 90°). In other words, the M3 site is significantly more distorted because its bond angles show the most variation. This information, along with peak areas, then informs the assignment of Mössbauer doublets because Δ, in particular, tends to increase with increasing polyhedral distortion. So Bustamante et al. (2005) revised the assignments of the three doublets from those of Nomura and Ujihira (1982) suggesting that their doublet with Δ = 1.29 is M2, Δ = 1.38 is M1, and Δ = 2.53 mm/s is M3.

In this study, hureaulite sample ML-P31-A (Fig. 2) contains solely Fe^{2+} but only in two different doublets with δ = 1.22 and 1.23 mm/s, and Δ = 1.23 and 2.37 mm/s, respectively, for M2 and M3 occupancy. XRD analysis suggested that this sample has a pentamanganese impurity but it may have a closely related structure. This sample could not be fit with three doublets, suggesting that its composition may be more Mn-rich than the synthetic samples previously studied.

Jahnsite. Jahnsite [$CaMnFe_2Fe_2(PO_4)_4(OH)_2 \cdot 8(H_2O)$] contains chains of Fe^{3+}-OH-Fe^{3+} corner-sharing octahedra parallel to the *b*-axis that are also linked to $[PO_4]^{3-}$ tetrahedra. Other chains that alternate Ca-O and Mn^{2+}-O octahedra also run in the *b* direction forming slabs with the Fe chains. The slabs are bridged by $[PO_4]^{3-}$ tetrahedra that link to MgO octahedra (Moore 1974a). Jahnsite forms a solid solution and is isostructural with whiteite, $(Mn^{2+},Ca)(Fe^{2+},Mn^{2+})Mg_2Al_2(PO_4)_4(OH)_2 \cdot 8(H_2O)$ (Moore and Ito 1978). It is also related to both the childrenite-eosphorite and laueite-pseudolaueite structures.

Although no jahnsite was included in this study, Hochleitner and Fehr (2010) reported the Mössbauer parameters for the Fe^{3+} end-member, keckite, for four Fe^{3+} doublets and one Fe^{2+} doublet as follows: δ = 0.41–0.51 mm/s and Δ = 0.81–0.86 mm/s for Fe^{3+} in the M1 site; δ = 0.37–0.48 mm/s and Δ = 1.22–1.26 mm/s for Fe^{3+} in the M2 site; δ = 0.39–0.50 mm/s and Δ = 0.30–0.54 mm/s for Fe^{3+} in the M1 site; δ = 0.41 mm/s and Δ = 0.55 mm/s for Fe^{3+} in the M2 site. The first published spectrum of whiteite DD329 (Fig. 2) has Mössbauer parameters of δ = 0.24 and 1.21 mm/s and Δ = 0.74 and 2.12 mm/s for Fe^{3+} and Fe^{2+}, respectively. Based on the fact that the Mn site is very distorted (λ = 1.0745) compared to the M1 site [λ = 1.0076 and 1.0016 from Grey et al. (2010)] and the parameters are consistent with relatively symmetrical sites, both Fe^{3+} and Fe^{2+} are assigned to the M2 site. The very low value for δ of Fe^{3+}, which might be assigned to a 4-coordinated site in a typical silicate phase, must in this case be assigned to an octahedral site. Perhaps the low-δ value arises from a highly distorted steric 6-coordinated environment in which four O atoms are significantly closer to the cation than the other two.

Kulanite. Kulanite [$BaFe_{1.3}^{2+}Mn_{0.6}^{2+}Mg_{0.2}Al_2(PO_4)_3(OH)_3$] is the

only member of the bjarebyite group of minerals obtained for this (or any other) Mössbauer study. As described by Cooper and Hawthorne (1994), the kulanite structure contains chains of edge- and corner-sharing Al (M2) octahedra along the *y* axis direction that are cross-linked through Fe (M1) octahedra as well as 10-coordinated Ba (X) polyhedra and PO_4 tetrahedra. They refined Al and Fe^{3+} in the M1 site and Fe^{2+}, Mn^{2+}, and Mg in the M2 site.

This study includes two different kulanite samples, MDD16 and ML-P32 (Fig. 3), from the type locality at Rapid Creek in the Yukon Territories of Canada for which the first Mössbauer spectra are reported. Parameters are somewhat similar for both samples. Each contains three Fe^{2+} different doublets with δ = 1.20–1.26 mm/s and Δ = 1.35–1.95 mm/s that should all be assigned to M2 per Cooper and Hawthorne (1994). Fe^{3+} in these samples is represented by a doublet with δ = 0.36–0.39 mm/s and Δ = 0.47–0.56 mm/s, presumably in the M1 site.

Landesite. Landesite $[(Mn,Mg)_9Fe_3^{3+}(PO_4)_8(OH)_3 \cdot 9H_2O]$ is a member of the phosphoferrite group and is described under that section below.

Laueite. The laueite structure is based on an infinite chain of corner-sharing, Fe^{3+}-bearing octahedra parallel to the *c* axis. The chains cross-link via PO_4^{3-} tetrahedra to isolated octahedra containing Mn^{2+} (Moore 1965). This structure is analogous to that of vivianite, in which the Fe^{3+}-bearing octahedra are edge-sharing rather than corner-sharing. In laueite and ferrolaueite, there are three distinct transition metal cation sites, M1 corresponds to Mn^{2+} or Fe^{2+} in the $[Mn^{2+}(H_2O)_4(PO_4)_2]$

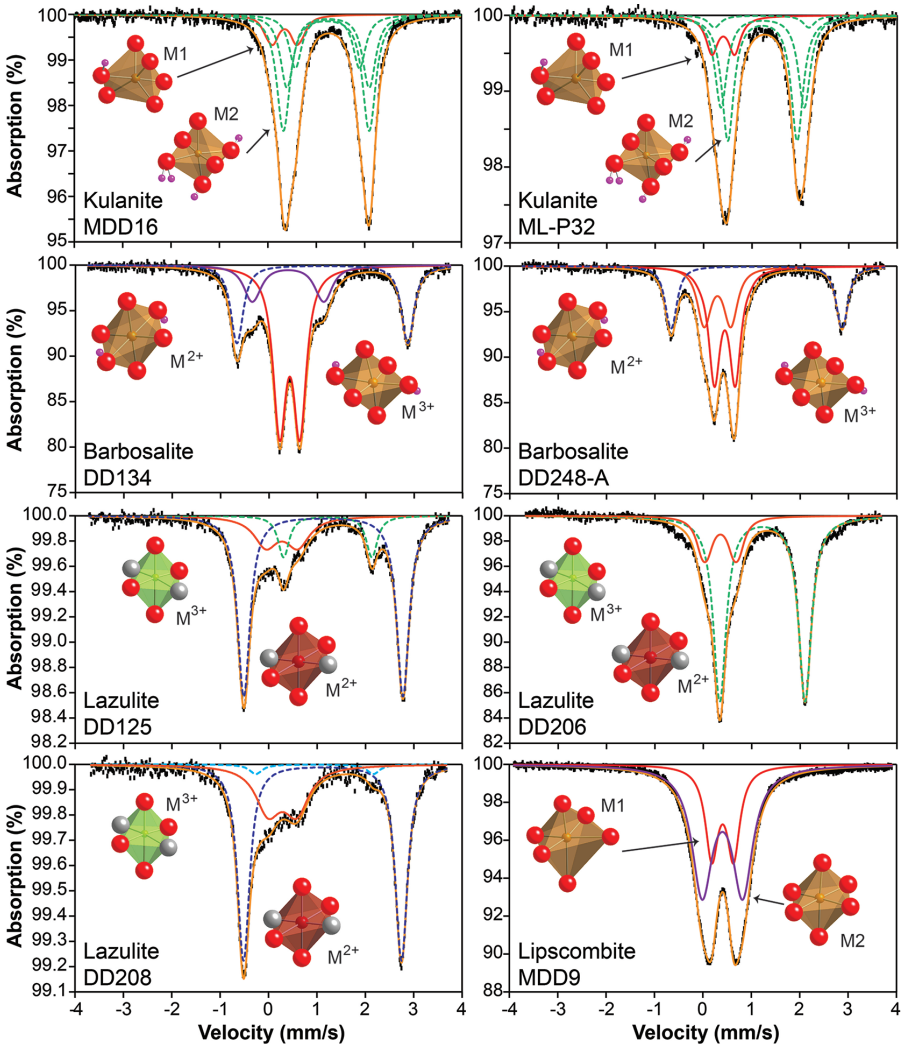

FIGURE 3. Mössbauer spectra and Fe coordination polyhedra, with conventions as in Figure 1. Kulanites (Cooper and Hawthorne 1994) MDD16 and ML-P32 are both dominated by doublets from Fe^{2+} in varying permutations of the M2 sites, likely caused by different next nearest neighbors. Five lazulite group minerals were studied here. Barbosalites (Redhammer et al. 2000) DD134 and DD248-A were modeled with three doublets: two for Fe^{3+} in the trivalent M^{3+} site and one for Fe^{2+} in the divalent octahedron. Three lazulites (Lindberg and Christ 1959), DD125, DD206, and DD208, also contained a combination of both valence states and were assigned as for barbosalite. Lipscomite (Vencato et al. 1989) MDD9 has only two doublets, both Fe^{3+}, occupying the M1 and M2 sites. (Color online.)

octahedron, M2 to the $[Fe^{3+}(OH)_2(PO_4)_4]$ octahedron, and M3 to the $[Fe^{3+}(H_2O)_2(OH)_2(PO_4)_2]$ octahedron. The M1 octahedron does not link to another octahedron, but M2 and M3 link to form corner-sharing octahedral chains through bridging $(OH)^-$ ligands. As a result its formula can be expressed as $(Mn^{2+},Fe^{2+})(H_2O)_4Fe^{3+}_2(H_2O)_2(OH)_2(PO_4)_2 \cdot 2H_2O$.

The Mössbauer spectrum of ferrolaueite was published by Segeler et al. (2012), who describe ferrolaueite from Monmouth County, New Jersey, that was rerun and refit in this study. Its spectrum shows one Fe^{2+} doublet in M1 (δ = 1.25 mm/s and Δ = 3.13 mm/s) and two Fe^{3+} doublets with nearly identical areas at δ = 0.42 and 0.38 mm/s and Δ = 1.27 and 0.71 mm/s, respectively, assigned to some combination of the M2 and M3 sites. In this study, laueite DD210 (Fig. 2) shows parameters similar to the ferrolaueite just discussed (Table 2[1]).

Lazulite group. The lazulite mineral group includes the lazulite species $[MgAl_2(PO_4)_2(OH)_2]$, scorzalite $[(Fe^{2+},Mg)Al_2(PO_4)_2(OH)_2]$, barbosalite $[Fe^{2+}Fe^{3+}_2(PO_4)_2(OH)_2]$, and hentschelite $[Cu^{2+}Fe^{3+}_2(PO_4)_2(OH)_2]$. All have very similar structures (Lindberg and Christ 1959) so they will be discussed together here. These minerals have face-sharing $Fe^{3+}_2Fe^{2+}O_8(OH)_4$ octahedral trimers forming chains along the *c*-axis with every fourth octahedron vacant (Redhammer et al. 2000). The resultant triplets were designated as *h*-clusters by Moore (1970) and are also found in many other phosphate minerals. Lipscombite is a related structure (see below) in which the vacancy is disordered among the face-sharing octahedra. Between those chains are corner-sharing $Fe^{3+}O_4(OH)_2$ octahedra that share two corners with bridging phosphate tetrahedra; these run parallel to the [101] direction.

The Mössbauer parameters of these related minerals have been well-studied by previous workers, including Mattievich et al. (1979), Amthauer and Rossman (1984), Rouzies and Millet (1993a), Millet et al. (1995), Schmid-Beurmann et al. (1997), Redhammer et al. (2000), and Grodzicki et al. (2003). All of them report parameters covering the same ranges of δ = 0.31–0.43 mm/s and Δ = 0.39–0.71 mm/s for Fe^{3+} and δ = 1.04–1.17 mm/s and Δ = 2.08–3.54 mm/s for Fe^{2+}. Up to five highly overlapping doublets are typically fit to the spectra of these minerals. Millet et al. (1995) also report a mixed valence site in lipscombite, with δ = 0.70 mm/s and Δ = 1.97 mm/s, that is not present in barbosalite despite the close distances between the face-sharing octahedra.

Lazulite and scorzalite were studied by Amthauer and Rossman (1984), Grodzicki et al. (2003), and Schmid-Beurmann et al. (1997). These two minerals form a solid solution with a miscibility gap between 30 and 60 mol% (Duggan et al. 1990) so their Mössbauer parameters are identical. Amthauer and Rossman (1984) studied a natural lazulite with δ = 1.12 mm/s and Δ = 3.32 mm/s. Schmid-Beurmann et al. (1997) report values for synthetic scorzalite as δ = 1.14 mm/s and Δ = 3.22 mm/s and δ = 0.40 and 1.13 mm/s and Δ = 0.47 and 3.30 mm/s for natural samples. In this study, the two barbosalite samples, DD134 and DD248-A (Fig. 3), each was modeled with three doublets: two for Fe^{3+} and one for Fe^{2+}, with parameters within the ranges of previous workers with one exception. Sample DD134 contains a Fe^{3+} doublet with a slightly larger Δ value of 1.21 mm/s.

Lazulite samples (DD125, DD206, and DD208; Fig. 3) in the current study were similar. All contain Fe^{3+} (δ = 0.27–0.35 mm/s and Δ = 0.64–0.77 mm/s) in the smaller Al/Fe^{3+} site and Fe^{2+} in the M^{2+} site (δ = 1.12–1.22 mm/s and Δ = 1.76–3.29 mm/s). In summary, the lazulite group minerals share both structures and indistinguishable Mössbauer parameters.

Leucophosphite. Leucophosphite $[KFe^{3+}_2(PO_4)_2(OH)\cdot 2H_2O)]$ was first described by Simpson (1931–1932), Axelrod et al. (1952), Lindberg (1957), and Simmons (1964). It forms in sedimentary rocks associated with bird guano and in pegmatites. Its structure was refined by Moore (1972a), and consists of two octahedral sites in an edge-sharing dimer (Fe2), which links by corner-sharing to two other Fe1 octahdra by PO_4 tetrahedra, forming a five-membered cluster in a structure similar to that of the sulfate mineral amarantite $[Fe_2(SO_4)_4O\cdot 7H_2O]$. K cations occupy channels between clusters of octahedra. The Mössbauer parameters of synthetic leucophosphite were reported by de Resende et al. (2008). They observed two doublets with δ = 0.41 and 0.41 mm/s and Δ = 0.84 (tentatively Fe1) and 0.55 (Fe2), respectively.

Lipscombite. The structure of lipscombite $[(Fe^{2+},Mn)Fe^{3+}_2(PO_4)_2(OH)_2]$ is closely related to mineral species in the lazulite group described above. All these minerals have chains of corner-sharing $Fe^{2+}O_4(OH)_2$ octahedra that share two corners with phosphate tetrahedra and run parallel to the [101] direction. What distinguishes lazulite from lipscombite is the occupancy of the other chains, which are face-sharing Fe^{3+} and Fe^{2+} octahedra running along the *x* direction. Every fourth octahedron is vacant in barbosalite (Redhammer et al. 2000), but in lipscombite the location of the vacancy is disordered, with the Fe3 site fully occupied by Fe^{3+} and the Fe1 and Fe2 sites partially occupied by Fe^{2+} (Rouzies and Millet 1993a; Rouzies et al. 1995). Thus the Mössbauer spectra of lipscombite typically include up to two Fe^{3+} and two Fe^{2+} doublets (Vochten and De Grave 1981; Vochten et al. 1983; Rouzies et al. 1993a, 1995; Yakubovich et al. 2006; Chukanov et al. 2007). For example, Vochten and De Grave (1981) give parameters of δ = 0.44 and 0.45 mm/s and Δ = 0.32 and 0.51 mm/s for Fe^{3+} in the M1 and M2 sites, respectively, and δ = 1.11 and 1.17 mm/s and Δ = 3.54 and 2.53 mm/s for Fe^{2+} in the M1 and M2 sites, again, respectively. Sample MDD9 from this study (Fig. 3) was fit to only two doublets, both Fe^{3+}, with δ = 0.41 and 0.40 mm/s and Δ = 0.44 and 0.85 mm/s, respectively, likely occupying the M1 and M2 sites.

Lithiophilite. Lithiophilite, $LiMnPO_4$, forms a solid solution with triphylite ($LiMnPO_4$-$LiFePO_4$), and has quite similar Mössbauer parameters in the sample studied here, which is a ferrolithophilite. It structure is based upon two chains parallel to the *c* axis: one consisting of M1 otahedra occupied by Li^{1+} cations and vacancies, and the other of M2 sites containing Fe and Mn (Hatert et al. 2012). The spectrum of DD135 (Fig. 4) includes one small (6% of the peak area) Fe^{3+} peak in the M2 site, like those seen in purpurite (see discussion below), with δ = 0.35 mm/s and Δ = 0.62 mm/s. However, the spectrum is dominated by Fe^{2+} in a doublet (94% of the total peak area) also in M2. Its parameters are δ = 1.24 mm/s and Δ = 2.97 mm/s.

Lomonosovite group. The lomonosovite $[Na_5Ti_2O_2(Si_2O_7)(PO_4)]$ group of minerals includes eight alkali-rich Ti-bearing silicates, murmanite, epistolite, innelite, vuonnemite, β-lomonosovite, quadruphite, polyphite, and sobolevite. Lomonosovite was described by Khalilov et al. (1965) and sub-

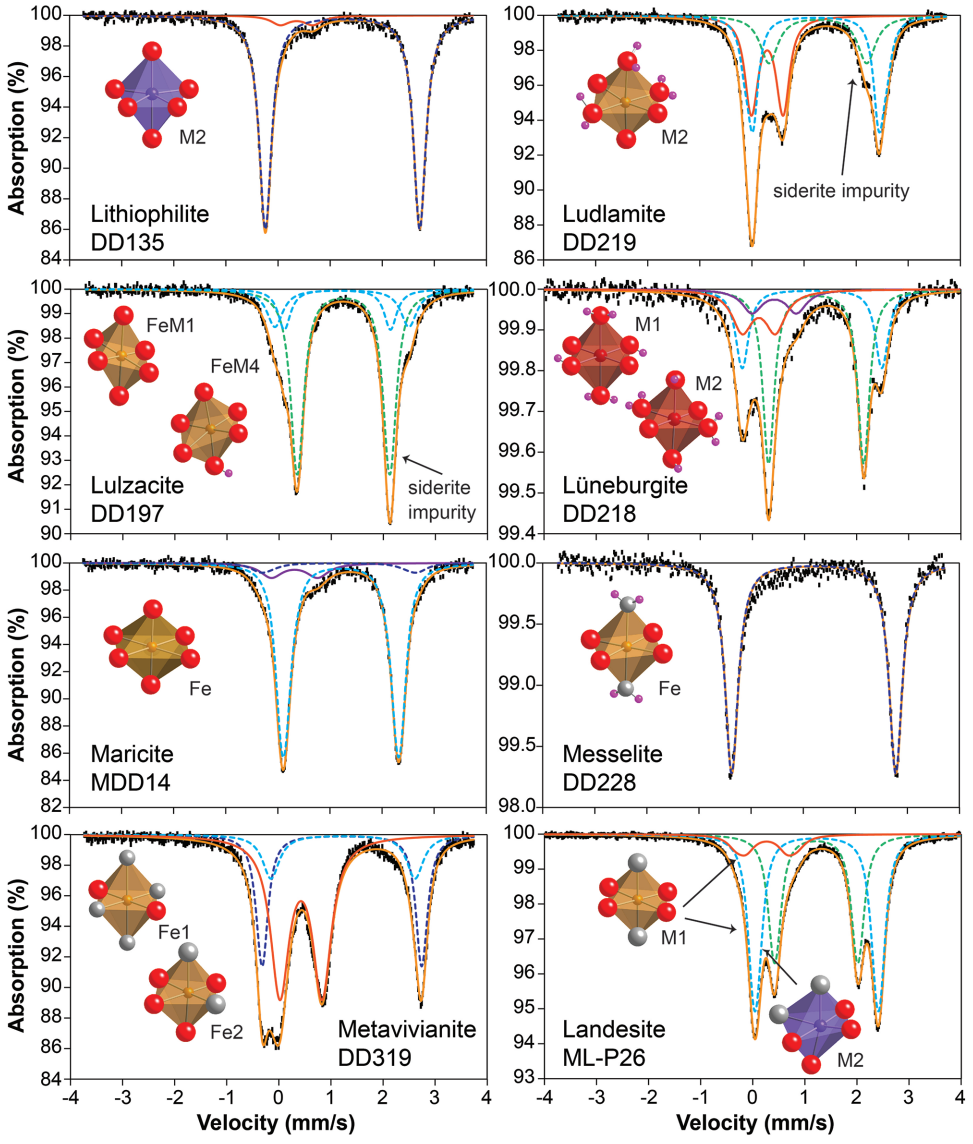

FIGURE 4. Mössbauer spectra and Fe coordination polyhedra, with conventions as in Figure 1. Lithiophilite (Losey et al. 2004) DD135 contains a small amount of Fe^{3+} but its spectrum is dominated by Fe^{2+}; both are in the M2 site. The spectrum of ludlamite (Abrahams and Bernstein 1966) DD219 has a small siderite impurity as well as doublets from Fe^{2+} and Fe^{3+} assigned to the M2 site. Lulzacite (Léone et al. 2000) DD197, although dominated by siderite, has two Fe^{2+} doublets assigned to M1 and M4. Lüneburgite (Sen Gupta et al. 1991) DD218 has a distinct Fe^{3+} doublet with δ more typical of tetrahedral Fe^{3+}, but are more reasonably attributed to M1 and M2. Maricite (Le Page and Donnay 1977) MDD14 contains both Fe^{2+} and Fe^{3+} in the Fe site. In messelite (Fleck and Kolitsch 2003) DD228, Fe is only in the Fe site. In metavivianite (Chukanov et al. 2012) DD319, Fe^{2+} is distributed between two octahedral sites and Fe^{3+} occupies only one site, though it is unclear if it is Fe1 or Fe2. In landesite (Moore et al. 1980) ML-P26, three doublets represent Fe^{3+} in Fe1, Fe^{2+} in M2, and Fe^{2+} in M1, respectively. (Color online.)

sequent workers (Khalilov and Makarov 1966; Rastsvetaeva 1971; Rastsvetaeva et al. 1971; Belov et al. 1977; Sokolova et al. 1987; Ercit et al. 1998). All the structures are based upon nets of TiO_6 octahedra and Si_2O_7 groups with Na atoms in the net voids (Massa et al. 2000). Only a single Mössbauer spectrum of any of the minerals in this group has been published. Cámara et al. (2008) fitted two doublets, one for Fe^{2+} and one for Fe^{3+}, to a Fersman Mineralogical Museum sample of lomonosovite. Parameters were δ = 0.31 and 1.15 mm/s and Δ = 0.70 and 2.54 mm/s. Presumably both occupy the Fe site in the structure.

Ludlamite. Ludlamite $[Fe_3^{2+}(PO_4)_2(H_2O)_4]$ has been found at many localities (e.g., Glass and Vhay 1949; Wolfe 1949). Its crystal structure was described by Ito and Mori (1951), Abrahams (1966), Abrahams and Bernstein (1966), and Forsyth et al. (1990) among many others. The structure contains Fe in two different octahedral sites, Fe1 with four PO_4 and two H_2O and Fe2 with three PO_4 and three H_2O.

Mössbauer spectra of ludlamite were published by Chandra

and Hoy (1967) and Mattievich and Danon (1977). The former study focused on magnetic properties, but Mattievich and Danon (1977) analyzed a natural and a synthetic sample at room temperature. Each was a single doublet with $\delta = 1.18$ mm/s and $\Delta = 2.41$ mm/s, the same parameters for both samples. In this study, sample DD219 (Fig. 4) also has the same doublet at $\delta = 1.23$ mm/s and $\Delta = 2.42$ mm/s, along with a Fe^{3+} doublet with $\delta = 0.29$ mm/s and $\Delta = 0.65$ mm/s. A third doublet ($\delta = 1.27$ mm/s and $\Delta = 1.87$ mm/s) likely shows Fe^{2+} in the siderite impurity. Paster et al. (1990) also reported 4 K parameters of $\delta = 1.34$ mm/s and $\Delta = 2.56$ mm/s for Fe1 and $\delta = 1.34$ mm/s and $\Delta = 2.37$ mm/s for Fe2.

Lulzacite. Lulzacite $[Sr_2Fe^{2+}(Fe^{2+},Mg)_2Al_4(PO_4)_4(OH)_{10}]$ was first described by Moëlo et al. (2000) and Léone et al. (2000) to contain five octahedral sites, one Fe^{2+} (M4), one containing Fe^{2+} and Mg (M1), and three sites occupied by Al^{3+} (M2, M3, and M5). Trimers of Al-(Fe,Mg)-Al form alternating rows, and chains of Fe and Al sites run parallel to *a*. The fifth type of octahedron (Al) cross-connects the rows and chains.

Sample DD197 (Fig. 4) from the type locality at Bois-de-la-Roche Quarry, Saint-Aubin-des-Châteaux, Loire-Atlantique, France, was studied here; it is important to note that some siderite remains in the sample despite careful handpicking. Its Mössbauer spectrum consists of three octahedral Fe^{2+} doublets with $\delta = 1.24$, 1.12, and 1.21 mm/s and $\Delta = 1.78$, 2.03, and 2.58 mm/s, respectively. The first of these is likely siderite (see ludlamite), but the other two represent the two Fe sites (M1 and M4) in lulzacite. Because the M1 site is slightly more distorted (Léone et al. 2000), it likely corresponds to the site with higher Δ.

Lüneburgite. The crystal structure of lüneburgite $\{Mg_3(H_2O)_6[B_2(OH)_6(PO_4)_2]\}$ was determined by Sen Gupta et al. (1991) from a sample from Bela Stenam Serbiam Yugoslavia and described later by Ewald et al. (2005). It consists of two types of Mg octahedra, M1 and M2, along with B and P tetrahedra that are ordered in a tetrahedral pair (Sen Gupta et al. 1991). The fundamental structural unit is a sheet of M2-B-P, with M1 sites in between. The M1 octahedra are more distorted, with $\lambda = 1.005$ and $\sigma^2 = 3.9$. By comparison, $\lambda = 1.002$ and $\sigma^2 = 6.5$ for the M2 site.

Sample DD218 (Fig. 4) studied here is from the same locality analyzed by Sen Gupta et al. (1991). It was modeled with four doublets: two containing Fe^{2+} with $\delta = 1.14$ and 1.22 mm/s and $\Delta = 2.63$ and 1.85 mm/s and two containing Fe^{3+} with $\delta = 0.42$ and 0.12 mm/s and $\Delta = 0.85$ and 0.63 mm/s. The Fe^{2+} doublets are easily assigned to M1 for the $\Delta = 2.63$ mm/s doublet and M2 for the $\Delta = 1.85$ mm/s feature. It is more difficult to assign the Fe^{3+} doublets. The lower δ doublet is typical of Fe^{3+} in tetrahedral coordination, but that seems unlikely in this mineral. The other Fe^{3+} doublet could be in either of the M sites.

Maricite. The structure of maricite ($NaFe^{2+}PO_4$) was described by Le Page and Donnay (1977) and Bridson et al. (1998) as a framework of distorted $Fe^{2+}O_6$ octahedra and PO_4 tetrahedra around 10-coordinated Na^{1+} cations. In this study, sample MDD14 (Fig. 4) comes from the same Big Fish River locality studied by Le Page and Donnay (1977); it is known from XRD to contain a small fraction of vivianite impurity. Its Mössbauer spectrum contains a doublet with $\delta = 0.31$ mm/s and $\Delta = 0.90$ mm/s for Fe^{3+} and two doublets for Fe^{2+}: $\delta = 1.17$ and 1.21 mm/s and $\Delta = 3.01$ and 2.21 mm/s; all of these must occupy the Fe site. These doublets are nearly identical to those found for vivianite (see description below and Table 2[1]). This suggests that the environments around the Fe polyhedra in these samples are quite similar.

Messelite. The crystal structure of messelite $[Ca_2(Fe^{2+},Mn)(PO_4)_2\cdot 2H_2O]$ from the Messel oil shale near Darmstadt, Germany, was refined by Fleck and Kolitsch (2003). It consists of a densely packed framework of 8-coordinated Ca^{2+}, 6-coordinated Fe^{2+}, and PO_4 tetrahedra. The Fe octahedra have two corners that share with H_2O and four that share with PO_4 tetrahedra. Five corners of the Ca polyhedra are shared with PO_4. In this study, a Mössbauer spectrum of messelite DD228 (Fig. 4), from the same locality was analyzed for the first time. It consists of a single doublet with $\delta = 1.20$ mm/s and $\Delta = 3.17$ mm/s, presumably in the Fe site.

Metavivianite. Rastsvetaeva et al. (2012) presented the most complete refinement and characterization of the structure of metavivianite $[Fe^{2+}_{3-x}Fe^{3+}_x(PO_4)_2(OH)_x\cdot(8–x)H_2O]$ with an update by Chukanov et al. (2012). The structure has sheets of alternating edge-sharing Fe2 octahedra that share apices and alternate with Fe1 octahedra. Fe1 is occupied by Fe^{2+}, and Fe^{3+}, Mg, and remaining Fe^{2+} occupy the smaller Fe2 site. A metavivianite was included in the study of Dormann and Poullen (1980), who fitted six doublets to its spectrum but interpreted them as different distributions on the Fe1 and Fe2 sites only. Five-doublet fits of a different metavivianite by Rodgers and Johnston (1985) included two Fe^{2+} doublets with $\delta = 0.99$ and 1.22 mm/s and $\Delta = 2.87$ and 2.94 mm/s for Fe1 and Fe2, respectively, and three Fe^{3+} doublets with $\delta = 0.43$, 0.40, and 0.42 mm/s and $\Delta = 0.42$, 0.70, and 1.06 mm/s for Fe2a, Fe1, and Fe2b, respectively.

In the current work on sample DD319 (Fig. 4), there are three Mössbauer doublets: one for Fe^{2+} in Fe1, one for Fe^{2+} in Fe2, and one for Fe^{3+} in Fe2. Because the average bond length is slightly longer for Fe1, the doublet with the larger QS ($\delta = 1.21$ mmm/s and $\Delta = 3.03$ mm/s) is assigned to that site in contradiction of the assignments of Dormann and Poullen (1980). The remaining two doublets ($\delta = 0.43$ and 1.23 mm/s and $\Delta = 0.77$ and 2.70 mm/s) represent the Fe2 site.

Phosphoferrite group. The phosphoferrite group includes the species $[(Fe^{2+},Mn)_3(PO_4)_2\cdot 3H_2O]$, along with landesite $[(Mn,Mg)_9Fe^{3+}_3(PO_4)_8(OH)_3\cdot 9H_2O]$, kryzhanovskite $[MnFe_2(PO_4)_2(OH)_2\cdot H_2O]$, garyansellite $[(Mg,Fe^{3+})_3(PO_4)_2(OH,O)\cdot 15(H_2O)]$, and reddingite $[Mn_3(PO_4)_2\cdot 3H_2O]$. These structures have been described in a series of papers by Moore (1964, 1971b, 1974b; Moore and Araki 1976; Moore et al. 1980). The group includes kinked chains of edge-sharing octahedra that linked together by corners to form sheets. PO_4 tetrahedra lie between the sheets and link them by corner-sharing into a rigid octahedral framework (Moore and Araki 1976) There are two distinct octahedral sites, Fe1 and Fe2, and they are linked into trimers in the order Fe1-Fe2-Fe2-Fe1-Fe2-Fe2, so there are twice as many Fe2 sites as Fe1 (Moore 1974b). Different species in the group are distinguished on the basis of cation ordering, with smaller cation in the M1 site (Moore 1971b). For example, in kryzhanovskite, Fe^{3+} fills the Fe1 site while Mn^{2+}, Ca, and Mg occupy Fe2. Moore et al. (1980) demonstrated that the average M-O distance is high and nearly identical in landesite and phosphoferrite and much lower in kryzhanovskite. These differences ought to be manifested in Mössbauer data of this mineral group.

Mattievich and Danon (1977) synthesized phosphoferrite with Fe^{2+} in two different sites with area ratios of 2:1. At 295 K, Fe^{2+} in M1 has parameters of $\delta = 1.18$ mm/s and $\Delta = 2.37$ mm/s, while for M2, $\delta = 1.19$ mm/s and $\Delta = 1.55$ mm/s. Moreira et al. (1994) studied the low-temperature spectra of synthetic phosphoferrite, and Moreira et al. (1996) followed the successive oxidation of phosphoferrite with heating. In this study, landesite ML-P26 (Fig. 4) has three doublets with $\delta = 0.26$, 1.22, 1.23 mm/s and $\Delta = 0.79$, 1.59, and 2.38 mm/s. These would represent Fe^{3+} in M1, Fe^{2+} in M2, and Fe^{2+} in M1, respectively.

Phosphosiderite. Phosphosiderite [$Fe^{3+}PO_4(H_2O)_2$] and its dimorph strengite have similar structures to variscite [$AlPO_4(H_2O)_2$] and its dimorph metavariscite. The structure was described by Taxer and Bartl (2004). The Fe octahedron has two corners that are H_2O and two that bridge to PO_4 tetrahedra. The Mössbauer spectrum of sample ML-P22 (Fig. 5) in this study has two Fe^{3+} doublets with $\delta = 0.43$ and 0.45 mm/s and $\Delta = 0.47$ and 0.23 mm/s, likely representing two slight geometrical modifications of the same Fe site.

Plimerite. Plimerite [$ZnFe_4^{3+}(PO_4)_3(OH)_5$] is a Zn analog of rockbridgeite described by Elliott et al. (2009); it is discussed with the other rockbridgeite minerals under that heading below.

Purpurite. The structure of purpurite, $MnPO_4$, which occurs in solid solution with heterosite ($MnPO_4$-$FePO_4$) is discussed in detail under the listing above for ferrisicklerite. Its Mössbauer characteristics have been well described. Li et al. (1986) and Li and Shinno (1997) find three Fe^{3+} doublets in the M2 site of purpurite, with $\delta = 0.27$, 0.40, and 0.29 mm/s and $\Delta = 1.69$, 0.96, and 0.56 mm/s. They interpret the different doublets to represent varying populations of next nearest M2 neighbors such as Mn^{2+}, Mn^{3+}, Fe^{2+}, and Fe^{3+}. Liu et al. (2005) fit quadrupole splitting distributions to purpurite spectra to test this hypothesis. They find no Fe in the vacant M1 sites of purpurite, but two Fe^{3+} doublets with $\delta = 0.48$ and 0.46 mm/s and $\Delta = 1.71$ and 0.83 mm/s, quite similar to those of the earlier workers. In this study, purpurite DD270 (Fig. 5) also has two Fe^{3+} doublets with $\delta = 0.43$ and 0.40 mm/s and $\Delta = 1.71$ and 0.74 mm/s, while the Fe^{3+} doublets in DD227 (Fig. 5) have $\delta = 0.43$ and 0.48 mm/s and $\Delta = 1.48$ and 0.58 mm/s.

Pyrophosphate. Although all the other minerals in this paper are based on isolated PO_4 tetrahedra, pyrophosphates such as the mineral canaphite ($CaNa_2P_2O_7 \cdot 4H_2O$) do exist in nature, albeit very rarely (Rouse et al. 1988). However, the diphosphates have been well studied because they are synthesized in all organisms, including the human body, in large amounts (Russell 1976). Baran et al. (2004) report a single doublet with $\delta = 0.45$ mm/s and $\Delta = 0.45$ mm/s for $BaFe_2(P_2O_7)_2$ and two Fe^{3+} doublets each in $PbFe_2(P_2O_7)_2$ ($\delta = 0.44$ and 0.42 mm/s and $\Delta = 0.84$ and 1.07

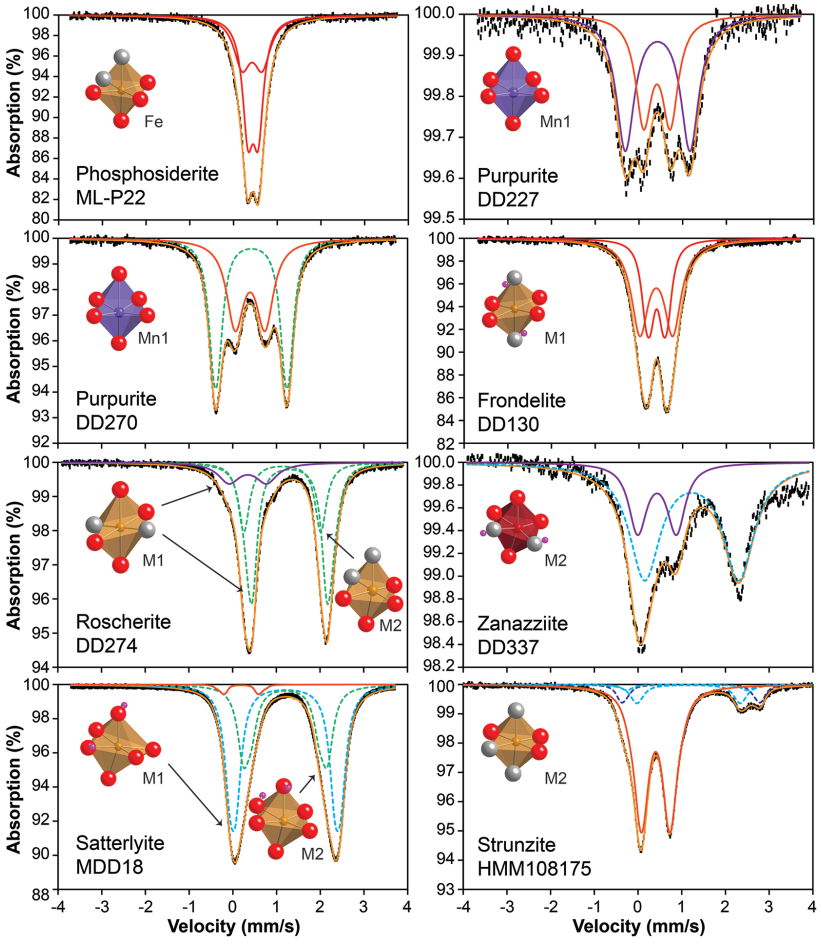

FIGURE 5. Mössbauer spectra and Fe coordination polyhedra, with conventions as in Figure 1. Phosphosiderite (Moore 1966) ML-P22 has two Fe^{3+} doublets corresponding to occupancy of the Fe site. Purpurites DD270 and DD227 (Bjoerling and Westgren 1938) each have two Fe^{3+} doublets assigned solely to M2 following the convention established by Li and Shinno (1997) and Liu et al. (2005). Frondelite DD130 (Redhammer et al. 2006), which belongs to the rockbridgeite groups, has Fe^{3+} only located in the M1 site. Both roscherite (Fanfani et al. 1977) and zanaziite (Rastsvetaeva et al. 2009) are members of the roscherite group; roscherite has Fe^{3+} in only M1 and Fe^{2+} in both M1 and M2. Zanazziite has Fe^{2+} and Fe^{3+}, both assigned to M2. The spectrum of satterlyite (Kolitsch et al. 2002) MDD18 is dominated by two Fe^{2+} doublets in the M1 and M2 sites and a very small Fe^{3+} doublet. Most of the Fe in strunzite (Fanfani et al. 1978) 108175 is Fe^{3+} in the M2 site, while the remaining Fe^{2+} is distributed among unspecified octahedral sites. (Color online.)

mm/s, respectively) and $SrFe_2(P_2O_7)_2$ (δ = 0.43 and 0.41 mm/s and Δ = 0.90 and 1.14 mm/s). These parameters are consistent with those in the orthophosphates, suggesting that the environment surrounding the Fe octahedra in these structures is little affected by the type of phosphate that is present.

Rockbridgeite group. There are three minerals in the rockbridgeite group: the species $(Fe,Mn)Fe_4(PO_4)_3(OH)_5$, frondelite, $MnFe_4(PO_4)_3(OH)_5$, and plimerite, $ZnFe_4(PO_4)_3(OH)_5$. First described by Moore (1970), these structures consist of face-sharing octahedra in Fe2-Fe1-Fe2 clusters connected to Fe3 octahedra by corner sharing. There is one Fe1 site for every two Fe2 and Fe3. $P1O_4$ tetrahedra share corners with all three Fe sites, while $P2O_4$ tetrahedra share only with Fe2 and Fe3. The Fe1 site is occupied only by Fe^{3+} and its bond length closely resembles the Fe1 site in barbosalite (Redhammer et al. 2000). The Fe2 site is larger and compares to the Fe2 site in barbosalite, so it is favored by Fe^{2+}; its distortion is attributed to partial occupancy by the smaller Mn^{3+} cation (Redhammer et al. 2006). The Fe3 site is only half occupied; it is less distorted than the Fe1 site as represented by λ and σ^2, and also is favored by Fe^{3+}.

Mössbauer spectra of rockbridgeite were first described by Amthauer and Rossman (1984); at 295 K they report two Fe^{3+} doublets [δ = 0.38 and 0.46 mm/s, Δ = 0.48 (Fe1) and 0.75 (Fe3) mm/s] and two Fe^{2+} doublets [δ = 1.11 and 1.05 mm/s, Δ = 2.77 (Fe3) and 3.05 (Fe2) mm/s]. However, they acknowledge that their site assignments do not agree with the crystal structure refinements by Moore (1970). In Rouzies et al. (1994), parameters for Fe^{3+} assigned to M1, M2, and M3 are given as δ = 0.42, 0.43, and 0.44 mm/s and Δ = 0.99, 0.66, and 0.38 mm/s, respectively, based on areas and site distortion as represented by Δ. Redhammer et al. (2006) report five doublets but assign them differently based on peak area arguments: Fe^{3+} has δ = 0.52, 0.45, and 0.41 mm/s and Δ = 0.87 (Fe2), 0.72 (Fe1), and 0.44 (Fe3) mm/s, respectively. Both Fe^{2+} doublets must occupy the Fe2 site, but they likely have two different populations of next nearest neighbors: δ = 1.12 and 1.07 mm/s and Δ = 2.73 and 3.01 mm/s, respectively. These are hypothesized by Redhammer et al. (2006) to arise from Fe^{2+}-Fe^{2+} and Fe^{2+}-Mn neighbors in the clusters.

Elliott et al. (2009) describe the crystal structure and Mössbauer spectrum of plimerite, the latter with three doublets assigned to Fe^{2+} (δ = 1.10 mm/s, Δ = 3.44 mm/s), Fe^{3+} in the M3 site (δ = 0.40 mm/, Δ = 0.35 mm/s), and Fe^{3+} in M1 (δ = 0.38 mm/s, Δ = 0.92 mm/s). In this study, frondelite has similar parameters but for Fe^{3+} only: δ = 0.40 and 0.41 mm/s with Δ = 0.76 and 0.26 mm/s, respectively for DD130 (Fig. 5).

Roscherite group. The hydrous beryllophosphate group of minerals is represented in this study by specimens of roscherite $[Ca(Mn,Fe)_5Be_4(PO_4)_6(OH)_4 \cdot 6H_2O]$ and zanazziite $[Ca_2(Mg,Fe)(Mg,Fe,Al,Mn,Fe)_4Be_4(PO_4)_6(OH)_4 \cdot 6H_2O]$. The crystal structure of roscherite was first described by Fanfani et al. (1975), with other specimens described by Fanfani et al. (1977), Clark et al. (1983), and Rastsvetaeva et al. (2005). The sample studied here is from the Minas Gerais locality of Lindberg (1958). Several species related to roscherite have subsequently been identified, including greifensteinite (Rastsvetaeva et al. 2002), atensioite (Rastsvetaeva et al. 2004), footemineite (Atencio et al. 2007a; Rastsvetaeva et al. 2007), Fe^{3+}-rich ruifrancoite (Atencio et al. 2007b), Zn- greifensteinite (Barinova et al. 2004), and the Mg-rich zanazziite (Fanfani et al. 1975, later renamed by Leavens et al. 1990; see also Rastsvetaeva et al. 2009). Minerals of this group are composed of chains of BeO_4 and PO_4 tetrahedra that run in the [101] direction (Huminicki and Hawthorne 2002). These crystal structures all contain two octahedral sites designated M1 and M2; M1 is slightly larger but because it is distorted, tends to be occupied by smaller cations (Al and vacancies) than the smaller but less distorted M2 site that generally contains Mg and Fe^{2+} (Rastsvetaeva et al. 2005).

In this study, roscherite DD274 (Fig. 5) and zanazziite DD337 (Fig. 5) show both Fe^{3+} and Fe^{2+}. For roscherite, there are two Fe^{2+} doublets with δ = 1.14 and 1.30 mm/s and Δ = 1.77 and 1.69 mm/s, respectively, and one Fe^{3+} doublet with δ = 0.35 mm/s and Δ = 0.84 mm/s. According to Rastsvetaeva et al. (2005), Fe^{2+} in roscherite occupies both larger M1 and smaller M2 sites, so the doublet with Δ = 1.77 mm/s may represent M1 and the Δ = 1.69 mm/s doublet M2. Fe^{3+} likely follows Al, which is found in the M1 site. For zanazziite, the sole Fe^{2+} doublet has δ = 1.23 mm/s and Δ = 2.13 mm/s, while Fe^{3+} is represented by δ = 0.43 mm/s and Δ = 0.95 mm/s. Both Fe^{2+} and Fe^{3+} occupy the M2 site (Fanfani et al. 1975).

Rosemaryite. Members of the wyllieite group have the same basic structure as the alluaudite group described above, based on the original descriptions by Moore and Ito (1973) and Moore and Molin-Case (1974). However, wyllieite group minerals have significantly more cation ordering. The M2 site in alluaudite is split into M2a (occupied by Fe^{2+}) and M2b (Al^{3+}), creating an ordered edge-sharing chain of octahedra. Alkali elements also order in the wyllieite group: Na^{1+} occupies the X1a site, with Mn^{2+} and Ca^{2+} in X1b. The X2 site is only partially occupied by Na^{1+}.

Rosemaryite, $NaMnFe^{3+}Al(PO_4)_3$, and ferrorosemaryite, $NaFe^{2+}Fe^{3+}Al(PO_4)_3$, are the only members of the wyllieite group [general formula of X2 X1a X1b M1 M2a M2b $(PO_4)_3$] of minerals for which Mössbauer data have been reported (Hatert et al. 2005, 2006). According to Moore and Ito (1973), Fe^{3+} occupies the M2b site and Fe^{2+} is in M1. The 80 K Mössbauer parameters from Hatert et al. (2005) include three Fe^{3+} doublets (δ = 0.54, 0.51, and 0.53 mm/s and Δ = 1.03, 0.52, and 0.74 mm/s) assigned to M1, M2a, and M2b, respectively. Fe^{2+} occurs in only two doublets (δ = 1.37 and 1.37 mm/s, Δ = 1.37 and 3.28 mm/s) assigned to M2a and M1. Based on those assignments, Hatert et al. (2006) report δ = 0.41 and 0.40 mm/s and Δ = 0.57 and 0.77 mm/s for Fe^{3+} in M2a and M2b, respectively, and δ = 1.23 and 1.24 mm/s and Δ = 2.18 and 2.88 mm/s, for Fe^{2+} in M2a and M1, respectively, in 295 K spectra of rosemaryite.

Sarcopside. Although the formula of sarcopside, $Fe^{2+}_3(PO_4)_2$ resembles those of the graftonite group, its structure is a derivative of olivine with ordered vacancies, related to those of triphyllite and related minerals (Huminicki and Hawthorne 2002; Moore 1972b). The M1 sites share two edges with adjacent M2 sites and two edges with PO_4 tetrahedra. Every second M1 site is vacant. Each PO_4 tetrahedron also shares an edge with an M2 octahedron. The Fe atoms thus occupy the same positions as Li and Mn in the lithiophilite structure, so their Mössbauer spectra should be similar; two Fe^{2+} cations and an ordered vacancy substitute for four Li^{1+} cations in triphylite-lithophilite (Moore 1972b).

Mattievich and Danon (1977) include the first published Mössbauer spectra of sarcopside, with only a single doublet hav-

ing δ = 1.19 and Δ = 2.92 mm/s that was not assigned to either M1 or M2. However, Ericsson and Khangi (1988) reported that Mössbauer parameters of both M1 and M2 sites were very similar at 295 K though they resolved two doublets with δ = 1.18 and 1.24 mm/s and Δ = 2.87 and 2.93 mm/s. These are indeed quite similar to those reported by Sklute et al. (2006) for two-doublet fits to 295 K olivine spectra.

Satterlyite. The satterlyite [$(Fe^{2+},Mg)_2(PO_4)(OH)$] structure is built on pairs of face-sharing, distorted $(Fe,Mg)O_6$ octahedra linked by edge-sharing to form double chains along [001] (Kolitsch et al. 2002). Each double chain shares corners with six other double chains to produce a framework with three different PO_4 tetrahedra linked by sharing corners with (Fe,Mg) O_6 octahedra. There are two unique $(Fe,Mg)O_6$ octahedra that are characterized by different occupancies; Fe partitions into the M1 site slightly more than in M2 (Evans and Groat 2012). Although the nominal formula includes only divalent cations, Chandrasekhar et al. (2003) investigated satterlyite by EPR and observed both Fe^{3+} and Fe^{2+}.

This study reports the first Mössbauer spectrum of satterlyite (Fig. 5). Although sample MDD18 from Rapid Creek, Yukon, Canada, has a minor vivianite impurity, its spectrum is dominated by Fe^{2+}, which has parameters of δ = 1.20 and 1.20 mm/s and Δ = 1.03 and 2.26 mm/s. On the basis of areas, the Δ = 1.03 mm/s doublet must be M2 and the Δ = 2.26 mm/s doublet is M1. These parameters are too low for vivianite, so they must represent satterlyite. A small Fe^{3+} doublet with only 2% of the total Fe is also observed with parameters suggestive of tetrahedral coordination at δ = 0.19 mm/s and Δ = 0.73 mm/s.

Scorzalite. Scorzalite [$(Fe^{2+},Mg)Al_2(PO_4)_2(OH)_2$] results are discussed with the other species in the lazulite group under the heading for barbosalite, above.

Strengite. Strengite ($Fe^{3+}PO_4 \cdot 2H_2O$) is the only member of the variscite group [$M(PO_4)(H_2O)_2$, where M = Al or Fe^{3+} and P may be P or As] for which Mössbauer data were obtained; none has been published previously. This mineral group has structures with alternating corner-sharing octahedra and tetrahedra (Moore 1966). Each octahedron has two *cis* H_2O corners and four corners shared with PO_4 (Taxer and Bartl 2004).

In this paper, two strengites were analyzed with slightly different parameters: δ = 0.42 and 0.39 mm/s and Δ = 0.30 and 0.55 mm/s for ML-P16 (Fig. 6) while δ = 0.45 and 0.42 mm/s and Δ = 0.33 and 0.34 mm/s for DD293-A (Fig. 6). Both contain solely Fe^{3+} as expected. The two doublets likely represent different distributions of next nearest neighbors around the octahedral sites.

Strunzite. The structure of strunzite, $MnFe_2(PO_4)_2(OH)_2] \cdot 6H_2O$, is composed of three types of octahedra: Fe1 and Fe2 octahedra [$FeO_5(OH)$] alternate in corner-sharing chains along the *z* direction, and chains of $Mn(H_2O)_4O_2$ octahedra are linked to them by PO_4 tetrahedra (Fanfani et al. 1977; Vogel and Evans 1980). Ferristrunzite was studied by Vochten and De Grave (1990), whose preferred fit included three doublets: Fe1 (δ = 0.39 mm/s, Δ = 0.89 mm/s), Fe2 (δ = 0.39 mm/s, Δ = 0.74 mm/s), and D3/Mn (δ = 0.40 mm/s, Δ = 0.64 mm/s). Reported parameters for mangano-ferristrunzite from Vochten et al. (1995) were Fe1 (δ = 0.30 mm/s, Δ = 0.79 mm/s), Fe2 (δ = 0.30 mm/s, Δ = 0.63 mm/s), and Fe substituting on the Mn site (δ = 0.31 mm/s, Δ = 0.61 mm/s). Finally, Van Alboom and De Grave (2005) analyzed three strunzites at 4.2 K; their results support the assignment of the third doublet in the 295 K spectra to the Mn site. In this study, sample HMM 108175 (Fig. 5) from the Harvard Mineralogical Museum has three small Fe^{2+} doublets at δ = 1.16, 1.12, and 1.21 mm/s and Δ = 2.36, 2.75, and 3.19 mm/s representing some distribution between M1, M2, and the Mn site, but is dominated by Fe^{3+} in M2 at δ = 0.40 mm/s and Δ = 0.65 mm/s.

Tarbuttite. Finney (1966) and Cocco et al. (1966) described the crystal structure of tarbuttite [$Zn_2(PO_4)(OH)$], in which Zn is 5-coordinated in two different sites; it is a member of the paradamite group (Bennett 1980; Hawthorne 1979). Zn1 sites form edge-sharing chains in the y direction, while Zn2 sites also share edges but along the [111] direction. Sample DD306 (Fig. 6) in this study from the Reaphook Hill locality in the Flinder Range of South Australia, the first published Mössbauer spectrum of this mineral, has two Fe^{3+} doublets with parameters of δ = 0.37 and 0.37 mm/s and Δ = 0.48 and 0.71 mm/s. Based on the distortion of the polyhedra in this mineral (σ^2_{Zn1} = 1.1651 and σ^2_{Zn2} = 1.1428), the higher Δ doublet is assigned to Zn1 and the doublet with lower Δ to Zn1.

Tinsleyite. Tinselyite [$KAl_2(PO_4)_2(OH) \cdot 2(H_2O)$] has the same structure as leucophosphite, described above, and the sulfate mineral amarantite (Moore 1972a). There are two edge-sharing $(Al,Fe^{3+})O_6$ M1 octahedra and a second type of $(Al,Fe^{3+})O_6$ M2 octahedra between them sharing corners with PO_4 (Dick 1999). Tunnels in the structure accommodate K^{1+} cations.

Mössbauer spectra of tinsleyite were reported by Da Costa and Viana (2001). At 293 K, there are two Fe^{3+} doublets with δ = 0.37 and 0.39 mm/s and Δ = 0.57 and 0.88 mm/s. Although the authors do not assign these doublets to specific sites, the later work of de Resende et al. (2008) on leucophosphite suggests that the doublet with higher Δ is M1 and the smaller Δ doublet is M2.

Triphylite. Triphylite ($LiFePO_4$) forms a solid solution with lithiophilite ($LiFePO_4$-$LiMnPO_4$), and has the same structure as ferrisicklerite-sickerlite [$Li(Fe,Mn)PO_4$-$Li(Mn,Fe)PO_4$], heterosite-purpurite ($FePO_4$-$MnPO_4$), natrophilite ($NaMnPO_4$), and simferite $Li(Mg,Fe,Mn)_2(PO_4)_2$. Many studies have examined Mössbauer spectroscopy of triphylite because this substitution has implications for extraction and insertion of Li in rechargeable batteries.

Aldon et al. (2010) finds ~300 K parameters for Fe^{2+} in triphylite to be δ = 1.22 mm/s and Δ = 2.97 mm/s while Andersson et al. (2000) reports nearly identical values of δ = 1.22 mm/s and Δ = 2.96 mm/s. Liu et al. (2005) resolved two doublets, one with δ = 1.28 mm/s and Δ = 2.97 mm/s assigned to the M2 site and one with δ = 1.29 mm/s and Δ = 1.77 mm/s for the M1 site. Fehr et al. (2007) report Fe^{2+} in M2 parameters of δ = 1.15 mm/s and Δ = 2.95 mm/s. Finally, a detailed study of the temperature dependence of Mössbauer spectra of triphylite by Van Alboom et al. (2011) reports a single 295 K doublet with δ = 1.22 mm/s and Δ = 2.93 mm/s.

In the current study, we examine eight triphylite samples (Fig. 7), many of which contain both Fe^{2+} and Fe^{3+}. For example sample DD193-B has Fe^{2+} features with δ = 1.21 and 1.26 mm/s and Δ = 2.98 and 1.35 mm/s and Fe^{3+} doublets at δ = 0.47 and 0.41 mm/s and Δ = 1.23 and 0.43 mm/s, resembling those for Fe^{3+} in purpurite and ferrisicklerite (Liu et al. 2005). Other samples studied, such as DD301, have solely Fe^{2+}: δ = 1.09 and 1.23

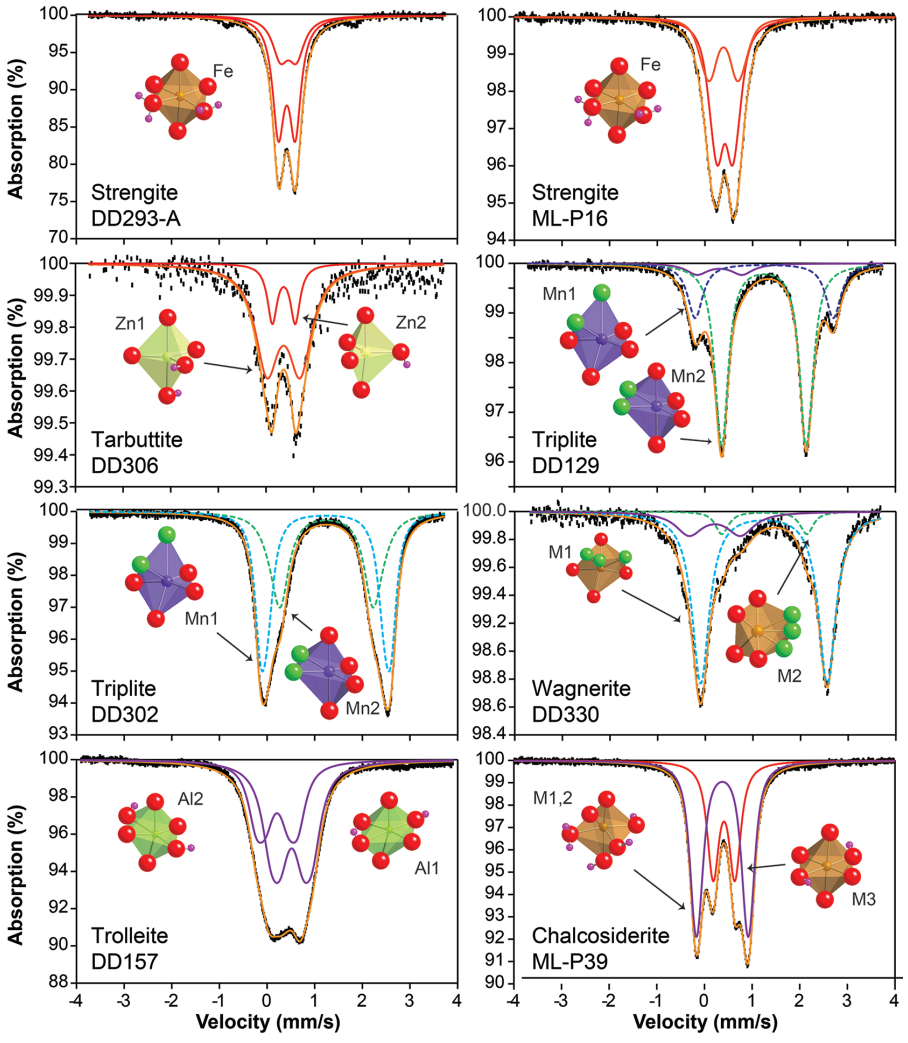

FIGURE 6. Mössbauer spectra and Fe coordination polyhedra, with conventions as in Figure 1. Strengites (Taxer and Bartl 2004) ML-P13 and DD293-A contain Fe^{3+} only in the Fe site. Tarbuttite (Genkina et al. 1985) DD306 is solely Fe^{3+} distributed among the Zn1 and Zn2 sites. Both triplite (Rea and Kostiner 1972) DD129 and DD309 samples contain Fe^{2+} in both M1 and M2, and wagnerite (Tadini 1981) DD330, also from the triplite-triplodite group, is similar. Trolleite DD157 has two doublets with the same Δ but different δ; the Al2 site has the lower δ. Chalcosiderite ML-P39, a member of the turquois family, has Fe^{3+} distributed among M1, M2, and M3 sites. (Color online.)

mm/s and Δ = 3.49 and 2.97 mm/s. A Fe^{2+} doublet with lower Δ is found in the spectra of samples MDD7 (δ = 1.23 mm/s and Δ = 1.68 mm/s) and DD308 (δ = 1.11 and 1.24 mm/s and Δ = 1.66 and 2.25 mm/s, respectively). These doublets must be relatively undistorted to have such low-Δ values, and they likely represent variations in the next nearest neighbor environment around the M2 site. Finally, samples DD193-B and DD271-A are unusual in that they contain predominantly Fe^{3+}. This sample has a known impurity of paraschulzite, which does not contain Fe^{3+}, so DD271A may well be an ozidized version of triphyllite worthy of additional future work.

Triplite-triploidite group. Waldrop (1969, 1970), Rea and Kostiner (1972), and Tadini (1981) described the crystal structures of triplite, $(Mn,Fe)_2FPO_4$, and triploidite, $(Mn,Fe^{2+})_2(PO_4)OH$; zweiselite and wolfeite are related due to their similar structure. Wagnerite, $(Mg,Fe^{2+})_2(PO_4)F$, is also related (Ren et al. 2003). In the *b* direction, isolated PO_4 tetrahedra share corners with MO_4F_2 octahedra, which are then linked into chains by shared edges. In the *a* direction, M2 octahedra similarly link to PO_4. Fe and Mn are distributed into both M1 and M2 sites.

Kostiner (1972) studied triplite with Mössbauer spectroscopy and reported parameters of δ = 1.27 and 1.23 and Δ = 2.01 and 2.70 mm/s for Fe^{2+} in the M2 and M1 sites, respectively.

In this study, triplites DD129 and DD302 (Fig. 6) are from different localities (Table 1) but share similar Mössbauer characteristics. DD302 has the same two Fe^{2+} doublets, with δ = 1.25 and 1.23 and Δ = 1.93 and 2.76 mm/s. In DD129, 7% of the total Fe is octahedral Fe^{3+} (δ = 0.31 mm/s and Δ = 0.94 mm/s) but the remaining two Fe^{2+} doublets resemble those of the other samples, with δ = 1.24 and 1.25 mm/s and Δ = 1.74 and 2.89

mm/s. Kostiner (1972) also reported Mössbauer parameters for triploidite (δ = 1.20 and 1.19 mm/s; Δ = 1.78 and 2.15 mm/s for M2 and M1, respectively), wolfeite (δ = 1.16 and 1.16 mm/s; Δ = 1.76 and 2.22 mm/s for M2 and M1), and zweiselite (δ = 1.29 and 1.24 mm/s; Δ = 1.95 and 2.62 mm/s for M2 and M1). They note that δ values for the F-bearing minerals are systematically higher than those for OH, likely resulting from the effectiveness of F, with its high electronegativity, and pulling *s*-electron density away from the Fe nucleus. F also has an effect on the electric field gradient, causing differences in Δ.

Finally the Mössbauer spectrum of wagnerite DD330 (Fig. 6) is published here for the first time. Two of its three Fe^{2+} doublets match the others in this group, with δ = 1.23 and 1.24 mm/s and Δ = 1.83 and 2.64 mm/s. A smaller (6% of the total area) Fe^{2+} doublet at δ = 1.14 and Δ = 3.21 is observed, along with 17% of the total area in a Fe^{3+} doublet with δ = 0.20 mm/s and Δ = 0.88 mm/s. Given the complexity of the wagnerite structure (e.g. Tadini 1981; Ren et al. 2003), it is unclear which sites each of these doublets represents.

Triploidite. Triploidite [$(Mn,Fe^{2+})_2(PO_4)OH$] is the OH-bearing equivalent of triplite, and is discussed above under that heading.

Trolleite. The trolleite [$Al_4(PO_4)_3(OH)_3$] structure is close to that of lazulite (Moore and Araki 1974; Huminicki and Hawthorne 2002; Yakubovich 2008). Al1 and Al2 octahedral sites share faces to form dimers that link by sharing OH^- corners to form double chains in the [001] direction. PO_4 tetrahedra bridge the chains, creating a very dense structure. The Al1 octahedra are slightly bigger than Al2.

Data presented here for trolleite DD157 represent the first published Mössbauer spectrum of this mineral (Fig. 6). It has two Fe^{3+} doublets with δ = 0.21 and 0.52 mm/s and Δ = 0.90 and 0.90 mm/s. Because the Al2 site is smaller and slightly more distorted, it may be represented by the δ = 0.21 mm/s doublet, leaving δ = 0.52 mm/s to be assigned to the Al1 site. Attempts to re-fit this spectrum with two doublets having more similar isomer shifts were unsuccessful. Parameters of lazulite spectra in the current study were indeed similar to trolleite, with parameters for Fe^{3+} of δ = 0.27–0.35 mm/s and Δ = 0.64–0.77 mm/s and for Fe^{2+} with δ = 1.12–1.22 mm/s and Δ = 1.76–3.29 mm/s.

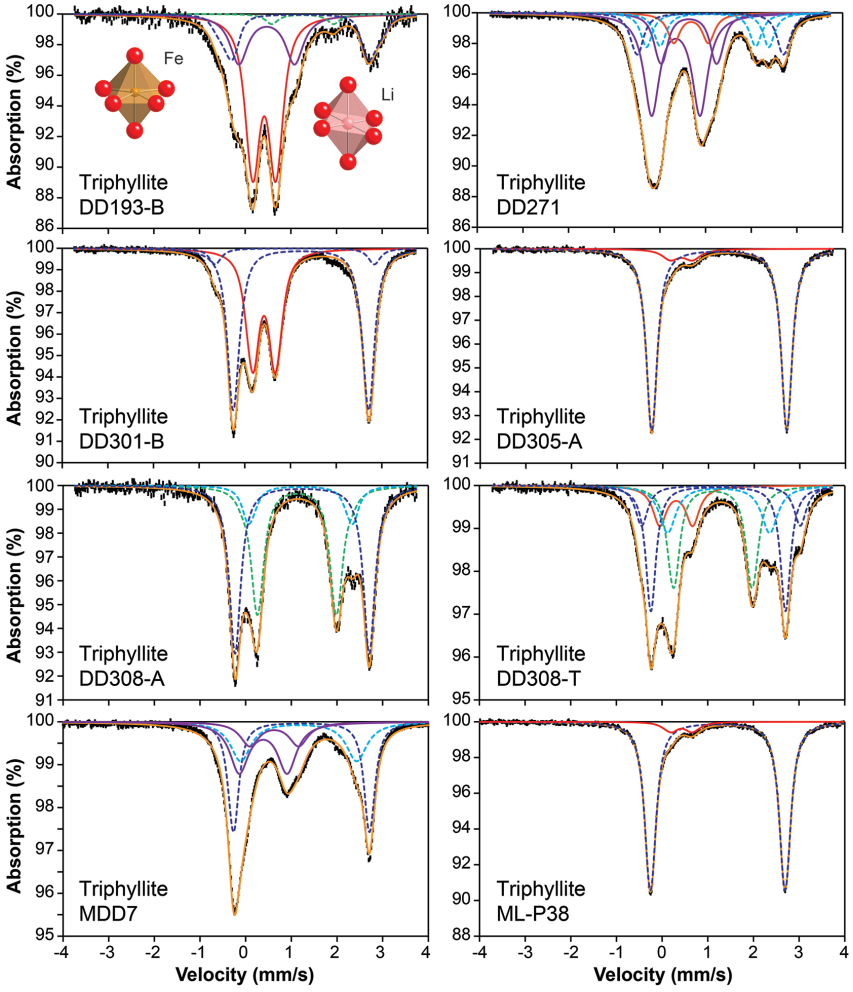

Figure 7. Mössbauer spectra and Fe coordination polyhedra, with conventions as in Figure 1. Triphyllite (Losey et al. 2004) spectra from the eight samples in study. All spectra show evidence for Fe^{2+} in the M1 and M2 sites. Samples DD193-B and DD271-A are unusual because they contain mostly Fe^{3+}. (Color online.)

Turquoise group. The turquoise group includes the species turquoise [$CuAl_6(PO_4)_4(OH)_8 \cdot 4H_2O$], coeruleolactite [$(Ca,Cu)Al_6(PO_4)_4(OH)_8 \cdot 4H_2O$], faustite [$(Zn,Cu)Al_6(PO_4)_4(OH)_8 \cdot 4H_2O$], chalcosiderite [$CuFe_6(PO_4)_4(OH)_8 \cdot 4H_2O$], aheylite [$(Fe,Zn)Al_6(PO_4)_4(OH)_8 \cdot 4H_2O$], and planerite [$Al_6(PO_4)_2(PO_3OH)_2(OH)_8 \cdot 4H_2O$]. Members vary by occupancy of the A-site (□, Cu, Zn, Fe^{2+}, Ca) and the B-site (Al or Fe^{3+}), with vacancies in the A-site charge-balanced by protonation of the PO_4 tetrahedra (Foord and Taggart 1998). The structures of turquoise and chalcosiderite were determined by Cid-Dresdner (1964, 1965), Giuseppetti et al. (1989), and Abdu et al. (2011). Four octahedral sites include the M1-M3 B sites and a larger X site (corresponding to B in the formula) containing the larger divalent cations. Two tetrahedral sites are occupied by P. The structure includes pairs of edge-sharing M1 and M2 octahedra that share corners with tetrahedra forming chains in the *b* direction. The chains also share corners with M3 octahedra and edges with X octahedra. The M1 and M2 sites are very similar (Abdu et al. 2011) and therefore should have the same Mössbauer parameters, while the M3 is very different.

The first Mössbauer study of turquoise by Sklavounos et al. (1992) reported two doublets with $\delta = 0.39$ and 0.35 mm/s and $\Delta = 0.52$ and 1.09 mm/s, respectively. Based on site geometry, they assigned the lower Δ doublet to M3 and the larger Δ doublet to M1 and M2. This assignment was supported by the combined single-crystal structure refinement and Mössbauer study of Abdu et al. (2011). They resolved two Fe^{3+} quadrupole splitting distributions, with the same site assignments, with the smaller $\Delta = 0.48$–0.61 mm/s doublet to M3 and the larger $\Delta = 1.10$–1.14 mm/s doublet to M1 and M2. In this study, chalcosiderite ML-P39 (Fig. 6) had the same two doublets ($\delta = 0.41$ and 0.38 mm/s and $\Delta = 0.43$ and 1.09 mm/s, respectively.

Varulite. Varulite [$NaCaMn(Mn,Fe^{2+},Fe^{3+})_2(PO_4)_3$], is discussed with the other alluaudite group phases under the alluaudite heading above.

Vivianite group. The vivianite group of hydrated phosphates includes the species vivianite [$Fe_3(PO_4)_2 \cdot 8H_2O$], baricite [$(Mg,Fe)_3(PO_4)_2 \cdot 8H_2O$], erythrite [$Co_3(AsO_4)_2 \cdot 8H_2O$], annabergite [$Ni_3(AsO_4)_2 \cdot 8H_2O$], köttigite [$Zn_3(AsO_4)_2 \cdot 8H_2O$], parasymplesite [$Fe_3(AsO_4)_2 \cdot 8H_2O$], hörnesite [$Mg_3(AsO_4)_2 \cdot 8H_2O$], arupite [$(Ni,Fe)_3(PO_4)_2 \cdot 8H_2O$], and pakhomovskyite [$Co_3(PO_4)_2 \cdot 8H_2O$]. The vivianite structure as first described by Mori and Ito (1950) has two different octahedral sites. The Fe1 sites are $Fe^{2+}O_2(H_2O)_4$ octahedra where the *trans* O^{2-} corners are the apices of PO_4 tetrahedra. The Fe2 sites are $Fe^{2+}O_4(H_2O)_2$ octahedra that share edges in pairs; two of the O^{2-} corners of each are the PO_4 groups that link to the Fe1 octahedra, forming chains that link in the *a* direction to form sheets (e.g., Fejdi et al. 1980). Bobierrite [$Mg_3(PO_4)_2 \cdot 8H_2O$] has the same structure with slightly different linkages between sheets.

Although Fe probably substitutes to some extent in all these phases, only vivianite and baricite have previously been characterized with Mössbauer spectroscopy. However, vivianite is perhaps the best-studied of all the phosphate minerals. A partial list of relevant papers includes Hrynkiewicz and Kulgawczuk (1964), Gonser and Grant (1967), Lerman et al. (1967), Janot et al. (1968a, 1968b), Takashima and Ohashi (1968), Mattievich and Danon (1971), Shinno and Takada (1971), Mattievich and Danon (1977), Vochten et al. (1979), Burns et al. (1980), De Grave et al. (1980), Dormann and Poullen (1980), McCammon and Burns (1980), Nembrini et al. (1983), Amthauer and Rossman (1984), Waerenborgh and Figueiredo (1986), Hanzel et al. (1990a, 1990b), Rouzies and Millet (1993b), and Rodgers et al. (1993). Parameters from a subset of these papers are given in Table 2[1].

Spectra from this study for vivianite and bobierrite (Fig. 8) are very similar. There are generally two Fe^{2+} doublets in vivianite with $\delta = 1.17$ and 1.22 mm/s and $\Delta = 2.47$ and 2.93 mm/s assigned to M1 and M2, respectively. Fe^{3+} is modeled by McCammon and Burns to occupy the M2 site. Bobierrite MDD11 has two Fe^{2+} doublets at $\delta = 1.21$ and 1.18 mm/s and $\Delta = 3.24$ and 2.41 mm/s, respectively. It has one Fe^{3+} doublet at $\delta = 0.26$ mm/s and $\Delta = 0.85$ mm/s. Five vivianite samples were examined. Their Mössbauer spectra were somewhat variable but generally resemble those of bobierrite (Fig. 8). All have at least two Fe^{2+} doublets, one with $\Delta \approx 2.5$ mm/s [assigned by McCammon and Burns (1980) to the Fe1 site] and a second with $\Delta \approx 3.0$ mm/s (Fe2 site). The Fe^{3+} doublet has $\delta = 0.31$–0.37 mm/s and $\Delta = 0.65$–0.86 mm/s. These fits and assignments are consistent with those in the literature listed above.

No sample of baricite could be obtained for the current study, but Yakubovich et al. (2001) provides Mössbauer data on a sample from its type locality in the Big Fish River area in the NE Yukon Territory of Canada. Their work demonstrates the preference of Mg for the M2 site, while the M1 site is mostly occupied by Fe. Their Mössbauer results are quite similar to those from this and previous studies of vivianite: $\delta = 0.31$ and 1.18 mm/s and $\Delta = 0.47$ and 2.46 mm/s for Fe^{3+} and Fe^{2+} in the M1 site, respectively, and $\delta = 0.29$ and 1.21 mm/s and $\Delta = 1.11$ and 3.26 mm/s for Fe^{2+} in M2.

Wagnerite. As described by Ren et al. (2003) and Coda et al. (1967), the structure of wagnerite [$(Mg,Fe^{2+})_2(PO_4)F$] makes it part of the triplite/triploidite group of minerals, so it is discussed under that heading above.

Whiteite. Whiteite [$(Mn^{2+},Ca)(Fe^{2+},Mn^{2+})Mg_2Al_2(PO_4)_4(OH)_2 \cdot 8(H_2O)$] forms a solid solution with jahnsite and so is discussed under that heading above.

Wolfeite. Wolfeite [$(Fe^{2+},Mn)_2(PO_4)OH$] is related to the triplite-triploidite group and is discussed with that group above.

Zanazziite. Zanazziite [$Ca_2(Mg,Fe)(Mg,Fe,Al,Mn,Fe)_4Be_4(PO_4)_6(OH)_4 \cdot 6H_2O$] is a member of the roscherite group and is discussed under that heading above.

Zwieselite. Zwieselite [$(Fe^{2+},Mn)_2(PO_4)F$] is related to the triplite-triploidite group and is discussed with that group above.

Summary of results

Site assignments for phosphate doublets. Parameters from all samples studied are shown in Figure 9, where they are compared against data from the literature, as well as Mössbauer results for sulfates (Dyar et al. 2013), silicates, and oxides (Burns and Solberg 1990). The sulfate data set includes only samples (many different species and multiple specimens of some) analyzed by Dyar et al. (2103), while the Burns and Solberg (1990) data deliberately only show one set of doublets for each mineral species, so that plot is more sparse. Several trends are apparent here.

In the silicate mineral groups, both δ and Δ vary consider-

ably within doublets of each valence state, and δ is a sensitive indicator of coordination number. For example, Fe^{2+} in silicates produces δ = 0.90–1.05 mm/s for 4-coordination, 1.05–1.19 mm/s for 6-coodination, and >1.20 mm/s for 8-coordination and larger sites. The vast majority of Mössbauer spectra of silicates with Fe^{2+} doublets show octahedral coordination with δ in that middle range ca. 1.14 mm/s. In phosphates and sulfates, Fe^{2+} in octahedral coordination in phosphate minerals also varies little, but the typical δ value is slightly higher, averaging 1.21 mm/s in the samples studied here. With one possible exception, there are no examples in this paper or in any of the reviewed literature in which there was unequivocal justification for assigning Fe^{2+} to a site in a phosphate mineral with a coordination number >6. The exception is a small (16% of the total area) peak in the varulite spectrum with δ = 1.42 mm/s that, if real, might indicate Fe^{2+} occupancy in the 8-coordinated Ca/Na site.

Figure 9 also shows that phosphate minerals have a wide range of isomer shift values. In silicates, values of δ = 0.30 mm/s and lower are generally interpreted to represent tetrahedral Fe^{3+}. However, the SiO_4 tetrahedra that form the building blocks for silicates are sometimes Si-deficient, so substitution of Al^{3+} and Fe^{3+} is relatively common. However, as noted above, tetrahedral Fe^{3+} occupancy in phosphate structures is rare because phosphates commonly contain only stoichiometric PO_4^{3-} tetrahedra. Thus the low values for δ (e.g., δ = 0.21 mm/s for trolleite and 0.31 mm/s for doublets in gormanite, lazulite, lomonosovite, and maricite) reported in this paper must represent 6-coordinated sites. Either these are poorly resolved doublets with small areas or they represent highly distorted sites, such that four corners of the octahedra are significantly closer to the central cation than the other two.

Electron delocalization. As has long been known, there is a fairly clear distinction between the groups of data for Fe^{3+} and Fe^{2+}. Doublets with δ values below 0.5 mm/s are assigned to Fe^{3+}, and those above 0.90 mm/s to Fe^{2+}. The few mineral species that lie beteen those values are usually interpreted to be "$Fe^{2.5+}$" with electrons delocalized (ED) or shared between Fe^{2+} and Fe^{3+} in adjacent sites. Their Mössbauer parameters fall between the typical ranges for each. This phenomenon is observed in magnetite, deerite, ilvaite, conrdtedtite, etc. (Burns 1981; Amthauer and Rossman 1984) but apparently does not occur in either phosphates or sulfates. ED is activated by thermal exchange, and is related to the optically activated effect of intervalence charge transfer of electrons in electronic absorption spectra. Amthauer and Rossman (1984) cite vivianite as a type example of intervalence charge transfer (IVCT) between isolated Fe^{2+}/Fe^{3+} pairs, so ED is certainly possible in phosphates. There is one report in the literature (Moreira et al. 1996) of ED in the phosphate mineral phosphosferrite. However, that paper does not give parameters for the ED doublets, and there is no sign of an ED feature in the landesite ML-P26 studied here. However, none of the phosphates studied here (nor any of the sulfate minerals in Dyar et al. 2013) shows evidence for $Fe^{2.5+}$ doublets.

This lack has been noted by previous workers (Vochten et al. 1979), even in the phosphate minerals with structures where octahedra share both edges or sides, bringing the Fe in those

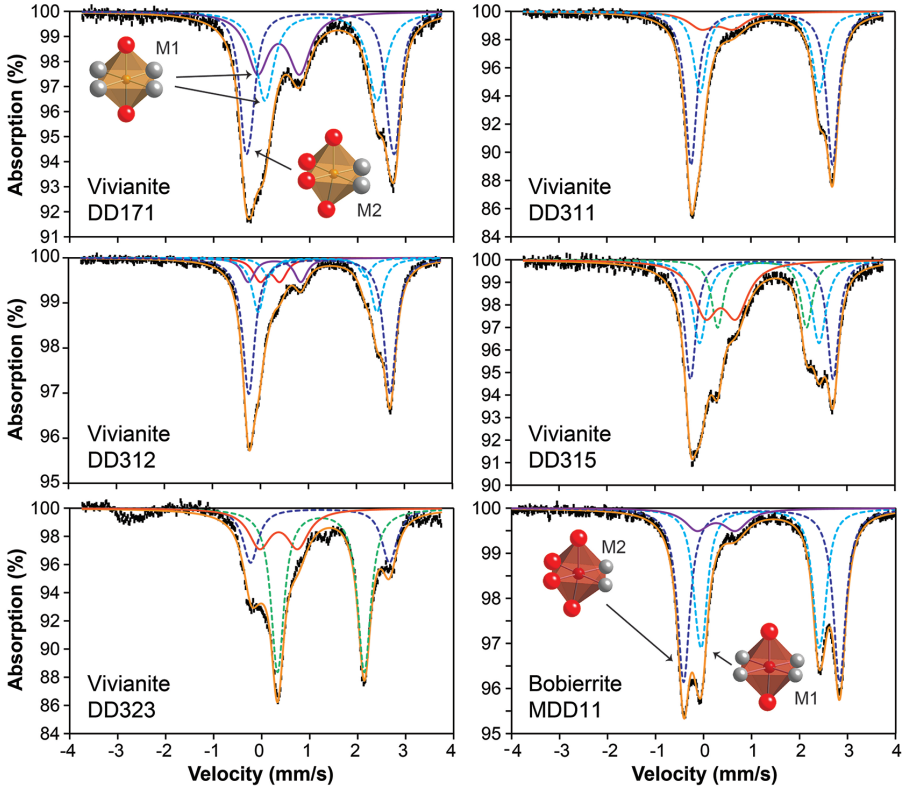

FIGURE 8. Mössbauer spectra and Fe coordination polyhedra, with conventions as in Figure 1. Vivianite group spectra of vivianite (Fejdi et al. 1980) and bobierite (Takagi et al. 1986). Fe^{2+} occupies both the M1 and M2 sites while Fe^{3+} is in M1. (Color online.)

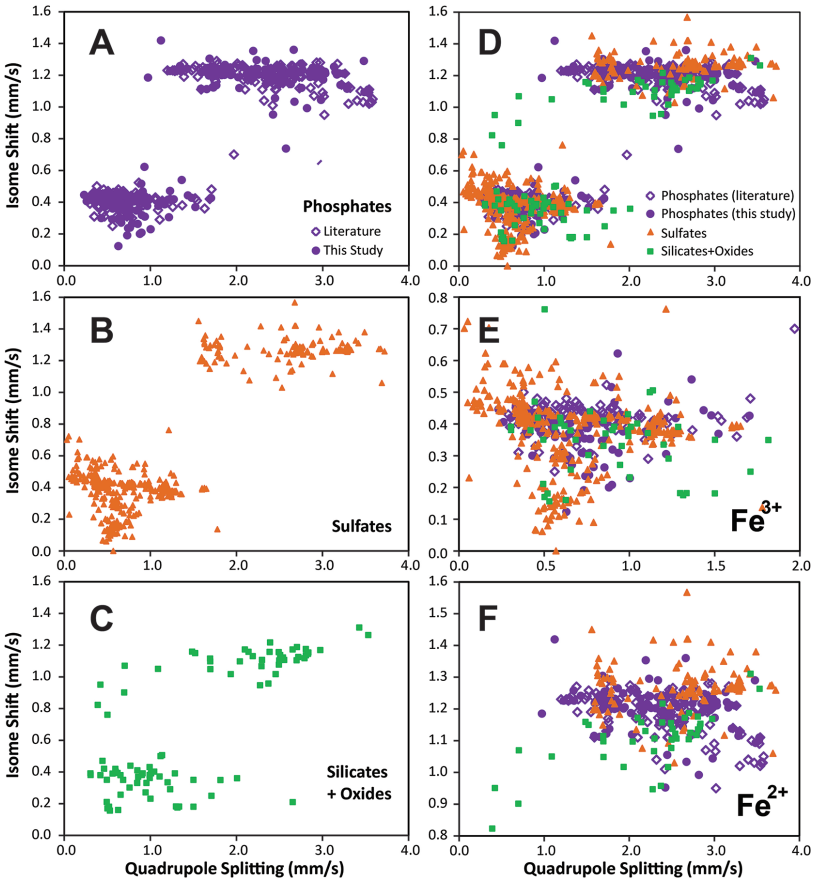

FIGURE 9. Mössbauer parameters of phosphates measured in this study (**a**), compared to parameters for sulfates (**b**, from Dyar et al. 2013), silicates, and oxides (Burns and Solberg 1990). All these data are superimposed in **d**, with close-ups of ranges corresponding to Fe^{3+} and Fe^{2+} in **e** and **f**, respectively. (Color online.)

adjacent cation sites close enough to exchange electrons (Fig. 10). Close inspection shows that edge-sharing chains in phosphates, such as those in graftonite and rosemaryite, have slightly longer Fe-Fe distances between neighboring cation sites, above the longest ED distance observed in silicates. However, in the face-sharing octahedra that occur in phosphates, the cation-cation distances are close enough to allow ED, but yet it still does not occur. Amthauer and Rossman (1984) postulate that electron exchange is seen in Mössbauer spectra only in minerals with structures involving infinite chains of structural units. Apparently the dimer, trimer, and tetramer linkages common in phosphates are simply too short for ED to occur. There are examples of infinite chains of octahedral sites in the phosphate group, such as graftonite shown here, but the cation-cation distances are apparently too long (Fig. 10).

RELATIONSHIPS AMONG COORDINATION POLYHEDRA GEOMETRIES AND MÖSSBAUER PARAMETERS

As noted earlier, Mössbauer parameters are related to the geometries of the individual coordination polyhedra surrounding the Fe cations in each site. In particular, distortion of the octahedral environment may lead to unequal occupancy of the *d* orbitals and a large contribution to Δ from the electronic field. Thus, it should be possible to directly correlate Mössbauer parameters with the characteristics of the octahedral sites in each mineral studied. This analysis was attempted by Burns and Solberg (1990) for oxide and silicate minerals, but their results only showed that Fe^{3+} and Fe^{2+} in sites with different coordination numbers could be distinguished. They concluded that "correlations between the various crystal structure parameters and Mössbauer spectral data are not good." However, their survey included a wide variety of silicate and oxide minerals with very dissimilar structures. As an alternative, the phosphate minerals, with only a single coordination number (6), might provide a more tractable subject for this analysis.

For this comparison, single-crystal structure refinements (SREF) of phosphate minerals were collected from the American Mineralogist Crystal Structure Database using data from the same species (though not the exact same samples) studied here. References to the SREF studies employed are given in captions to Figures 1 to 8. Using those crystal structure data and the CrystalMaker software package, parameters describing the six-coordinated sites in each of the phosphates studied were evaluated. On the basis of the atomic coordinates, calculated mean bond length, mean octahedral quadratic elongation (λ), and angular variance (σ) of each cation site where Fe may reside in these minerals were calculated. These structural data were compared with Mössbauer parameters for the samples studied here. Refinements where the composition was low in Fe were not used, because those site characteristics are more reflective of the other cation than of Fe occupancy.

As noted by Burns and Solberg (1990), δ should be affected most by oxidation state, increased covalent bond character, and shortened bond distances. Thus they expected cation-oxygen distances to be reflected in δ values. However, none of the following parameters yielded any kind of correlation to δ: polyhedral volume,

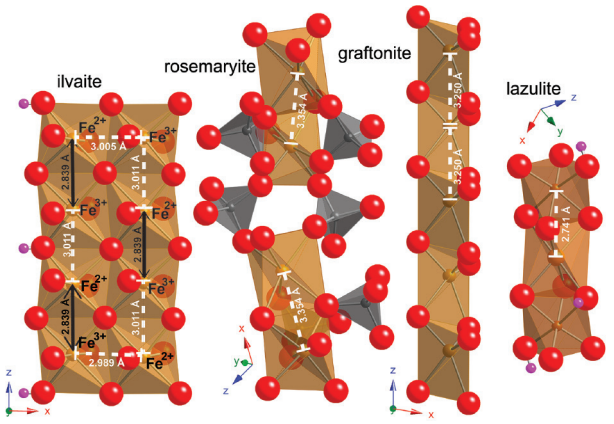

FIGURE 10. Crystal structures of ilvaite, rosemaryite, graftonite, and lazulite, showing distances between cations in adjacent sites. Ilvaite is a classic example of a mineral in which infinite chains of edge-sharing octahedra allow electrons to be exchanged between adjacent sites, resulting in a Mössbauer spectrum with a doublet of averaged δ values, assigned to $Fe^{2.5+}$. This type of electron delocalization (ED) does not occur in any of the phosphate minerals studied here, despite the common occurrence of edge- and face-sharing octahedral dimers, trimers, and tetramers like those in rosemaryite and lazulite shown here. Amthauer and Rossman (1984) suggest that because these chains are discontinuous, ED is inhibited. There are examples of infinite chains of octahedral sites in the phosphate group, such as graftonite shown here, but the cation-cation distances are likely too long. (Color online.)

mean bond length, λ, mean bond angle, or σ. For the same set of crystal structure characteristics, Δ is not correlated with any of these except possibly mean bond length, where longer bonds suggest higher quadrupole splitting (Fig. 11). This is the same result found for Fe^{3+} in sulfate minenals in a parallel study. So it appears that the best (albeit poor) predictor of quadrupole splitting is the size of the coordination polyhedron in any given mineral species.

IMPLICATIONS: WHERE IS THE PHOSPHORUS ON MARS?

Results from the α particle X-ray spectrometer (APXS) on the Spirit and Opportunity rovers provided more than 200 P_2O_5 analyses for rocks and soils on Mars. Phosphorus was uniformly assumed to be present as Ca-phosphates, likely apatite and/or brushite (e.g., Ming et al. 2006), in keeping with their presence in martian meteorites. However, remote sensing data suggest that many of the rocks containing Ca-phosphates and Ca-sulfates also contain various types of Mg-sulfates formed through aqueous processes and not found in meteorites. This raises the possibility (likelihood?) that Mg or even Fe-phosphates might also occur on Mars, albeit in small abundances. If the MIMOS II Mössbauer spectrometers on the Mars Exploration Rovers had measured samples including Fe-containing phosphate minerals, what would their Mössbauer signatures look like?

Morris et al. (2006a) summarizes the Mössbauer evidence from the 95 targets acquired during Opportunity rover's traverse across Meridiani Planum, while Morris et al. (2006b) provides a parallel analysis of 82 spectra from the Spirit rover, which landed at Gusev crater and traveled to the Columbia Hills. Using these data and correlations with APXS data, Opportunity and Spirit found an overlapping set of minerals: olivine, pyroxene, ilmenite, nanophase oxide, Fe^{3+} sulfate, jarosite, magnetite, goethite, and hematite. Setting aside the magnetic phases, the average parameters reported for these phases at Gusev were δ = 1.15 mm/s and Δ = 2.99 mm/s for olivine, δ = 1.16 mm/s and Δ = 2.14 mm/s for pyroxene, δ = 0.37 mm/s and Δ = 0.91 mm/s for nanophase oxide, δ = 1.07 mm/s and Δ = 0.80 mm/s for ilmenite, and δ = 0.43 mm/s and Δ = 0.58 mm/s for Fe^{3+} sulfate. Parameters for the olivine, pyroxene, and nanophase oxide were similar at Meridiani, and also included a second pyroxene site (δ = 1.18 mm/s and Δ = 2.21 mm/s) as well as a doublet interpreted to be jarosite with δ = 1.07 mm/s and Δ = 0.80 mm/s. Note that because these data were acquired at an average temperature of 220 K, their 295 K equivalents would have Δ values roughly 0.02–0.07 mm/s lower (Klingelhöfer et al. 2004; Rothstein 2006). If Fe-containing phosphate minerals were present, would they have been distinguishable from the other minerals present on the basis of these parameters?

Figures 12 and 13 show close-ups of Figure 9 with the positions of the doublets detected on Mars as reported by Morris et al. (2006a, 2006b) superimposed. As noted in Dyar et al. (2013), jarosite has a fairly unique set of Mössbauer parameters among sulfate minerals, and there are few phosphate minerals that would produce those parameters (Fig. 10). Figures 12 and 13 demonstrate that there is complete overlap between phosphates (and sulfates) and the regions surrounding the Mars doublets interpreted to result from sulfate, pyroxene, olivine, and nanophase oxide. Given the 2σ standard deviations from Morris et al. (2006a, 2006b) and shown in Figure 13, it would be impossible

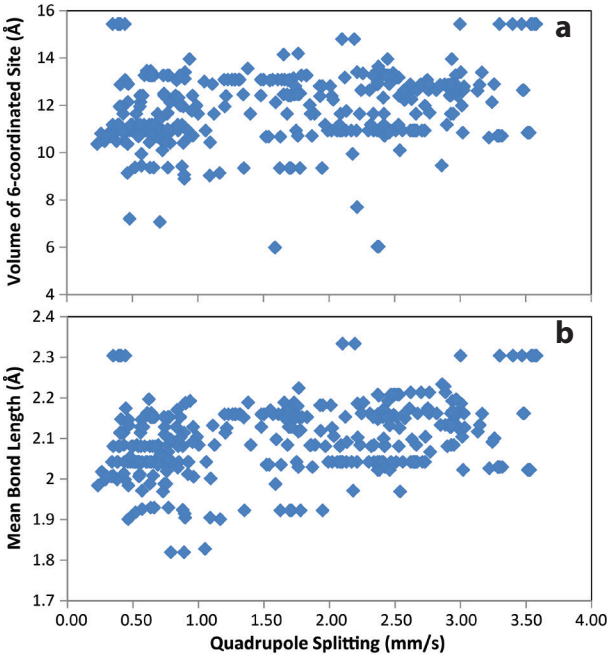

FIGURE 11. Comparison of quadrupole splitting in phosphate minerals with characteristics of the Fe coordination polyhedra. There is no observed correlation between Δ and octahedral site volume, but there is some hint that Δ may be related to mean bond length. (Color online.)

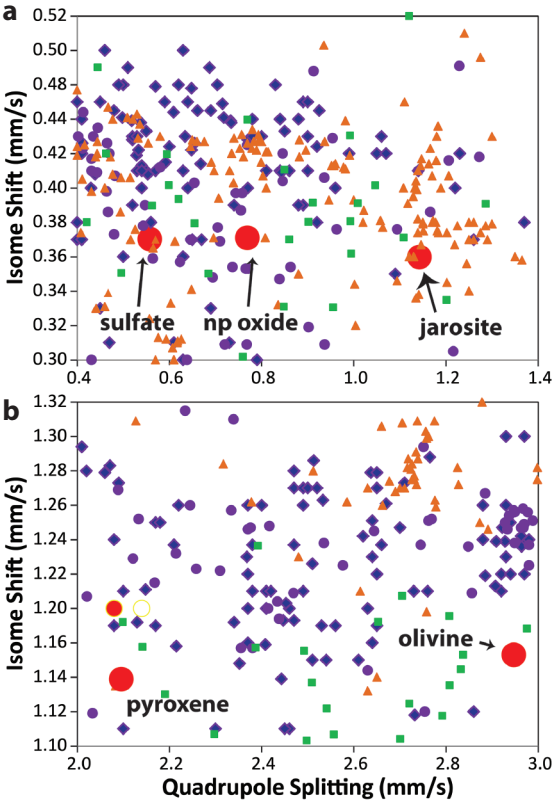

◀**FIGURE 12.** Mössbauer spectra and Fe coordination polyhedra in phosphates (purple diamonds are literature data; purple circles are data from this study), sulfates (orange triangles) from Dyar et al. (2013), and silicates and oxides (green squares) from Burns and Solberg (1990). Large red dots indicate the positions of doublets in Mössbauer spectra reported by Morris et al. (2006a, 2006b). These plots demonstrate the non-uniqueness of mineral identifications based on Mössbauer spectra alone. (Color online.)

to unequivocally assign any of the Mars doublets to specific phases on the basis of Mössbauer data alone. Of course, the team benefitted from the additional chemical data and images to make their assignments, which are very reasonable.

This conclusion illustrates why Mössbauer spectroscopy is rarely used in terrestrial applications for the purpose of mineral identification in paramagnetic minerals. Similarities among coordination polyhedra in naturally occurring minerals and the limited range of δ and Δ values for Fe^{3+} and Fe^{2+} result in so much overlap between parameters that it is difficult to distinguish contributions from coexisting minerals on the basis of Mössbauer spectra alone. Spectra of commonly occurring rock-forming minerals such as pyroxene, amphibole, and mica with octahedral sites will be generally indistinguishable because the structures are all so similar. In other words, the number of mineral species is large and the range of hyperfine parameters is limited, such that in many cases, specific phases cannot be uniquely identified with Mössbauer spectra alone. This is particularly true for Fe^{3+}-rich

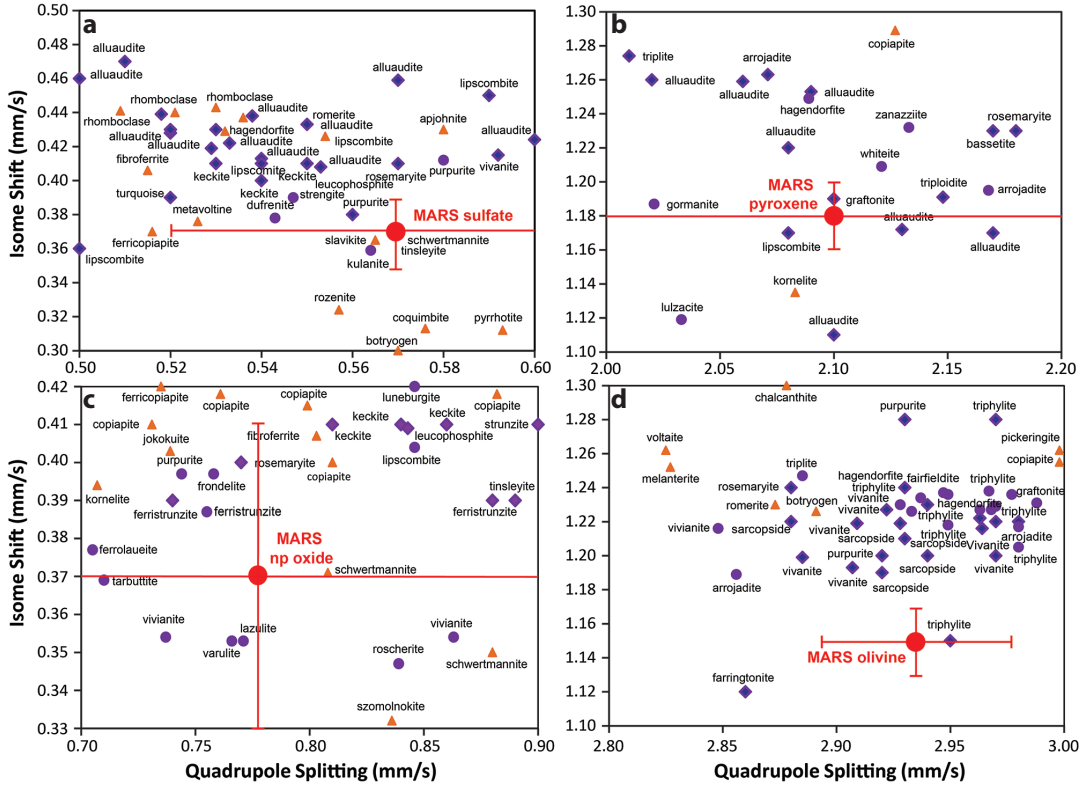

FIGURE 13. Close-up of Figure 12 showing phosphate minerals near reported positions of doublets in spectra from Mars. Errors on isomer shift and quadrupole splitting are ideally ±0.02 mm/s but may be slightly higher for Δ because its temperature shift varies with mineralogy and is thus poorly constrained. Mars data are plotted as average values with 2σ standard deviations from Morris et al. (2006b). (Color online.)

phases, because the absolute range of Mössbauer parameters for Fe^{3+} in any coordination number is so small.

On Mars, the MIMOS spectrometers were used for valence state determinations and mineral identification in conjunction with bulk chemical results from the α particle X-ray spectrometer instrument and deductions based on phase equilibria of likely martian assemblages. The success of the MER missions owes much to constraints placed on mineral identification by the Mössbauer spectrometers based on comparisons to contemporary databases of spectra. However, interpretations of Mössbauer data are such that phases can only be excluded, and unequivocal species identifications are extremely difficult for paramagnetic phases (like silicates, phosphates, and sulfates), particularly in rocks where there are multiple Fe-bearing phases.

The true strength of the Mössbauer technique lies in its ability to measure valence states and site occupancies of Fe and identify magnetic phases. Highly reproducible spectra can be acquired under a range of conditions and instrument geometries from transmission to backscatter mode, in the laboratory or on the surface of Mars. However, spectral parameters can be only qualitatively related to the geometries of the individual Fe coordination polyhedra. This study shows that Mössbauer data remain difficult to relate to specifics of the local environment around the Fe polyhedra in phosphates; the same conclusions were reached by Burns and Solberg (1990) for silicates and Dyar et al. (2013) for sulfates. Data from other techniques are still needed to facilitate accurate identifications of specific phases from Mössbauer spectroscopy of paramagnetic materials. This study provides a wealth of new data on Fe-bearing phosphate minerals to bolster future analyses of Mössbauer on Mars.

Acknowledgments

We are grateful to Ed Cloutis, the Harvard Mineralogical Museum, and the NMNH for the loan of samples, and for support from NASA Grant NNX08AP42G. Student support for this project was provided by the Massachusetts Space Grant Consortium. We thank David Palmer for help with the CrystalMaker models. Mertzman salutes the NSF for award MRI-0923224, which enabled the purchase of PANalytical XRD system X'Pert PRO equipped with a 15 position sample changer used in this study. This is PSI Contribution Number 608.

References cited

Abdu, Y.R., Hill, S.K., Fayek, M., and Hawthorne, F.C. (2011) The turquoise-chalcosiderite $Cu(Al,Fe^{3+})_6(PO_4)_4(OH)_8 \cdot 4H_2O$ solid-solution series: A Mössbauer spectroscopy, XRD, EMPA, and FTIR study. American Mineralogist, 96, 1433–1442.

Abrahams, S.C. (1966) Ferromagnetic and crystal structure of ludlamite, $Fe_3(PO_4)_2(H_2O)_4$ at 4.2 K. Journal of Chemical Physics, 44, 2230–2237.

Abrahams, S.C., and Bernstein, J.L. (1966) Crystal structure of paramagnetic ludlamite, $Fe_3(PO_4)_2 \cdot 4H_2O$, at 298K. Journal of Chemical Physics, 44, 2223–2229.

Afanasev, A.M., Gorobchenko, V.D., Kulgawczuk, D.S., and Lukashevich, I.I. (1974) Nuclear γ-resonance in iron sulphates of the jarosite group. Physica Status Solidi, 26, 697–701.

Alberti, A. (1976) The crystal structure of ferrisicklerite, $Li_{<1}(Fe^{3+},Mn^{2+})PO_4$. Acta Crystallographica, B, 31, 1522–1526.

Aldon, L., Perea, A., Womes, M., Ioncia-Bousquet, C.M., and Jumas, J.-C. (2010) Determination of the Lamb-Mössbauer factors of $LiFePO_4$ and $FePO_4$ for electrochemical in situ and operando measurements in Li-ion batteries. Journal of Solid State Chemistry, 183, 218–222.

Alves, K.M.B., Garg, R., and Garg, V.K. (1980) A Mössbauer resonance study of brasilian childrenite. Radiochemical and Radioanalytical Letters, 45, 129–132.

Amthauer, G., and Rossman, G.R. (1984) Mixed valence of iron in minerals with cation clusters. Physics and Chemistry of Minerals, 11, 37–51.

Andersson, A.S., Kalska, B., Häggström, and Thomas, J.O. (2000) Lithium extraction/insertion in LiFePO: An X-ray diffraction and Mössbauer spectroscopy study. Solid State Ionics, 130, 41–52.

Atencio, D., Matioli, P.A., Smith, J.B., Chukanov, N.V., Coutinho, J.M.V., Rastsvetaeva, R.K., and Möckel, S. (2007a) Footemineite, the Mn-analog of atencioite, from the Foote mine, Kings Mountain, Cleveland County, North Carolina, U.S.A., and its relationship with other roscherite-group minerals. American Mineralogist, 93, 1–6.

Atencio, D., Chukanov, N.V., Coutinho, J.M.V., Menezes, L.A.D., Dubinchuk, V.T., and Möckel, S. (2007b) Ruifrancoite, a new Fe^{3+}-dominant monoclinic member of the roscherite group from Galileia, Minas Gerais, Brazil. Canadian Mineralogist, 45, 1263–1273.

Axelrod, J.M., Carron, M.K., Milton, C., and Thayer, T.P. (1952) Phosphate mineralization at Bomi Hill and Bambuta, Liberia, West Africa. American Mineralogist, 37, 883–909.

Banin, A., Clark, B.C., and Wänke, H. (1992) Surface chemistry and mineralogy. In H.H. Kieffer, B.M. Jakosky, C.W. Snyder, and M.S. Matthews, Eds., Mars, pp. 594–625. University of Arizona Press, Tucson.

Baran, E.J., Mercader, R.C., Massaferro, A., and Kremer, E. (2004) Vibrational and ^{57}Fe-Mössbauer spectra of some mixed cation diphosphates of the type $M^{II}Fe^{III}_2(P_2O_7)_2$. Spectrochimica Acta A, 60, 1001–1005.

Barinova, A.V., Rastsvetaeva, R.K., Chukanov, N.V., and Pietraszko, A. (2004) Refinement of the crystal structure of Zn-containing greifensteinite. Crystallography Reports, 49, 942–945.

Belov, N.V., Gavrilova, G.S., Solovieva, L.P., and Khalilov, A.D. (1977) More precisely determined structure of lomonosovite. Doklady Akademii Nauk USSR, 235, 1064–1067.

Bennett, T.J. (1980) Crystal structure of paradamite. American Mineralogist, 353–354.

Bjoerling, C., and Westgren, A. (1938) Minerals of the Varutrask pegmatite. IX. X-ray studies on triphylite, varulite, and their oxidation products. Geologiska Foreningens i Stockholm Forhandlingar, 60, 67–72.

Blount, A.M. (1974) The crystal structure of crandallite. American Mineralogist, 59, 41–47.

Boctor, N.Z., Wang, J., Alexander, C.M.O., Hauri, E., Bertka, C.M., and Fei, Y. (1998) Hydrogen-isotopic studies of carbonate and phosphate in Martian meteorite Allan Hills 84001. Meteoritics and Planetary Science, 33, A18–A19.

Bouvier, A., Blichert-Toft, J., Vervoort, J.D., and Albarède, F. (2005) The age of SNC meteorites and the antiquity of the Martian surface. Earth and Planetary Science Letters, 240, 221–233.

Bridges, J.C., and Grady, M.M. (1999) A halite-anhydrite-chlorapatite assemblage in Nakhla: Mineralogical evidence for evaporates on Mars. Meteoritics and Planetary Science, 34, 407–415.

Bridges, J.C., and Warren, P.H. (2003) The SNC meteorites: Basaltic igneous processes on Mars, Journal of the Geological Society, 163, 229–251.

Bridson, J.N., Quinlan, S.E., and Tremaine, P.R. (1998) Synthesis and crystal structure of maricite and sodium iron(III) hydroxyphosphate. Chemistry of Materials, 10, 763–768.

Brückner, J., Dreibus, G., Gellert, R., Squyres, S., Wänke, H., Yen, A., and Zipfel, J. (2008) Mars Exploration Rovers: Chemical composition by the APXS. In J. Bell, Ed., The Martian Surface, 58–101. Cambridge University Press, New York.

Burns, R.G. (1981) Intervalence transitions in mixed-valence minerals of iron and titanium. Annual Review of Earth and Planetary Sciences, 9, 345–383.

Burns, R.G., and Solberg, T.C. (1990) ^{57}Fe-bearing oxide, silicate, and aluminosilicate minerals, crystal structure trends in Mossbauer spectra, in L.M. Coyne, S.W.S. McKeever, and D.F. Blake, Spectroscopic Characterization of Minerals and their Surfaces, 415, pp. 262–283. American Chemical Society, Washington, D.C.

Burns, R.G., Nolet, D.A., Parkin, K.M., McCammon, C.A., and Schwartz, K.B. (1980) Mixed valence minerals of iron and titanium: Correlations of structural, Mössbauer, and electronic spin data. NATO Advanced Study Institute Series, C, 58, 295–336.

Bustamante, A., Mattievich, E., de Amoim, H.S., Vencato, I., and Silviera, M.M. (2005) The Mössbauer spectrum of synthetic hureaulite: $Fe^{2+}_5(H_2O)_4(PO_4H)_2(PO_4)_2$. Hyperfine Interactions, 166, 599–603.

Calvo, C. (1968) The crystal structure of graftonite. American Mineralogist, 53, 742–750.

Cámara, F., Oberti, R., Chopin, C., and Medenbach, O. (2006) The arrojadite enigma: I. A new formula and a new model for the arrojadite structure. American Mineralogist, 91, 1249–1259.

Cámara, F., Sokolova, E., Hawthorne, F.C., and Abdu, Y. (2008) From structure topology to chemical composition. IX. Titanium silicates: revision of the crystal chemistry of lomonosovite and murmanite, Group-IV minerals. Mineralogical Magazine, 72, 1207–1228.

Campbell, J.L., Lee, M., Jones, B.N., Andrushenko, S.M., Holmes, N.G., Maxwell, J.A., and Taylor, S.M. (2009) A fundamental parameters approach to calibration of the Mars Exploration Rover alpha particle X-ray spectrometer. Journal of Geophysical Research, 114, E04006, doi: 10.1029/2008JE003272.

Catti, M., Ferraris, G., and Ivaldi, G. (1979) Refinement of the crystal structure of anapaite, $Ca_2Fe(PO_4)_2 \cdot 4H_2O$—Hydrogen bonding and relationships with the bihydrated phase. Bulletin de Minéralogie, 102, 314–318.

Chandra, S., and Hoy, G.R. (1967) Detection of two internal magnetic fields in $Fe_3(PO_4)_2 \cdot 4H_2O$. Physical Letters, 24A, 377–378.

Chandrasekhar, A.V., Ramanaiah, M.V., Reddy, B.J., Reddy, Y.P., Rao, P.S., and Ravikumar, R.V.S.S.N. (2003) Optical and EPR studies of iron bearing phosphate miernals: satterylite and gormanite from Yukon Territory, Canada. Spectrochimnimca Acta A, 2115–2121.

Chopin, C., Oberti, R., and Cámara, F. (2006) The arrojadite enigma: II. Compositional space, new members, and nomenclature of the group. American Mineralogist, 91, 1260–1270.

Chukanov, N.V., Pekov, I.V., Möckel, S., Xadov, A.E., and Dubinchuk, V.T. (2007)

Zinclipscombite, $ZnFe_2^{3+}(PO_4)_2(OH)_2$, a New Mineral Species. Geology of Ore Deposits, 49, 509–513.

Chukanov, N.V., Scholz, R., Aksenov, S.M., Rastsvetaeva, R.K., Pekov, I.V., Belakovskiy, D.I., Krambrock, K., Paniago, R.M., Righi, A., Martins, R.F., Belotti, F.M., and Bermanec, V. (2012) Metavivianite, $Fe^{2+}Fe_2^{3+}(PO_4)_2(OH)_2 \cdot 6H_2O$: new data and formula revision. Mineralogical Magazine, 76, 725–741.

Cid-Dresdner, H. (1964) The determination and refinement of the crystal structure of turquoise, $CuAl_6(PO_4)_4(OH)_8 \cdot 4H_2$. Zeitschrift für Kristallogtaphie, 121, 87–113.

——— (1965) X-ray study of chalcosiderite, $CuFe_6(PO_4)_4(OH)_8 \cdot 4H_2O$. American Mineralogist, 50, 227–231.

Clark, A.M., Fejer, E.E., Couper, A.G., von Knorring, O., Turner, R.W., and Barstow, R.W. (1983) Iron-rich roscherite from Gunnislake, Cornwall. Mineralogical Magazine, 47, 81–83.

Clark, B.C., Baird, A.K., Weldon, R.J., Tsusaki, D.M., Schnabel, L., and Candelaria, M.P. (1982) Chemical composition of Martian fines. Journal of Geophysical Research, 87, 10059–10067.

Clark, B.C., Morris, R.V., McLennan, S.M., Gellert, R., Joliff, B., Knoll, A.H., Squyres, S.W., Lowenstein, T.K., Ming, D.W., Tosca, N.J., and others. (2005) Chemistry and mineralogy of outcrops at Meridiani Planum. Earth and Planetary Science Letters, 240, 73–94.

Cocco, G., Fanfani, L., and Zanazzi, P.F. (1966) The crystal structure of tarbuttite, $Zn_2(OH)PO_4$. Zeitschrift für Kristallographie, 123, 312–329.

Coda, A., Giuseppetti, G., Tadini, C., and Carobbi, S.G. (1967) The crystal structure of Wagnerite. Atti della Accademia Nazionale dei Lincei, 43, 212–224.

Cooper, M., and Hawthorne, F.C. (1994) Refinement of the crystal-structure of kulanite. Canadian Mineralogist, 32, 15–19.

Corbin, D.R., Whitney, J.F., Fultz, W.C., Stucky, G.D., Eddy, M.M., and Cheetham, A.K. (1986) Synthesis of open-framework transition metal phosphates using organometallic precursors in acidic media—Preparation and structural characterization of $Fe_3P_4O_{20}H_{10}$ and $NaFe_3P_3O_{12}$. Inorganic Chemistry, 25, 2279–2280.

Da Costa, G.M., and Viana, R.R. (2001) The occurrence of tinsleyite in the archaeological site of Santana do Riacho, Brazil. American Mineralogist, 86, 1053–1056.

De Grave, E., and Vochten, R. (1988) Temperature dependence of the Mössbauer effect in iron uranyl phosphate. Hyperfine Interactions, 39, 107–116.

De Grave, E., Vochten, R., Desseyn, H.O., and Chambäre, D.C. (1980) Analysis of some oxidized vivianites. Journal de Physique Colloques, 41, C1-407–C1-408.

de Resende, V.G., da Costa, G.M., De Grave, E., and Van Alboom, A. (2008) Mössbauer spectroscopic study of synthetic leucophosphite, $KFe_2(PO_4)_2(OH) \cdot 2H_2O$. American Mineralogist, 93, 483–487.

Deniard, P., Dulac, A.M., Rocquefelte, X., Grigorov, V., Lebacq, O., Pasturel, A., and Jobic, S. (2004) High potential positive materials for lithium–ion batteries: transition metal phosphates. Journal of Physics and Chemistry of Solids, 65, 229–233.

Dick, S. (1999) Über die Struktur von synthetischem Tinsleyit $K(Al_2(PO_4)_2(OH)(H_2O)) \cdot (H_2O)$. Zeitschrift für Naturforschung, 54, 1358–1390.

Dormann, J.L., and Poullen, J.F. (1980) Étude par spectroscopie Mössbauer de vivianites oxydees naturelles. Bulletin de Minéralogie, 103, 633–639.

Dreibus, G., and Haubold, R. (2004) Phosphorus sorption by terrestrial basalt and granite and implications for the Martian crust. Icarus, 167, 166–169.

Dreibus, G., Jagoutz, E., Spettel, B., and Wänke H. (1996) Phosphate-mobilization on Mars? Implications from leach experiments on SNCs. In Lunar and Planetary Science Conference XXVII, Abstract 323, Lunar and Planetary Institute, Houston.

Duggan, M.D., Jones, M.T., Richards, D.N.G., and Kamprad, J.L. (1990) Phosphate minerals in altered andesite from Mount Perry, Queensland, Australia. Canadian Mineralogist, 28, 125–131.

Dyar, M.D. (1984) Precision and interlaboratory reproducibility of measurements of the Mössbauer effect in minerals. American Mineralogist, 69, 1127–1144.

Dyar, M.D. Agresti, D.G., Schaefer, M., Grant, C.A., and Sklute, E.C. (2006) Mössbauer spectroscopy of earth and planetary materials. Annual Reviews of Earth and Planetary Science, 34, 83–125.

Dyar, M.D., Schaefer, M.W., Sklute, E.C., and Bishop, J.L. (2008) Mössbauer spectroscopy of phyllosilicates: Effects of fitting models on recoil-free fractions and redox ratios. Clay Minerals, 43, 3–33.

Dyar, M.D., Breves, E.A., Jawin, E.R., Marchand, G.J., Nelms, M., O'Connor, V., Peel, S., Rothstein, Y., Sklute, E., Lane, M.D., Bishop, J.L., and Mertzman, S. (2013) Mössbauer parameters of iron in sulfate minerals. American Mineralogist, 98, 1943–1965.

Eeckhout, S.G., De Grave, E., Vochten, R., and Blaton, N.M. (1999) Mössbauer effect study of anapaite, $Ca_2Fe^{2+}(PO_4)_2 \cdot 4H_2O$, and of its oxidation products. Physics and Chemistry of Minerals, 26, 506–512.

Elliott, P., Kotlitsch, U., Giester, G., Libowitzky, E., McCammon, C., Pring, A., Birch, W.D., and Brugger, J. (2009) Description and crystal structure of a new mineral plimerite, $ZnFe_4^{3+}(PO_4)_3(OH)_5$- the Zn-analogue of rockbridgeite and frondelite, from Broken Hill, New South Wales, Australia. Mineralogical Magazine, 73, 131–148.

Ercit, T.S., Cooper, M.A., and Hawthorne, F.C. (1998) The crystal structure of vuonnemite, $Na_{11}Ti^{4+}Nb_2(Si_2O_7)_2(PO_4)_2O_3(F,OH)$, a phosphate-bearing sorosilicate of the lomonosovite group. The Canadian Mineralogist, 36, 1311–1320.

Ericsson, T., and Khangi, F. (1988) An investigation of $Fe_3(PO_4)_2$–sarcopside between 1.6K-721K: Comparison with fayalite. Hyperfine Interactions, 41, 783–786.

Evans, R.J., and Groat, L.A. (2012) Structure and topology of dumortierite and dumortierite-like materials. The Canadian Mineralogist, 50, 1197–1231.

Ewald, B., Öztan, Y., Prots, Y., and Kniep, R. (2005) Structural patterns and dimensionality in magnesium borophosphates: The crystal structures of $Mg_3(H_2O)[BP_3O_9(OH)_4]$ and $Mg(H_2O)_2[B_2P_2O_8(OH)_2 \cdot H_2O]$. Zeitschrift für Anorganische und Aligemeine Chemie, 631, 1615–1621.

Fanfani, L., Nunzi, A., and Zanazzi, P.F. (1970) Crystal structure of fairfieldite. Acta Crystallographica B, 26, 640–645.

Fanfani, L., Nunzi, A., Zanazzi, P.F., and Zanzari, A.R. (1975) Crystal structure of roscherite. Tschermaks Mineralogische und Petrographische Mitteilunger, 22, 266–277.

Fanfani, L., Zanazzi, P.F., and Zanzari, A.R. (1977) Crystal structure of a triclinic roscherite. Tschermaks Mineralogische und Petrographische Mitteilunger, 24, 169–178.

Fanfani, L., Tomassini, M., Zanazzi, P.F., and Zanzari, A.R. (1978) The crystal structure of strunzite, a contribution to the crystal chemistry of basic ferric-manganous hydrated phosphates. Tschermaks Mineralogische und Petrographische Mitteilungen, 25, 77–87.

Fehr, K.T., Hochleitner, R., Schmidbauer, E., and Schneider, J. (2007) Mineralogy, Mössbauer spectra and electrical conductivity of triphylite $Li(Fe^{2+},Mn^{2+})PO_4$. Physics and Chemistry of Minerals, 34, 485–494.

Fehr, K.T., Hochkeitner, R., Laumann, A., Schmidbauer, E., and Schneider, J. (2010) Mineralogy, Mössbauer spectroscopy and electrical conductivity of heterosite (Fe^{3+}, Mn^{3+})PO_4. Physics and Chemistry of Minerals, 37, 179–189.

Fejdi, P., Poullen, J.F., and Gasperin, M. (1980) Affinement de la structure de la vivianite $Fe_3(PO_4)_2 \cdot 8H_2O$. Bulletin de Mineralogie 103, 135–138.

Finney, J.J. (1966) The unit cell of tarbuttite, $Zn_2(PO_4)(OH)$, and paradamite, $Zn_2(AsO_4)(OH)$. American Mineralogist, 51, 1218–1220.

Fleck, M., and Kolitsch, U. (2003) Natural and synthetic compounds with kröhnkite-type chains. An update. Zeitschrift für Kristallographie, 218, 553–567.

Foley, N.C., Economou, T., and Clayton, R.N. (2003) Final chemical results from the Mars Pathfinder alpha proton X-ray spectrometer. Journal of Geophysical Research, 108, 8096, doi: 10.1029/2002JE002019.

Foord, E.E., and Taggart, J.E. Jr. (1998) A reexamination of the turquoise group: The mineral aheylite, planerite (redefined), turquoise and coeruleolactite. Mineralogical Magazine, 62, 93–111.

Forsyth, J.B., Wilkinson, C., and Paster, S. (1990) Magnetism in ludlamite, $Fe_3(PO_4)_2 \cdot 4H_2O$. Journal of Physics: Condensed Matter, 2, 8381–8390.

Gellert, R., Rieder, R., Anderson, R.C., Brückner, J., Clark, B.C., Dreibus, G., Economou, T., Klingelhöfer, G., Lugmair, G.W., Ming, D.W., and others. (2004) Chemistry of rocks and soils in Gusev crater from the alpha particle X-ray spectrometer. Science, 305, 829–832.

Gellert, R., Rieder, R., Brückner, J., Clark, B.C., Dreibus, G., Klingelhöfer, G., Lugmair, G., Ming, D.W., Wänke, H., Yen, A., Zipfel, J., and Squyres, S.W. (2006) Alpha Particle X-Ray Spectrometer (APXS): Results from Gusev crater and calibration report. Journal of Geophysical Research, 111, E02S05, doi:10.1029/2005JE002555.

Genkina, E.A., Maksimov, B.A., and Mel'nikov, O.K. (1985) Crystal structure of synthetic tarbittite. Doklady Akademii nauk SSSR, 282, 314–317.

Giuseppetti, G., and Tadini, C. (1984) The crystal structure of childrenite from Tavistock (SW England) $Ch_{89}Eo_{11}$ term of children-eosphorite series. Neues Jahrbuch für Mineralogie Monatshefte, 6, 263–271.

Giuseppetti, G., Mazzi, F., and Tadini, C. (1989) The crystal structure of chalcosiderite, $CuFe_6(PO_4)_4(OH)_8 \cdot 4H_2O$. Neues Jahrbuch für Mineralogie Monatschefte, 5, 227–239.

Glass, J.J., and Vhay, J.S. (1949) A new locality for ludlamite. American Mineralogist, 34, 335–336.

Gonser, U., and Grant, R.G. (1967) Determination of spin directions and electric field gradient axes in vivianite by polarized recoil-free gamma rays. Physica Status Solidi, 21, 331–342.

Gooding, J.L. (1992) Soil mineralogy and chemistry on Mars: Possible clues from salts and clays in SNC meteorites, Icarus, 99, 28–41.

Gooding, J.L., and Wentworth, S.J. (1991) Origin of "white druse" salts in the EET79001 meteorite. In Lunar and Planetary Science Conference XXII, Abstract 461, Lunar and Planetary Institute, Houston.

Gooding, J.L., Wentworth, S.J., and Zolensky, M.E. (1988) Calcium carbonate and sulfate of possible extraterrestrial origin in the EETA79001 meteorite. Geochimica et Cosmochimica Acta, 52, 909–915.

Goreaud, M., and Raveau, B. (1980) Alunite and crandallite: A structure derived from that of pyrochlore. American Mineralogist, 65, 953–956.

Greenwood, J.P., and Blake, R.E. (2006) Evidence for an acidic ocean on Mars from phosphorus geochemistry of Martian soils and rocks. Geology, 34, 953–956.

Greenwood, J.P., Blake, R.E., and Coath, C.D. (2003) Ion microprobe measurements of $^{18}O/^{16}O$ ratios of phosphate minerals in the martian meteorites ALH84001 and Los Angeles. Geochimica et Cosmochimica Acta, 67, 2289–2298.

Grey, I., Mumme, W.G., Neville, S.M., Wuilson, N.C., and Birch, W.D. (2010) Jahnsite-whiteite solid solutions and associated minerals in the phosphate pegmatite at Hagendorf-Süd, Bavaria, Germany. Mineralogical Magazine, 74, 969–978.

Grodzicki, M., Redhammer, G.J., Amthauer, G., Schünemann, V., Trautwein, A.X., Velickov, B., and Schmid-Beurmann, P. (2003) Electronic structure of Fe-bearing lazulites. American Mineralogist, 88, 481–488.

Guidry, M.W., and Mackenzie, F.T. (2003) Experimental study of igneous and sedimentary apatite dissolution: Control of pH, distance from equilibrium, and temperature on dissolution rates. Geochimica et Cosmochimica Acta, 67, 2949–2963.

Hanzel, D., Meisel, W.P.E., Hanzel, D., and Gütlich, P. (1990a) Mössbauer effect study of the oxidation of vivianite. Solid State Communications, 76, 307–310.
——— (1990b) Conversion electron Mössbauer study of vacuum and thermally treated vivianite. Hyperfine Interactions, 57, 2201–2207.
Hatert, F., Keller, P., Lissner, F., Antenucci, D., and Fransolet, A.M. (2000) First experimental evidence of alluaudite-like phosphates with high Li-content: the $(Na_{1-x}Li_x)MnFe_2(PO_4)_3$ series (x = 0 to 1). European Journal of Mineralogy, 12, 847–857.
Hatert, F., Hermann, R.P., Long, G.J., Fransolet, A.-M., and Grandjean, F. (2003) An X-ray Rietveld, infrared, and Mössbauer spectral study of the $NaMn(Fe_{1-x}In_x)_2(PO_4)_3$ alluaudite-type solid solution. American Mineralogist, 88, 211–222.
Hatert, F., Long, G.J., Hautot, D., Fransolet, A.-M., Delwiche, J., Hubin-Franskin, M.J., and Grandjean, F. (2004) A structural, magnetic, and Mössbauer spectral study of several Na-Mn-Fe-bearing alluaudites. Physics and Chemistry of Minerals, 31, 487–506.
Hatert, F.D., Lefevre, P., Fransolet, A.M., Spirlet, M.R., Rebbouth, L., Fontan, F., and Keller, P. (2005) Ferrorosemaryite, $NaFe^{2+}Fe^{3+}Al(PO_4)_3$, a new phosphate mineral from the Rubindi pegmatite, Rwanda. European Journal of Mineralogy, 17, 749–759.
Hatert, F., Hermann, R.P., Fransolet, A,-M., Long, G.J., and Grandjean, F. (2006) A structural, infrared, and Mössbauer study of rosemaryite, $NaMnFe^{3+}Al(PO_4)_3$. European Journal of Mineralogy, 18, 775–785.
Hatert, F., Ottolini, L., Wouters, J., and Fontan, F. (2012) A structural study of the lithiophilite-sicklerite series. The Canadian Mineralogist, 50, 843–854.
Hausrath, E.M., Golden, D.C., Morris, R.V., Agresti, D.G., and Ming, D.W. (2013) Acid sulfate alteration of fluorapatite, basaltic glass, and olivine by hydrothermal vapors and fluids: Implications for fumarolic activity and secondary phosphate phases in sulfate-rich Paso Robles soil at Gusev Crater, Mars. Journal of Geophysical Research, 118, 1–13.
Hawthorne, F.C. (1979) Paradamite. Acta Crystallographica B, 35, 720–722.
Hermann, R.P., Hatert, F., Fransolet, A.-M., Long, G.J., and Grandjean, F. (2002) Mössbauer spectra evidence for next-nearest neighbor interactions within the alluaudite structure of $Na_{1-x}Li_xMnFe_2(PO_4)_3$. Solid State Sciences, 4, 507–513.
Herwig, S., and Hawthorne, F.C. (2006) The topology of hydrogen bonding in brandtite, coliinsite, and fairfieldite. Canadian Mineralogist, 44, 1181–1196.
Hochleitner, R., and Fehr, K.T. (2010) The keckite problem and its bearing on the crystal chemistry of the jahnsite group: Mössbauer and electron-microprobe studies. The Canadian Mineralogist, 48, 1445–1453.
Hrynkiewicz, A.Z., and Kulgawczuk, D.S. (1964) Hyperfine structure of the 14.4 keV gamma line of ^{57}Fe in some iron oxy-hydroxides investigated with the Mössbauer effect. Acta Physica Polonica, 24, 689–692.
Hrynkiewicz, A.Z., Kubisz, J., and Kulgawczuk, D.S. (1965) Quadrupole splitting of the 14.4 keV gamma line of ^{57}Fe in iron sulphates of the jarosite group. Journal of Inorganic Nuclear Chemistry, 27, 2513–2517.
Hui, H.J., Peslier, A.H., Lapen, T.J., Shafer, J.T., Brandon, A.D., and Irving, A.J. (2011) Petrogenesis of basaltic shergottite Northwest Africa 5298: Closed-system crystallization of an oxidized mafic melt. Meteoritics and Planetary Science, 46, 1313–1328.
Huminicki, D.M.C., and Hawthorne, F.C. (2002) The crystal chemistry of phosphate minerals. In M.L. Kohn, J. Rakovan, and J.M. Hughes, Eds., Phosphates, 48, 123–253. Reviews in Mineralogy and Geochemistry, Mineralogical Society of America, Chantilly, Virginia.
Hurowitz, J.A., McLennan, S.M., Tosca, N.J., Arvidson, R.E., Michalski, J.R., Ming, D.W., Schröder, C., and Squyres, S.W. (2006) In situ and experimental evidence for acidic weathering of rocks and soils on Mars. Journal of Geophysical Research, 111, E02S19, doi:10.1029/2005JE002515.
Ikeda, Y., Kimura, M., Takeda, H., Shimoda, G., Kita, N.T., Morishita, Y., Suzuki, A., Jagoutsz, E., and Dreibus, G. (2006) Petrology of a new basaltic meteorite. Antactica Meteorite Research, 19, 20–44.
Ito, T., and Mori, H. (1951) The crystal structure of ludlamite. Acta Crystallographica, 4, 412–416.
Janot, C., Chabanel, M., and Herzog, Ch. (1968a) Étude par effet Mössbauer des constituants d'une limonite phosphoreuse provenant d'une Minette Lorraine. Comptes Rendus Hebdomadaires des Seances de l'Academie des Sciences, C, 266, 103–106.
——— (1968b) Étude d'une limonite par effet effet Mössbauer. Bulletin de la Société Française de Minéralogie et de Crystallographie, 91, 166–171.
Jull, A.J., Donahue, D.J., Swindle, T.D., Burkland, M.K., Herzog, G.F., Albrecht, A., Klein, J., and Middleton, R. (1995) Isotopic composition of carbonate in the SNC meteorites. Meteoritics, 30, 311–318.
Kampf, A.R., Colombo, F., and del Tanago, J.G. (2010) Gayite, a new dufrénite-group mineral from the Gigante granitic pegmatite, Córdoba province, Argentina. American Mineralogist, 95, 386–391.
Kang, B., and Ceder, G. (2009) Battery materials for ultrafast charging and discharging. Nature, 458, 190–193.
Khalilov, A.D., and Makarov, E.S. (1966) Crystal chemistry of murmanite-lomonosovite group of minerals. Geochemistry International USSR, 3, 197–208.
Khalilov, A.D., Makarov, E.S., Mamedov, K.S., and Pyanzina, L.Y. (1965) On the crystalline structure of minerals of mourmanite-lomonosovite group. Doklady Akademii Nauk USSR, 162, 179–185.
Klingelhöfer, G., Morris, R.V., Bernhardt, B., Rodionov, D., de Souza, P.A. Jr., Squyres, S.W., Foh, J., Kankeleit, E., Bonnes, U., and others. (2003) Athena MIMOS II Mössbauer spectrometer investigation. Journal of Geophysical Research, 108, DOI: 10.1029/2003JE002138.
Klingelhöfer, G., Morris, R.V., Bernhardt, B., Schröder, C., Rodionov, D.S., deSouza, P.A., Yen, A., Gellert, R., Evlanov, E.N., Zubkov, B., and others. (2004) Jarosite and hematite at Meridiani Planum from Opportunities Mössbauer spectrometer. Science, 306, 1740–1745.
Kolitsch, U., Andrut, M., and Giester, G. (2002) Satterlyite, $(Fe,Mg)_{12}(PO_3OH)(PO_4)_5(OH,O)_6$: Crystal structure and infrared absorption spectra. European Journal of Mineralogy, 14, 127–133.
Korzenski, M.B., Schimek, G.L., Kolis, J.W., and Long, G.J. (1998) Hydrothermal synthesis, structure, and characterization of a mixed-valent iron(II/III) phosphate, $NaFe_{3.67}(PO_4)_3$: A new variation of the alluaudite structure type. Journal of Solid State Chemistry, 139, 152–160.
Kostiner, E. (1972) A Mössbauer effect study of triplite and related minerals. American Mineralogist, 57, 1109–1114.
Kovács, K., Kuzmann, E., Homonnay, Z., Vértes, A., Gunneriusson, L., and Sandstron, A. (2008) Mössbauer study of synthetic jarosites. Hyperfine Interactions, 186, 69–73.
Lane, M.D., Bishop, J.L., Dyar, M.D., King, P.L., Parente, M., and Hyde, B.C. (2008) Mineralogy of the Paso Robles soils on Mars. American Mineralogist, 93, 728–739.
Le Bail, A., Stephens, P.W., and Hubert, F. (2003) A crystal structure for the souzalite/gormanite series from synchrotron powder diffraction data. European Journal of Mineralogy, 15, 719–723.
Le Page, Y., and Donnay, G. (1977) The crystal structure of the new mineral maricite $NaFePO_4$. Canadian Mineralogist, 15, 518–521.
Leavens, P.B., White, J.S., and Nelen, J.A. (1990) Zanazziite a new mineral from Minas Gerais Brazil. The Mineralogical Record, 21, 413–417.
Léone, P., Palvadeau, P., and Moëlo, Y. (2000) Structure cristalline d'un nouvel hydroxyphosphate naturel de strontium, fer et aluminium (lulzacite), $Sr_2Fe(Fe_{0.63}Mg_{0.37})_2Al_4(PO_4)_4(OH)_{10}$. Chimie de l'etat Solide et Cristallochimie, 3, 301–308.
Lerman, A., Stiller, M., and Hermon, E. (1967) Mössbauer quantitative analyses of Fe^{3+}/Fe^{2+} ratios in some phosphates and oxide mixtures: possibilities and limitations. Earth and Planetary Science Letters, 3, 409–416.
Li, Z., and Shinno, I. (1997) Next nearest neighbor effects in triphylite and related phosphate minerals. Mineralogical Journal, 19, 99–107.
Li, Z., Zuezheng, Z., Danian, Y., and Wei, H. (1986) The next nearest neighbor effect on the octahedral ferric iron in purpurite. Kexue Tongbao, 31, 1192–1194.
Liferovich, R.P., Sokolova, E.V., Hawthorne, F.C., Laajoki, K.V.O., Gehor, S., Pakhomovsky, Y.A., and Sorokhtina, N.V. (2000) Gladiusite, $Fe_2^{2+}(Fe^{2+},Mg)_4(PO_4)(OH)_{11}(H_2O)$, a new hydrothermal mineral species from the phoscorite-carbonatite unit, Kovdor complex, Kola Peninsula, Russia. Canadian Mineralogist, 38, 1477–1485.
Lindberg, M.L. (1957) Leucophosphite from the Sapucaia pegmatite mine, Minas Gerais, Brazil. American Mineralogist, 42, 214–221.
——— (1958) The beryllium content of roscherite from the Sapucaia pegmatite mine, Minas Gerais, Brazil, and from other localities. American Mineralogist, 43, 824–838.
Lindberg, M.L., and Christ, C.L. (1959) Crystal structures of the isostructural minerals lazulite, scorzalite, and barbosalite. Acta Crystallographica, 12, 695–697.
Liu, Z., Dong, D., Liu, M., Sui, Y., Su, W., Qian, Z., and Li, Z. (2005) Quadrupole splitting distributions in purpurite and related minerals. Hyperfine Interactions, 163, 13–27.
Losey, A., Rakovan, J.F., Hughes, J.M., Francis, C.A., and Dyar, M.D. (2004) Structural variationin the lithiophilite-triphylite series and other olivine-group structures. The Canadian Mineralogist, 42, 1105–1115.
Massa, W., Yakubovich, O.V., Kireev, V.V., and Mel'nikov, O.K. (2000) Crystal structure of a new vanadate variety in the lomonosovite group: $Na_5Ti_2O_2[Si_2O_7](VO_4)$. Solid State Sciences, 2, 615–623.
Mattievich, E., and Danon, J. (1971) Use of Mössbauer spectroscopy in the study of fossils. Notas de Fisica, 17, 237–253.
——— (1977) Hydrothermal synthesis and Mössbauer studies of ferrous phosphates of the homologous series $Fe_3^{2+}(PO_4)_2 \cdot 2(H_2O)$. Journal of Inorganic Nuclear Chemistry, 39, 569–580.
Mattievich, E., Vugman, N.V., Diehl, L.M.A., and Danon, J. (1979) Analytical interpretation of temperature-dependent combined quadrupole and magnetic hyperfine interaction in $Fe^{2+}Fe_2^{3+}(PO_4)_2(OH)_2$ (barbosalite). Journal de Physique, 40, 1195–1198.
McCammon, C.A., and Burns, R.G. (1980) The oxidation mechanism of vivianite as studied by Mössbauer spectroscopy. American Mineralogist, 65, 361–366.
McCoy, T.J., Wadhwa, M., and Keil, K. (1999) New lithologies in the Zagami meteorite: Evidence for fractional crystallization of a single magme unit on Mars. Geochimica et Cosmochimica Acta, 63, 1249–1262.
McGlynn, I.O., Fedo, C.M., and McSween, H.Y. (2012) Soil mineralogy at the Mars Exploration Rover landing sites: An assessment of the competing roles of physical sorting and chemical weathering. Journal of Geophysical Research—Planets, 177, E01006, DOI: 10.1029/2011JE003861.
McSween, H.Y. Jr. (1994) What we have learned about Mars from SNC meteorites. Meteoritics, 29, 757–779.
McSween, H.Y. Jr., Eisenhour, D.D., Taylor, L.A., Wadhwa, L.A., and Crozaz, G. (1996) QUE94201 shergottite: Crystallization of a martian basaltic magma. Geochimica et Cosmochimica Acta, 60, 4563–4569.
Millet, J.M.M., Rouzies, D., and Vedrine, J.C. (1995) Isobutyric acid oxidative dehydrogenation over iron hydroxyphosphates. II. Tentative description of the catalytic sited based on Mössbauer spectroscopic study. Applied Catalysis A, 124, 205–219.
Ming, D.W., Mittlefehldt, D.W., Morris, R.V., Golden, D.C., Gellert, R., Yen, A., Clark, B.C., Squyres, S.W., Farrand, W.H., Ruff, S.W., and others. (2006) Geochemical and

mineralogical indicators for aqueous processes in the Columbia Hills of Gusev crater, Mars. Journal of Geophysical Research, 111, E02S12, doi:10.1029/2005JE002560.
Mittlefehldt, D.W. (1994) ALH84001, a cumulate orthopyroxenite member of the Martian meteorite clan. Meteoritics, 29, 214–221.
Moëlo, Y., Lasnier, B., Palvadeau, P., Léone, P., and Fontan, F. (2000) Lulzacite, $Sr_2Fe^{2+}(Fe^{2+},Mg)_2Al_4(PO_4)_4(OH)_{10}$, a new strontium phosphate (Saint Aubin-des-Châteaux, Loire-Atlantique, France). Comptes rendus de l'Académie des sciences. Série II, Sciences de la terre et des planets, 330, 317–324.
Mojzsis, S.J., and Arrhenius, G. (1998) Phosphate and carbon on Mars: Exobiological implications and sample return considerations. Journal of Geophysical Research, 103, 28495–28511.
Moore, P.B. (1964) Investigations of landesite. American Mineralogist, 69, 1122–1125.
——— (1965) The crystal structure of laueite, $Mn^{2+}Fe^{3+}_5(OH)_2(PO_4)_2(H_2O)_8 \cdot 2H_2O$. American Mineralogist, 50, 1884–1892.
——— (1966) The crystal structure of metastrengite and its relationship to strengite and phosphophyllite. American Mineralogist, 51, 168–176.
——— (1970) Crystal chemistry of the basic iron phosphates. American Mineralogist, 55, 135–169.
——— (1971a) Crystal chemistry of the alluaudite structure type: Contribution to the paragenesis of pegmatite phosphate giant crystals. American Mineralogist, 56, 1955–1974.
——— (1971b) The $Fe^{3+}_3(H_2O)_n(PO_4)_2$ homologous series: Crystal-chemical relationships and oxidized equivalents. American Mineralogist, 56, 1–7.
——— (1972a) Octahedral tetramer in the crystal structure of leucophosphite, $K_2Fe^{3+}_4(OH)_2(H_2O)_2(PO_4)_4 \cdot 2H_2O$. American Mineralogist, 57, 397–410.
——— (1972b) Sarcopside: Its atomic arrangement. American Mineralogist, 57, 24–35.
——— (1974a) Jahnsite, segelerite, and robertsite, three new transition metal phosphate species. American Mineralogist, 59, 48–59.
——— (1974b) Evidence for a complete mixed valence solid solution series in $Fe^{2+}_2(H_2O)_3(PO_4)_2$ (phosphoferrite) $Fe^{3+}_3(OH)_3[PO_4]_2$ (kryzhanovskite). Nature, 251, 305–306.
Moore, P.B., and Araki, T. (1973) Hureaulite, $Mn^{2+}_5(H_2O)_4[PO_3(OH)]_2[PO_4]_2$: Its atomic arrangement. American Mineralogist, 58, 302–207.
——— (1974) Trolleite, $Al_4(OH)_3(PO_4)_4$: A very dense structure with octahedral face-sharing dimers. American Mineralogist, 59, 974–984.
——— (1976) A mixed-valence solid-solution series: Crystal structures of phosphoferrite, $Fe^{II}_3(H_2O)_3(PO_4)_2$, and kryzhanovskite, FeIII$(OH)_3(PO_4)_2$. Inorganic Chemistry, 15, 316–321.
Moore, P.B., and Ito, J. (1973) Wyllieite, $Na_2Fe^{2+}_2Al(PO_4)_3$, a new species. Mineralogical Record, 4, 131–136.
——— (1978) Whiteite, a new species. 1. Proposed nomenclature for jahnsite-whiteite complex series. 2. New data on xanthoxenite. 3. Samonsite discredited. Mineralogical Magazine, 42, 309–323.
——— (1979) Alluaudites, wyllieites, arrojadites—Crystal-chemistry and nomenclature. Mineralogical Magazine, 43, 227–235.
Moore, P.B., and Molin-Case, J. (1974) Contribution to pegmatite phosphate giant crystal paragenesis: II. The crystal chemistry of wyllieite, $Na_2Fe^{2+}_2Al(PO_4)_3$, a primary phase. American Mineralogist, 59, 280–290.
Moore, P.B., Araki, T., and Kampf, A.R. (1980) Nomenclature of the phosphoferrite structure type: Refinements of landesite and kryzhanovskite. Mineralogical Magazine, 43, 789–795.
Moore, P.B., Araki, T., Merlino, S., Mellini, M., and Zanazzi, P.F. (1981) The arrojadite-dickinsonite series, $KNaCa(Fe,Mn)^{2+}_{14}Al(OH)_2(PO_4)_{12}$ crystal structure and crystal chemistry. American Mineralogist, 66, 1043–1049.
Moreira, L.F., Diehl, L.M.A., Torres-Tapia, E.C., Domingues, P.H., and Mattievich, E. (1994) Magnetic studies on synthetic phosphoferrite $Fe^{3+}_3(H_2O)_3(PO_4)_2$. Hyperfine Interactions, 83, 193–197.
Moreira, L.F., Dominguez, P.H., and Mattievich, E. (1996) Study of the series phosphoferrite-kryzhanovskite $Fe^{3+}_3(PO_4)_2 \cdot (H_2O)_3 \rightarrow Fe^{2+}_3(PO_4)_2 \cdot (H_2O)_3$. International Conference on the Applications of the Mössbauer Effect, 95, 10–16.
Mori, H., and Ito, T. (1950) The structure of vivianite and symplesite. Acta Crystallographica, 3, 1–6.
Morris, R.V., Ming, D.W., Graff, T.G., Arvidson, R.E., Bell, J.F. III, Squyres, S.W., Mertzman, S.A., Gruener, J.E., Golden, D.C., Le, L., and Robinson, G.A. (2005) Hematite spherules in basaltic tephra altered under aqueous, acid-sulfate conditions on Mauna Kea volcano, Hawaii: Possible clues for the occurrence of hematite-rich spherules in the Burns formation at Meridiani Planum, Mars. Earth and Planetary Science Letters, 240, 168–178.
Morris, R.V., Klingelhöfer, G., Schröder, C., Rodionov, D.S., Yen, A., Ming, D.W., de Souza, P.A., Wdowiak, T., Fleischer, I., Gellert, R., and others. (2006a) Mössbauer mineralogy of rock, soil, and dust at Meridian Planum, Mars: Opportunity's journey across sulfate-rich outcrop, basaltic sand and dust, and hematite lag deposits. Journal of Geophysical Research, 111, E12S15, doi:10.1029/2006JE002791.
Morris, R.V., Klingelhöfer, G., Schröder, C., Rodionov, D.S., Yen, A., Ming, D.W., de Souza, P.A., Fleischer, I., Wdowiak, T., Gellert, R., and others. (2006b) Mössbauer mineralogy of rock, soil, and dust at Gusev Crater, Mars: Spirit's journey through weakly altered olivine basalt on the plains and pervasively altered basalt in the Columbia Hills. Journal of Geophysical Research, 111, E02S13, doi:10.1029/2005JE002584.
Nembrini, G.P., Capobianco, J.A., Viel, M., and Williams, A.F. (1983) A Mössbauer and chemical study of the formation of vivianite in sediments of Lago Maggiore (Italy). Geochimica et Cosmochimica Acta, 47, 1459–1464.
Nomura, K., and Ujihira, Y. (1982) Mössbauer spectrometric study of hureaulite. Noppon Kagaku Kaishi, 8, 1352–1356.
Nord, A.G., and Ericsson, T. (1982) Cation distributions in $(Fe_{1-z}Me_z)_3(PO_4)_2$ graftonite-type solid solutions determined by Mössbauer spectroscopy. Zeitschrift für Kristallographie, 161, 209–224.
——— (1985) Cation distribution of some ternary orthophosphates having the farringtonite structure. American Mineralogist, 70, 624–629.
Nord, A.G., and Kierkegaard, P. (1968) The crystal structure of $Mg_3(PO_4)_2$. Acta Chemica Scandinavica, 22, 1466–1474.
Paster, S., Wilkinson, C., Forsyth, J.B., Johnson, C.E., Pankhurst, Q.A., and Thomas, M.F. (1990) Magnetic structure of ludlamite, $Fe_3(PO_4)_2 \cdot 4H_2O$. Hyperfine Interactions, 54, 651–654.
Rastsvetaeva, R.K. (1971) Crystalline structure of lomonosovite $Na_5Ti_2(Si_2O_7)(PO_4)O_2$. Doklady Akademii nauk SSSR, 197, 81–84.
Rastsvetaeva, R.K., Simonov, V.I., and Belov, N.V. (1971) Crystalline structure of lomonosovite, $Na_5Ti_2Si_2O_7(PO_4)O_2$. Doklady Akademii Nauk USSR, 197, 81.
Rastsvetaeva, R.K., Gurbanova, O.A., and Chukanov, N.V. (2002) Crystal structure of greifensteinite $Ca_2Be_4(Fe^{2+},Mn)_5(PO_4)_6(OH)_4 \cdot 6H_2O$. Doklady Physical Chemistry, 383, 78–81.
Rastsvetaeva, R.K., Barinova, A.V., Chikanov, N.V., and Pietraszko, A. (2004) Crystal structure of a magnesium-rich triclinic analogue of greifensteinite. Doklady Chemistry, 398, 191–195.
Rastsvetaeva, R.K., Chukanov, N.V., and Verin, I.A. (2005) Crystal structure of roscherite. Doklady Chemistry, 403, 160–163.
Rastsvetaeva, R.K., Chukanov, N.V., Verin, I.A., and Atencio, D. (2007) The crystal structure of footemineite. Doklady Earth Sciences, 416, 1053–1056.
Rastsvetaeva, R.K., Rozenberg, K.A., Chukanov, N.V., and Möckel, S. (2009) The crystal structure of an iron-rich variety of zanazziite belonging to the heteropolyhedral framework roscherite-group beryllophosphates. Crystallography Reports, 54, 568–571.
Rastsvetaeva, R.K., Aksenov, S.M., and Chukanov, N.V. (2012) The first crystal structure determination of metavivanite $Fe^{2+}Fe^{3+}_2(PO_4)_2(OH)_2 \cdot 6H_2O$. Doklady Physical Chemistry, 445, 101–104.
Rea, J.R., and Kostiner, E. (1972) The crystal structure of manganese fluorophosphates, $Mn_2(PO_4)F$. Acta Crystallographica, B, 28, 2525–2529.
Redhammer, G.J., Tippelt, G., Roth, G., Lottermoser, W., and Amthauer, G. (2000) Structure and Mössbauer spectroscopy of barbosalite $Fe^{2+}Fe^{3+}_2(PO_4)_2(OH)_2$ between 80 K and 300 K Sample: $T = 298$ K. Physics and Chemistry of Minerals, 27, 419–429.
Redhammer, G.J., Tippelt, G., Bernroider, M., Lottermoser, W., Amthauer, G., and Roth, G. (2005) Hagendorfite $(Na,Ca)MnFe_2(PO_4)_3$ from type locality Hagendorf (Bavaria, Germany): Crystal structure determination and ^{57}Fe Mössbauer spectroscopy. European Journal of Mineralogy, 17, 915–932.
Redhammer, G.J., Roth, G., Tippelt, G., Bernroider, M., Lottermoser, W., Amthauer, G., and Hochleitner, R. (2006) Manganoan rockbridgeite $Fe_{4.32}Mn_{0.62}Zn_{0.06}(PO_4)_3(OH)_5$: Structure analysis and ^{57}Fe Mössbauer spectroscopy. Acta Crystallographica, C, 62, i24–i28.
Ren, L., Grew, E.S., Xiong, M., and Ma, Z. (2003) Wagnerite-*Ma5bc*, a new polytype of $Mg_2(PO_4)(F,OH)$, from granulite-facies paragneiss, Larsemann Hills, Prydz Bay, East Antartica. The Canadian Mineralogist, 41, 393–411.
Rieder, R., Wänke, H., Economou, T., and Turkevich, A. (1997) Determination of the chemical composition of martial soil and rocks: the alpha proton X-ray spectrometer. Journal of Geophysical Research, 102, 4027–4044.
Rieder, R., Gellert, R., Brückner, J., Klingelhöfer, G., Dreibus, G., Yen, A., and Squyres, S.W. (2003) The new Athena alpha particle X-ray spectrometer for the Mars Exploration Rovers. Journal of Geophysical Research, 108, 8066, doi: 10.1029/2003JE002150.
Rieder, R., Gellert, R., Anderson, C., Brückner, J., Clark, B.C., Driebus, G., Economou, T., Klingelhöfer, G., Lugmair, G.W., Ming, D.W., Squyres, S.W., d'Uston, C., Wänke, H., Yen, A., and Zipfel, J. (2004) Chemistry of rocks and soils at Meridiani Planum from the Alpha Particle X-ray Spectrometer. Science, 306, 1746–1749.
Rodgers, K.A., and Johnston, J.H. (1985) Type metavivianite: Mössbauer evidence for a revised composition. Neues Jahrbuch für Mineralogie Monatshefte, 1985, 539–542.
Rodgers, K.A., Kobe, H.W., and Childs, C.W. (1993) Characterization of vivianite from Catavit, Llallagua, Bolivia. Mineralogy and Petrology, 47, 193–208.
Rothstein, Y. (2006) Spectroscopy of jarosite and implications for the mineralogy of Mars. B.A. thesis, Mount Holyoke College, South Hadley, Massachusetts.
Rouse, R.C., Peacor, D.R., and Freed, R.L. (1988) Pyrophosphate groups in the structure of canaphite, $CaNa_2P_2O_7 \cdot 4H_2O$: The first occurrence of a condensed phosphate as a mineral. American Mineralogist, 73, 168–171.
Rouzies, D., and Millet, J.M.M. (1993a) Mössbauer spectroscopic study of synthetic lipscombite and barbosalite at room temperature. Hyperfine Interactions, 77, 11–18.
——— (1993b) Mössbauer spectroscopic study of synthetic oxidized vivianite at room temperature. Hyperfine Interactions, 77, 19–28.
Rouzies, D., Varloud, J., and Millet, J.M.M. (1994) Thermal behavior and physicochemical characterization of synthetic and natural iron hydroxyphosphates. Journal of the Chemical Society–Faraday Transactions, 90, 3335–3339.
Rouzies, D., Moral, P., and Millet, J.M.M. (1995) Synthesis and study by Mössbauer spectroscopy of lipscombite $(Fe^{3+}Fe^{2+}(P0_4)_2(0H)_2)$ partially substituted by

manganese, cobalt, and chromium cations. Journal of Physical Chemistry, 99, 12576–12580.
Russell, R.G.G. (1976) Metabolism of inorganic pyrophosphate (PP). Arthritis and Rheumatism, New York, 19, 465–479.
Schmidt, M.E., Farrand, W.H., Johnson, J.R., Schröder, C., Hurowitz, J.A., McCoy, T.J., Ruff, S.W., Arvidson, R.E., DesMarais, D.J., Lewis, K.W., and others. (2009) Spectral, mineralogical, and geochemical variations across Home Plate, Gusev Crater, Mars indicate high and low temperature alteration. Earth and Planetary Science Letters, 281, 258–266.
Schmid-Beurmann, P., Morteani, G., and Cemič, L. (1997) Experimental determination of the upper stability of scorzalite, $FeAl_2[OH/PO_4]_2$, and the occurrence of minerals with a composition intermediate between scorzalite and lazulite(ss) up to the conditions of the amphibolite facies. Mineralogy and Petrology, 61, 211–222.
Schwab, R.G., Götz, C., Herold, H., and Pinto de Oliveria, N. (1991) Compounds of the crandallite type: Synthesis and properties of pure (Ca, Sr, Ba, Pb, La, Ce to Eu) – arsenocrandallites. Neues Jahrbuch für Mineralogie Monatshefte 1991, 97–112.
Segeler, C.G., Moore, P.B., Dyar, M.D., Leans, F., and Ferraiolo, J.A. (2012) Ferrolaueite, a new mineral from Monmouth County, New Jersey, U.S.A. Australian Journal of Mineralogy, 16, 69–76.
Sen Gupta, P.K., Swihart, G.H., Dimitrijević, R., and Hossain, M.B. (1991) The crystal structure of lünebergite, $Mg_3(H_2O)_6[B_2(OH)_6(PO_4)_2]$. American Mineralogist, 76, 1400–1407.
Shinno, I., and Li, Z. (1998) Octahedral site Fe^{2+} quadrupole splitting distributions from the Mössbauer spectra of arrojadite. American Mineralogist, 83, 1316–1322.
Shinno, T., and Takada, T. (1971) Mössbauer experiments in external magnetic fields. Bulletin of the Institute for Chemical Research, Kyoto University, 49, 314–319.
Simmons, G.C. (1964) Leucophosphite, a new occurrence in the Quadrilitero Ferrifero, Minas Gerais, Brazil. American Mineralogist, 49, 377–386.
Simpson, C.S. (1931–1932) Contributions to the mineralogy of Western Australia. Royal Society of Western Australia Journal, 188, 61–74.
Sklavounos, S., Ericsson, T., Filippidis, A., Michailidis, K., and Kougoulis, C. (1992) Chemical, X-ray and Mössbauer investigation of a turquoise from the Vathi area volcanic rocks, Macedonia, Greece. Neues Jahrbuch für Mineralogie Monatshefte 1992, 469–480.
Sklute, E.C., Dyar, M.D., and Schaefer, M.W. (2006) Mössbauer spectroscopy of olivines across the Mg-Fe solid solution series. Lunar and Planetary Science, Abstract 2109.
Sokolova, E.V., Egorov-Tismenko, Yu.K., and Khomyakov, A.P. (1987) Crystal structure of lomonosovite and sulfohalite as a homolog of the structures of $Na_{14}CaMgTi_4(Si_2O_7)_2(PO_4)_4O_4F_2$. Mineralogicheskij Zhurnal, 9, 28–35.
Sokolova, E., Hawthorne, F.C., McCammon, C., and Liferovich, R.P. (2001) The crystal structure of Gladiusite, $(Fe^{2+},Mg)_4Fe^{3+}_2(PO_4)(OH)_{11}(H_2O)$. The Canadian Mineralogist, 39, 1121–1130.
Stopar, J.D., Taylor, G.J., Velbel, M.A., Norman, M.D., Vicenzi, E.P., and Hallis, L.J. (2013) Element abundances, patterns, and mobility in Nakhlite Miller Range 03346 and implications for aqueous alteration. Geochimica et Cosmochimica Acta, 112, 208–225.
Sturman, B.D., Mandarino, J.A., Mrose, M.E., and dunn, P.J. (1981) Gormanite, $Fe^{2+}_3Al_4(PO)_4(OH)_6 \cdot 2H_2O$, the ferrous analogue of souzalite, and new data for souzalite. Canadian Mineralogist, 19, 381–387.
Tadini, C. (1981) Magniotriplite: its crystal structure and relation to the triuplite-triploidite group. Bulletin de Minéralogie, 104, 677–680.
Takagi, S., Mathew, M., and Brown, W.E. (1986) Crystal structures of bobierrite and synthetic $Mg_3(PO_4)_2(H_2O)_8$. American Mineralogist, 71, 1229–1233.
Takahashi, M. Tobishima, S., Takei, K., and Sakura, Y. (2002) Reaction behavior of $LiFePO_4$ as a chathode materials for rechargeable lithium batteries. Solid State Ionics, 148, 283–289.
Takashima, Y., and Ohashi, S. (1968) The Mössbauer spectra of various natural minerals. Bulletin of the Chemical Society of Japan, 41, 88–93.
Taxer, K., and Bartl, H. (2004) On the dimorphy between the variscite and clinovariscite group: Refined finestructural relationship of strengite and clinostrengite, $Fe(PO_4) \cdot 2H_2O$. Crystal Research and Technology, 39, 1080–1088.
Tosca, N.J., McLennan, S.M., Clark, B.C., Grotzinger, J.P., Hurowitz, J.A., Knoll, A.H., Schröder, C., and Squyres, S.W. (2005) Chemical modeling of evaporation processes on Mars: Insight from the sedimentary record at Meridiani Planum. Earth and Planetary Science Letters, 240, 122–148.
Tosca, N.J., McLennan, S.M., Lindsley, D.H., and Schoonen, M.A. (2004) Acid-sulfate weathering of synthetic Martian basalt: The acid fog model revisited. Journal of Geophysical Research, 109, E05003, doi:10.1029/2003JE002218.
Toulmin, P., Baird, A.K., Clark, B.C., Keil, K., Rose, H.J., Christian, R.P., Evans, P.H., and Kelliher, W.C. (1977) Geochemical and mineralogical interpretation of the Viking inorganic chemical results. Journal of Geophysical Research, 82, 4625–4634.
Treiman, A.H. (1996) An early warm, wet Mars? Little support from the Martian meteorite ALH84001. LPI Technical Report 96-01, Part 1, Houston, Texas.
Usui, T., McSween, H.Y. Jr., and Clark, B.C. III (2008) Petrogenesis of high-phosphorus Wishstone Class rocks in Gusev Crater, Mars. Journal of Geophysical Research, 113, E12S44, doi: 10.1029/2008JE003225.
Van Alboom, A., and De Grave, E. (2005) Mössbauer effect in natural strunzite, ferristrunzite, and ferrostrunzite. Hyperfine Interactions, 166, 679–685.
Van Alboom, A., De Grave, E., and Wohlfahrt-Mehrens, M. (2011) Temperature dependence of the Fe^{2+} Mössbauer parameters in triphylite ($LiFePO_4$). American Mineralogist, 96, 408–416.
Vencato, I., Mattievich, E., and Mascarebhas, Y.P. (1989) Crystal structure of synthetic lipscombite: A redetermination. American Mineralogist, 74, 456–460.
Vochten, R., and De Grave, E. (1981) Crystallographic, Mössbauer and Electrokinetic Study of Synthetic Lipscombite. Physics and Chemistry of Minerals, 7, 197–203.
——— (1990) Mössbauer and infrared spectroscopic characterization of ferristrunzite from Blaton, Belgium. Neues Jahrbuch für Mineralogy Monatshefte, 176–190.
Vochten, R., van Acker, P., and De Grave, E. (1983) Mössbauer, electrokinetic and refined lattice parameters study of synthetic manganoan lipscombite. Physics and Chemistry of Minerals, 9, 263–268.
Vochten, R., De Grave, E., and Stoops, G. (1979) Petrographic, chemical, and Mössbauer study of some oxidized vivianite nodules from Retie (Province of Antwerp, Belgium). Neues Jahrbuch für Mineralogy Abhandlungen, 137, 208–222.
Vochten, R., De Grave, E., and Pelsmaekers, J. (1984) Mineralogical study of bassetite in relation to its oxidation. American Mineralogist, 69, 967–978.
Vochten, R., De Grave, E., van Springel, K., and van Haverbeke, L. (1995) Mineralogical and Mössbauer spectroscopic study of some strunzite varieties of the Silbergrube, Waidhaus, Oberpfalz, Germany. Neues Jahrbuch für Mineralogy Monatshefte, 1995, 11–25.
Vogel, R., and Evans, B.J. (1980) ^{57}Fe Mössbauer study of the crystal chemistry of strunzite, $MnFe_2(PO4)_2(OH)_2 \cdot 6H_2O$. Journal de Physique, C1-297–298.
Waerenborgh, J.C., and Figueiredo, M.O. (1986) X-ray powder diffraction and ^{57}Fe Mössbauer spectroscopy study of the thermal breakdown of vivianite $Fe_3(PO_4)_2 \cdot H_2O$. Hyperfine Interactions, 29, 1101–1104.
Waldrop, L. (1969) The crystal structure of triplite, $(Mn,Fe)_2FPO_4$. Zeitschrift für Kristallographie, 130, 1–14.
——— (1970) The crystal structure of triploidite and its relation to the structures of other minerals of the triplite-triploidite group. Zeitschrift für Kristallographie, 131, 1–20.
Wänke, H., and Dreibus, G. (1998) Chemical composition and accretion history of terrestrial planets. Philosophical Transactions of the Royal Society of London A, 325, 545–557.
Wise, M.A., Hawthorne, F.C., and Cerny, P. (1990) Crystal structure of a Ca-rich beusite from the Yellowknife pegmatite field, Northwest Territories. Canadian Mineralogist, 28, 141–146.
Wolfe, C.W. (1949) Ludlamite from the Palermo Mine, North Groton, New Hampshire. American Mineralogist, 34, 94–97.
Yakubovich, O.V. (2008) Phosphates with amphoteric oxo-complexes: From structural features to genetic conclusions. Zeitschrift für Kristallographie, 223, 126–131.
Yakubovich, O.V., Matvienko, E.N., Simonov, M.A., and Mel'nikov, O.K. (1986) Crystal structure of synthetic Fe^{3+}-arrojadite with ideal formula of $K_2Na_5Fe^{2+}_{14}Fe^{3+}(PO_4)_{12}(OH)_2$. Moscow University Geology Bulletin 1986, 35–47.
Yakubovich, O.V., Massa, W., Liferovich, R.P., and McCammon, C.A. (2001) The crystal structure of baricite, $(Mg_{1.70}Fe_{1.30})(PO_4)_2 \cdot 8H_2O$, the magnesium-dominant member of the vivianite group. The Canadian Mineralogist, 39, 1317–1324.
Yakubovich, O.V., Steele, I.M., Rusakov, V.S., and Urusov, V.S. (2006) Hole defects in the crystal structure of synthetic lipscmbite $(Fe^{3+}_{4.7}Fe^{2+}_{2.3})[PO_4]_4O_{2.7}(OH)_{1.3}$ and genetic crystal chemistry of minerals of the lipscombite-barbosalite series. Crystallography Reports, 51, 401–411.
Yang, S.F., Song, Y.N., Ngala, K., Zavalu, P.Y., and Whittingham, M.S. (2003) Performance of $LiFePO_4$ as lithium battery cathode and comparison with manganese and vanadium oxides. Journal of Power Source, 119–1121, 239–246.
Yen, A.S., Morris, R.V., Gellert, R., Clark, B.C., Ming, D.W., Klingelhöfer, G., McCoy, T.J., Schmidt, M.E., and the Athena Science Team (2007) Composition and formation of the "Paso Robles" class soils at Gusev Crater. In Lunar and Planetary Science Conference XXXVIII, Abstract 2030. Lunar and Planetary Institute, Houston.
Zanazzi, P.F., Fanfani, L., and Nunzi, A. (1969) Crystal structure of fairfieldite. Acta Crystallographica A, 25, 112–117.

Manuscript received July 31, 2013
Manuscript accepted December 16, 2013
Manuscript handled by Brian Phillips